C O M M U N I C A T I O N S

FACULTY OF SCIENCES
UNIVERSITY OF ANKARA

DE LA FACULTE DES SCIENCES
DE L'UNIVERSITE D'ANKARA

Series C: Biology

VOLUME: 32 **Number: 2** **YEAR: 2023**

Faculty of Sciences, Ankara University
06100 Beşevler, Ankara-Türkiye
ISSN 1303-5991 e-ISSN 2618-6470

C O M M U N I C A T I O N S

FACULTY OF SCIENCES
UNIVERSITY OF ANKARA

DE LA FACULTE DES SCIENCES
DE L'UNIVERSITE D'ANKARA

S e r i e s C : B i o l o g y

Volume: 32 **Number: 2** **Year: 2023**

This Journal is published two issues in a year by the Faculty of Sciences, University of Ankara. Articles and any other material published in this journal represent the opinions of the author(s) and should not be construed to reflect the opinions of the Editor(s) and the Publisher(s).

Correspondence Address:
COMMUNICATIONS EDITORIAL OFFICE
Ankara University, Faculty of Sciences,
06100 Tandoğan, ANKARA – TÜRKİYE
Tel: (90) 312-2126720 Fax: (90) 312-2235000
e-mail: commun@science.ankara.edu.tr
http://communications.science.ankara.edu.tr/index.php?series=A1

Print:
Ankara University Press
İncitaş Sokak No:10 06510 Beşevler
ANKARA – TÜRKİYE
Tel: (90) 312-2136655

C O M M U N I C A T I O N S

FACULTY OF SCIENCES
UNIVERSITY OF ANKARA

DE LA FACULTE DES SCIENCESDE
L'UNIVERSITE D'ANKARA

Series C: Biology

Volume: 32 **Number: 2** **Year: 2023**

http://communications.science.ankara.edu.tr

Commun.Fac.Sci.Univ.Ank.Ser. C Biology
Volume 32, Number 2, Pages 87-104 (2023)
ISSN 1303-6025 E-ISSN 2651-3749
DOI: 10.53447/ communc.1260170

Research Article; Received: March 4, 2023; Accepted: April 26, 2023

ECOLOGICAL RISK ASSESSMENT PROFILE OF LAKE SURFACE SEDIMENT USING METAL(LOID)S: A CASE STUDY, THE BORABOY LAKE, TÜRKİYE

ŞEYDA FİKİRDEŞİCİ ERGEN[1]

[1] Department of Biology, Faculty of Science, Ankara University, Ankara, TÜRKİYE

ABSTRACT. Anthropogenic activities have increasingly threatened aquatic ecosystems with the gradual increase of metalloids in the lake sediment. The profile of Al, As, Cd, Co, Cr, Cu, Fe, Mn, Mo, Ni, Pb, and Zn metal(loid)s that have been investigated in natural Boraboy Lake have been investigated in sediment. Their amounts in the sediment have been found as Mn>Fe>Al>Zn>Cu>Cr>Ni>Co>Pb>As>Mo>Cd. The findings have been analyzed using sediment quality values. The Enrichment Factor, one of the sediment quality values, has indicated that the lake has highly enriched in As, Cd, Co, Cr, Cu, Mn, Ni, Pb, and Zn. In addition to that, it has been detected that As, Ni, and Cu together constituted the 67% of the total toxic effect. While the mean value of Cu has been found to be higher than the reference value of the earth's crust at, 58.1±6.8 ppm, the mean values of As and Ni have been found to be lower than the reference value of the earth's crust (9.4±0.7 ppm) and (18.8±12.8 ppm) respectively. As and Cu have been detected above the Threshold Effect Level. Despite all these results, it has been revealed through sediment quality indexes that there is no threatening accumulation in the lake.

1. INTRODUCTION

Due to their ability to accumulate metal(loid)s (Ms), sediments are generally defined as aquatic cleaners of Ms [1]. Ms are found in the natural composition of the earth crust; however they have been gradually increasing in lake sediments with anthropogenic effects. Increasing Ms level has toxicological effects on both wetland and organisms in wetland when it is over a certain threshold value. Therefore, it is crucial to study the possible ecotoxicological effects of a metal(loid) and to reveal the Ms-Ms interactions of a lake [2]. Ms, which are harmless and naturally found in trace amounts in the earth crust, have been subject to many studies in which they generate ecotoxicological stress in wetlands due to anthropogenic effects such as industry, agriculture, trade, etc. [3-6]. It is very important to determine the distribution of Ms to stations in a sediment and to identify the spatial points where it is concentrated. Therefore, it is shown by these studies that such studies are of great importance in terms of timely intervention.

Keywords. Multivariate statical analysis, sediment quality guidelines, Ms-Ms interactions, ecotoxicity
seydafikirdesici@gmail.com- Corresponding author; 0000-0002-4623-1256

The Ms concentrations acquired from the sediment are not meaningful on their own. The results are only meaningful when they are evaluated with background level and sediment quality guides [6]. Thus, in investigation of the sources (natural/anthropogenic) of Ms, background levels such as probable effect level (PEL), threshold effect level (TEL), effects range low (ERL), and effects range median (ERM) and sediment evaluation methods such as Degree of Contamination (C_d), Modified Degree of Contamination (mC_d), Contamination factor (C_f^i) and Enrichment factor (EF), Geoaccumulation index (I_{geo}), Toxic unit (TU), Pollution Load Index (PLI), mean ERM quotients (m-ERM-q) and mean PEL quotients (m-PEL-q) have been frequently used in the literature [3-6] The separation of the source of an Ms in the sediment provides important information about the contamination degree of that Ms. It also offers advantages in determining and maintaining the health status of the lake water system [2].

Boraboy Lake is 750 m long in general and 100 m wide in the eastern half and 200 m wide in the western half. It has a perimeter of 2 km and an area of 11 ha (0.11 km^2). The lake is generally used for irrigation of agricultural areas and recreation [7]. In the study, 13 different Ms in the sediment of Boraboy Lake, which is an important natural lake, have been investigated in terms of both accumulation and ecological hazard. The amounts of these metals have been interpreted using the sediment quality guidelines (SQGs) limit values, and their effects have been evaluated through the sediment assessment indexes. Ms-Ms accumulation relations have also been examined using multivariate statistical analysis. The main objective of this study is to understand the current Ms composition of the lake by determining the distribution of Ms at the stations in the sediment of Lake Boraboy.

2. MATERIALS AND METHODS

A total of 15 samples were taken from the surface sediment at one time in October 2021 (Figure 1, Table 1). The samples collected were sent directly to Bureau Veritas Mineral Laboratories Canada (ACME LAB.) and analyzed according to the AQ270 method. Duplicate, reference material and blank results and detection limits are as in Table 2.

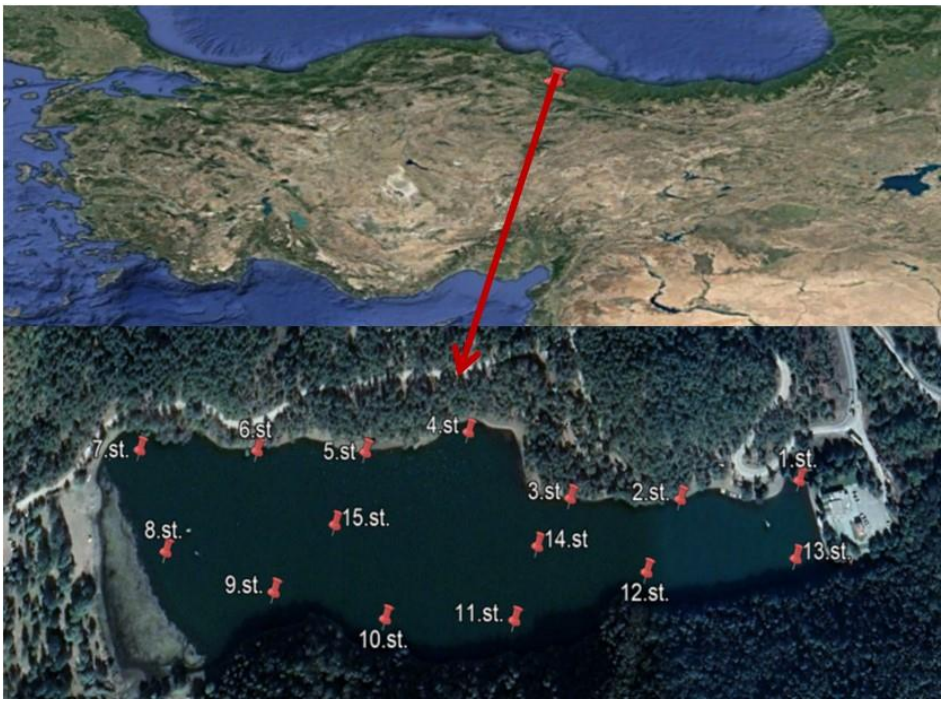

FIGURE 1. Boraboy Lake stations

TABLE 1. Coordinates of work stations

Station No	Latitude	Longitude
1	40°48'15.53"K	36° 9'29.03"D
2	40°48'15.02"K	36° 9'24.10"D
3	40°48'15.04"K	36° 9'19.59"D
4	40°48'16.84"K	36° 9'15.41"D
5	40°48'16.28"K	36° 9'11.15"D
6	40°48'16.31"K	36° 9'60.67"D
7	40°48'16.33"K	36° 9'10.81"D
8	40°48'13.59"K	36° 9'30.11"D
9	40°48'12.54"K	36° 9'70.56"D
10	40°48'11.85"K	36° 9'12.07"D
11	40°48'11.82"K	36° 9'17.26"D
12	40°48'13.08"K	36° 9'22.63"D
13	40°48'13.45"K	36° 9'28.70"D
14	40°48'13.76"K	36° 9'18.22"D
15	40°48'14.32"K	36° 9'90.96"D

TABLE 2. Duplicate samples, reference material, blank solution results and detection limits

	Al	**As**	**Cd**	**Co**	**Cr**	**Cu**	**Fe**	**Mn**	**Mo**	**Ni**	**Pb**	**Zn**
	(%)	(ppm)	(ppm)	(ppm)	(ppm)	(ppm)	(%)	(ppm)	(ppm)	(ppm)	(ppm)	(ppm)
Pulp Duplicates-1	3.38	5.8	0.23	24.2	9.7	60.97	4.30	968	0.37	10.8	29.61	240.4
Pulp Duplicates-2	3.47	6.0	0.23	24.0	9.9	61.87	4.37	982	0.39	11.1	29.64	248.4
Reference value BVGEO01	2.46	124.8	6.11	27.7	192.9	4604.86	3.86	788	10.75	179.3	191.33	1858.7
Reference value OREAS262	1.26	34.8	0.60	30.3	45.1	126.94	3.46	570	0.65	64.4	57.02	156.2
Blank	<0.01	<0.1	<0.01	<0.1	<0.5	0.02	<0.01	<1	<0.01	<0.1	<0.01	<0.1
Detection Limit	0.01	0.1	0.01	0.1	0.5	0.01	0.01	1	0.01	0.1	0.01	0.1

Sediment Quality Indexes

Source data from Turekian and Wedepohl [8] have been taken as reference. The scale including the meaning of the sediment quality indexes is as in Table 3.

Contamination factor (C_f^i) [9]

$$C_f^i = C^i / C_n^i \quad (1)$$

C^i= Amount of Ms
C_n^i= Reference value

Degree of Contamination (C_d) [9]

$$C_d = \sum_{i=1}^{n} C_f^i \quad (2)$$

C_f^i= Contamination factor

Modified Degree of Contamination (mC_d) [10]

$$mC_d = \frac{\sum_{i=1}^{n} C_f^i}{n} \quad (3)$$

C_f^i= Contamination factor
n= Number of Ms studied

Pollution load index (PLI) [11]

$$PLI = (C_{f1} \times C_{f2} \times C_{f3} \ldots . \times C_{fn})^{1/n} \quad (4)$$

C_{f1}= Contamination factor
n= Number of Ms studied

Enrichment factor (EF) [12]

$$EF = \frac{C_n/C_{ref}}{B_n/B_{ref}} \quad (5)$$

C_n= Amount of Ms
C_{ref}= Amount of Ms in the reference environment
B_n= Amount of reference element in sample
B_{ref}= The value of reference element in reference environment
AI has been preferred as reference element.

Geoaccumulation index (I_{geo}) [13]

$$I_{geo} = log_2 \frac{C_n}{1.5 \times B_n} \quad (6)$$

C_n= Amount of Ms
B_n= The amount of metal in the reference environment
1.5= natural oscillation coefficient

Mean effect range median ratio (m-ERM-Q) and average probable effect level ratio (m-PEL-Q) [14]

$$m - ERM - Q = \frac{\sum_{i=1}^{n} C_i/ERM_i}{n} \quad (7)$$

$$m - PEL - Q = \frac{\sum_{i=1}^{n} C_i/PEL_i}{n} \quad (8)$$

C_i=Amount of metal
ERM= effect range median of metal
PEL= average probable effect level of metal
n= number of Ms studied

Total toxic unit (Σ TU) and rational toxic unit

$$\Sigma TUs = \sum_{i=1}^{n} C_i/PEL_{C_i} \quad (9)$$

$$Proportional\ TU = \frac{C_i/PEL_{C_i}}{\Sigma TUs} X100 \quad (10)$$

Statistical Analysis

The relationship between Ms-Ms has been revealed through correlation, principal components analysis (PCA) and clustering (CA) analysis. SPSS 21v. has been used for all statistical analysis.

TABLE 3. Meaning scale of sediment quality indexes

Contamination factor [9]	
CF<1	low contamination
1≤CF<3	moderate contamination
3≤CF<6	considerable contamination
CF≥6	high contamination
Degree of contamination (C_d) [9]	
Cd≤8	low degree of contamination
8≤Cd≤16	moderate degree of contamination
16≤Cd≤32	considerable degree of contamination
Cd≥32	very high degree of contaminations
Modified degree of contamination (mCd) [10]	
mCd < 1.5	nil to very low degree of contamination
1.5 ≤ mCd < 2	low degree of contamination
2 ≤ mCd < 4	moderate degree of contamination
4 ≤ mCd < 8	high degree of contamination
8 ≤ mCd < 16	very high degree of contamination
16 ≤ mCd < 32	extremely high degree of contamination
mCd ≥ 32	ultra high degree of contamination
Pollution load index (PLI) [11]	
PLI <1	no pollution
PLI is >1	deterioration

TABLE 3 (continued)

Enrichment factor (EF) [12]	
<1	no enrichment
1 to 3	minor enrichment
3 to 5	moderate enrichment
5 to 10	significant enrichment
10 to 25	severe enrichment
25 to 50	very severe enrichment
>50	extremely severe enrichment
Geoaccumulation index (Igeo) [13]	
Igeo≤0	practically uncontaminated
0<Igeo<1	uncontaminated to moderately contaminated
1<Igeo<2	moderately contaminated
2<Igeo<3	moderately to strongly contaminated
3<Igeo<4	strongly contaminated
4<Igeo<5	strongly to extremely contaminated
Igeo≥5	extremely contaminated
Ratio of average effects range median (m-ERM-Q) [50]	
m-ERM-q<0.1	9%
0.11<m-ERM-q<0.5	21%
0.51 <m-ERM-q <1.5	49%
m-ERM-q>1.50	76% probability of being toxic
Ratio of average probable effect level (m-PEL-Q) [14]	
m-PEL-Q<0.1	unimpacted
0.1< m-PEL-Q<1	moderately impacted
m-ERM-Q>1	highly impacted

3. RESULTS AND DISCUSSION

As a result of the analysis, Ms accumulation in the sediment has been found as Mn>Fe>Al>Zn>Cu>Cr>Ni>Co>Pb>As>Mo>Cd, respectively (Table 4). Manganese (Mn) is in the form of Mn^{2+} in aquatic ecosystems [15]. The distribution of Mn in lakes may vary depending on the hydrophysical characteristics of the lakes and the redox changes of the lake habitat [16]. The Mn value in the study varied between 991 and 1675 ppm. The mean Mn value has been calculated as 1217.3±172.9 ppm. It is higher than the earth crust reference value. Due to its lower turbulence and higher pH compared to rivers,

the lake sediments act as an efficient sink for the iron element (Fe) [17]. Mn is affected more by redox changes than Fe [18]. The amount of Fe and Mn in a lake sediment does not only depend on redox changes. It also depends on the biogeochemical alteration of the lake water and the diagenesis of the sediment [19]. In the study, while the Fe concentration has varied between 351 and 682 ppm, the mean value has been calculated as 536.1±86.1 ppm. This result is low, compared to the earth crust reference value.

Although its content varies depending on the type of the rock, Aluminum (Al), one of the main elements of the earth crust, has been detected in all rocks. It constitutes approximately 7.91% of the lithosphere. Along with silicium and oxygen, it is one of the main elements of the earth crust and it is mostly in the form of Al^{+3} cation. It shows affinity for oxygen bonds [20]. Al is easily absorbed by sediment as it is in the form of metastable compounds and can activate as the acidity increases in water [21]. In the study, the Al value varied between 247 and 457 ppm. The mean value has been calculated as 368.1±63.6 ppm. It has been found to be lower than the earth crust reference value. On the basis of anthropogenic zinc (Zn) release, there is the production of energy, cement, medicine, cosmetics and rubber etc. as well as processes such as waste incineration [22]. The Zn value in the study varied between 72.1 and 94.1 ppm. The mean value has been calculated as 85.1±6.4 ppm. While some stations of the lake are close to the earth crust reference value, the mean value has been found to be low. Copper (Cu) is a very important trace element for carbohydrate metabolism and the functioning of some enzymes [23]. However, it can also cause the pollution of a lake when it exceeds the threshold value. Vehicle exhausts, pesticides, mining and burning coal are effective Cu resources [24, 25]. Cu values varied between 46.9 and 71.5 ppm, and the mean value has been calculated as 58.1±6.8 ppm. The Cu concentration in each station has been observed to be higher than the earth crust reference value. Cr contamination in lakes is associated with the discharge of wastewater from industrial facilities [26]. In this study, Cr concentration has been observed in the range of 8.1 to 40.1 ppm and the mean value has been calculated to be 24.2±12.1 ppm. The detected Cr concentration has been observed not to exceed the earth crust value at any of the stations.

Nickel (Ni) is a commercially important metal that is used in stainless steel, metallurgy and food industry. Therefore, its oscillation into lakes is both natural and anthropogenic and it is a metal commonly found in waters [27]. In the study, its concentration has been found in the range of 8.9 to 43.3 ppm, while the mean value has been calculated as 18.8±12.8 ppm. Its concentration at each station has remained low compared to the earth crust reference data. Cobalt (Co) is one of the trace elements for organisms; however, it has very dangerous effects when it exceeds the threshold value. It is found in the stable cobalt sulfate phase in sediments [28]. In the study, its concentration has been measured between 10.9 and 24.6 ppm. Its mean value has been calculated as 16.2±4.1 ppm. Although it exceeded the earth crust reference value at some stations, its average value has

been found to be lower. Adsorption and desorption speeds of lead (Pb) in the sediment vary due to the structure of the sediment. Pb ranks third in the world in Ms production. This makes Pb potentially dangerous among the lake pollutants [29]. It reaches the lake sediment easily due to its wide use in such as mining, ammunition, pipe construction, paint making and pesticides [30]. The mean value of Pb, which is detected between 7.8 and 24.6 ppm concentrations, has been calculated as 13.1±6.2 ppm. Except for a few stations, it has been observed to be below the earth crust reference value. Although in small amounts, Arsenic (As) is an Ms found in earth crust all over the world. Anthropogenic activities play a role in the distribution of As pollution. It is mostly used in wood preservatives and pesticides [31]. In the study, As concentrations have been found between 8.1 and 10.6 ppm. Its mean value has been calculated as 9.4±0.7 ppm. It has been observed to be lower than the earth crust reference value.

Molybdenum (Mo) is a metal that is naturally found in sediment and rocks, however, it has harmful effects when in high concentrations [32]. Mo can be absorbed by Al, Fe and Mn under acidic conditions and precipitated with cations such as Pb, Mn, Zn, and Cu [33]. While the mean Mo has been found to be 0.48±0.12 ppm in the study, it has been found in the range of 0.28-0.67 ppm throughout the lake. This amount is a lot less than the earth crust reference value. Cadmium (Cd) is a highly toxic and non-essential Ms for organisms [9]. Its toxic effect may increase with other Ms such as Zn [34]. In the study, the Cd concentration range has been found to be between 0.05-0.18 ppm, while the mean concentration has been calculated as 0.09 ppm. It is quite low compared to the earth crust reference data as well.

The result of the Ms has been compared with the limit values (Table 4). All the calculated metal(loid) values have been found to be below the Probable Effect Level (PEL). Only As and Cu values have been observed to exceed the Threshold Effect Level (TEL) value, and Ni, at the TEL limit value. Therefore, no toxic effects of Ms other than As, Cu and Ni are expected in the lake, and the effect of these Ms have been determined to be rare (Table 3) [35].

TABLE 4. Ms values and limit values in sediment

	Al	**As**	**Cd**	**Co**	**Cr**	**Cu**	**Fe**	**Mn**	**Mo**	**Ni**	**Pb**	**Zn**
Mean	368.1	9.41	0.091	16.25	24.17	58.08	536.1	1217	0.476	18.83	13.05	85.12
Min	247	8.1	0.05	10.9	8.1	46.87	351	991	0.28	8.9	7.77	72.1
Max.	457	10.6	0.18	24.6	40.1	71.52	682	1675	0.67	43.3	24.64	94.1
Std. Dev.	63.6	0.77	0.05	4.10	12.12	6.79	86.1	172.9	0.12	12.8	6.24	6.41
PEL	X	17.00	3.53	X	90.00	197.00	X	X	X	36.00	91.30	315.00
ERM		85.00	9.00		145.00	390.00				50.00	110.00	270.00
TEL		5.9	0.60		37.30	35.70				18.00	35.00	123.00
ERL		33.00	5.00		80.00	70.00				30.00	35.00	120.00
Earth Crust	80000	13.00	0.30	19.00	90.00	45.00	47200	850.00	2.6	68.00	20.00	95.00

Ms with the potential of toxic effects in the lake are As (26.6%), Ni (25.7%), Cu (14.2%), Zn (13.0%) and Cr (12.9%), respectively. Studies supporting this result are available in the literature [5, 36]. Although the rates seem high, they are not highly risky for the lake and CF supported this result. The CF value is one of the most important indexes to observe the time-dependent increase of an Ms in the sediment and to evaluate the Ms [9,37]. This index has been used by many researchers studying metal(loid) pollution in sediment [5, 25, 38, 39]. The CF values of Al, As, Cd, Co, Cr, Fe, Mo, Ni, Pb, and Zn have been calculated to be less than 1. Therefore, the effect of these Ms on the lake is low contamination. The CF value of Cu and Mn is higher than 1, and its effects have been observed to be moderate contamination (Table 5). Thus, Cu and Mn indicate a moderate pollution, while other Ms's potential to pollute is low.

However, according to EF data, it has been observed that there is extremely severe enrichment in terms of As, Cd, Co, Cr, Cu, Mn, Ni, Pb and Zn (>50) in the lake. The enrichment of all these Ms indicates that the anthropogenic release in the lake is high. In the study Withanachchi et al. [40] conducted in Mashavera River (Georgia), they reported that the EF value of Cd metal was similarly extremely severe enrichment at some stations. Seifi et al. [41] determined the EF value of Pb, Cd and Zn metals as significant enrichment in sediment samples they collected from places close to the urban and industrial areas of the Persian Gulf. EF, which is an important contamination index, provides powerful data in determining the raw information of the studied wetland and conveying this information to the necessary authorities [42]. Therefore, it has been determined that if the Boraboy Lake's exposure to the anthropogenic effect is not dealt with, these Ms may create a high potential ecotoxicological risk for the lake in the future. Ms do not disappear in nature and tend to accumulate increasingly. Therefore, preventing continuous input to the lake is very important for the lake ecosystem. Cd, mCd and PLI are indexes used to evaluate the quality of a lake sediment and provide very important information about the quality of the lake [43]. When the Cd, mCd and PLI levels of all Ms are evaluated, it cannot be mentioned that the lake is polluted by the detected Ms (Table 5).

The toxic profile of the lake has been revealed through m-ERM-Q and m-PEL-Q data. According to the result of the m-ERM-Q index, the lake is at level 1, which is 9% of rate. This indicates that the toxicity level of Ms, which have accumulated up to today in the lake, for the organisms in the lake is 9%. According to the m-PEL-Q index, it has been concluded that the lake is moderately impacted. According to the Igeo index result, it has been concluded that the lake is practically uncontaminated. The indexes used, have indicated consistent results in evaluating the presence and accumulation of Ms in the sediment (Table 5).

When similar studies conducted recently in our country are examined, Cd accumulation has been observed to be a common and general problem just as in our study, most of which has been conducted in wetland. Şimşek et al. [3]

investigated the pollution caused by the metals they detected in the sediment of the creeks on the Samsun-Tekkeköy border in the north of Türkiye, through indexes such as EF, CF, PERI and Igeo. They determined that Cd metal, which is common in all creeks, is risky. Yüksel et al. [44] examined the pollution in the sediment of Çavuşlu creek in Giresun through indexes such as EF, Igeo, CF, and PLI. They also stated that the Cd metal was the greatest danger. Cüce et al. [4] examined the metal accumulation profile of the Ömerli Dam Lake sediment in İstanbul through the sediment quality indexes and pointed out that the Cd and Pb moderately enriched. Algül and Beyhan [45] studied metals in the Bafa Lake sediment using EF, CF and Igeo indexes. As a result, they revealed that the lake is contaminated by Ni and Cd metals, while Cu, Mn and Zn metals are included from natural resources. Of course, our wetlands, which are not only under Cd stress but also under other Ms stresses, have been revealed through many studies. In their study in Çubuk-2, Asartepe and Kesikköprü dam lakes, Fikirdeşici-Ergen et al. [5] drew attention to the accumulation of As and Ni Ms in all the three lakes. Metal determination study in a surface sediment made in the Tigris river, Igeo, CF, EF, and PLI indices were used. The results indicated that river sediment moderately polluted because of Co, Cu, Zn and Pb according Igeo [46]. In a study in which heavy metals were detected on the surface of 77 protected lakes in Poland, the amounts of Cr, Ni, Cd, Pb, Zn, and Cu and their ecological effects were examined. They determined that the lake sediment surfaces were contaminated with metals, and that Pb and Cd metals were higher than the background reference data. They reported that the lake surface sediments were also highly contaminated in terms of Pb and Cu, according to the EF and Igeo indexes [47]. Similar indices were used in a similar study on the surface sediment of Lake Manzala (Egypt) (Igeo, PLI etc.). As a result of the study, the researchers reported that the metals that cause the most stress in the sediment are Cd and Cu [48].

TABLE 5. The results of sediment quality indexes

	Al	**As**	**Cd**	**Co**	**Cr**	**Cu**	**Fe**	**Mn**	**Mo**	**Ni**	**Pb**	**Zn**
CF	0.005	0.72	0.30	0.86	0.27	1.29	0.01	1.43	0.18	0.28	0.65	0.90
Cd	6.90											
MCd	0.57											
EF	1.00	157.27	65.69	185.85	58.38	280.51	2.47	311.28	39.85	60.20	141.87	194.75
Igeo	-8.35	-1.05	-2.31	-0.81	-2.48	-0.22	-7.05	-0.07	-3.03	-2.44	-1.20	-0.74
PLI	0.354											
m-ERM-Q	0.18											
m-PEL-Q	0.30											
TTU	2.08											
TU		26.62	1.24		12.92	14.18				25.17	6.88	13.00

Correlation, cluster, and principal component analyzes have been employed to reveal the results and relationships of Boraboy Lake Ms. The strongest positive correlations have been observed among Cu-Fe (r=0.876), Cr-Ni (r=0.860), Mn-Zn (r=0.793), Cd-Pb (r=0.780), and negative correlations among Mo-Ni (r). = -0.737) and Co-Mo (r= -0.713) (Table 6). According to CA, the metals that are at the closest distance to each other are, (Cr-Ni (0.132) and Cu-Fe (3.66)), similar to the correlation. The farthest distances have been detected between metals that show negative correlation (Table 7, Figure 2). The PCA result also supports all these findings (Table 8, Figure 3). It indicates that Ms with positive correlations originate from common resources, while those with negative correlations do not have a common origin and also do not show similar behaviors during migration [49].

TABLE 6. Correlation of Ms in sediment

	Al	As	Cd	Co	Cr	Cu	Fe	Mn	Mo	Ni	Pb	Zn
Al	1.000											
As	.343	1.000										
Cd	.669**	.305	1.000									
Co	-.221	.533*	.013	1.000								
Cr	-.009	.391	.436	.721**	1.000							
Cu	-.079	.286	-.281	.269	-.243	1.000						
Fe	-.294	-.005	-.542*	.093	-.363	.876**	1.000					
Mn	.155	.615*	.210	.584*	.468	.450	.290	1.000				
Mo	.357	-.329	.054	-.713**	-.634*	.254	.366	-.184	1.000			
Ni	-.009	.583*	.446	.771**	.860**	-.121	-.347	.461	-.737**	1.000		
Pb	.665**	.213	.780**	-.048	.377	-.567*	-.692**	.214	-.104	.397	1.000	
Zn	.184	.536*	.106	.473	.248	.768**	.599*	.793**	.014	.314	-.054	1.000

TABLE 7. CA proximity matrix

	Al	As	Cd	Co	Cr	Cu	Fe	Mn	Mo	Ni	Pb	Zn
Al	0.000	20.489	13.367	37.983	18.855	31.884	37.313	30.586	16.581	17.994	13.298	26.224
As		0.000	16.768	14.808	13.199	20.349	26.875	14.230	35.578	12.546	15.380	12.811
Cd			0.000	20.697	1.806	39.774	48.441	24.325	37.490	1.467	.744	29.870
Co				0.000	14.009	20.376	24.299	9.457	45.635	15.057	20.155	15.101
Cr					0.000	39.575	46.717	20.476	43.370	.132	1.091	27.787
Cu						0.000	3.664	15.696	19.916	39.317	41.952	5.282
Fe							0.000	15.527	16.964	47.131	49.181	9.272
Mn								0.000	31.305	21.493	23.956	9.683
Mo									0.000	43.319	39.582	25.430
Ni										0.000	.862	27.855
Pb											0.000	30.272
Zn												0.000

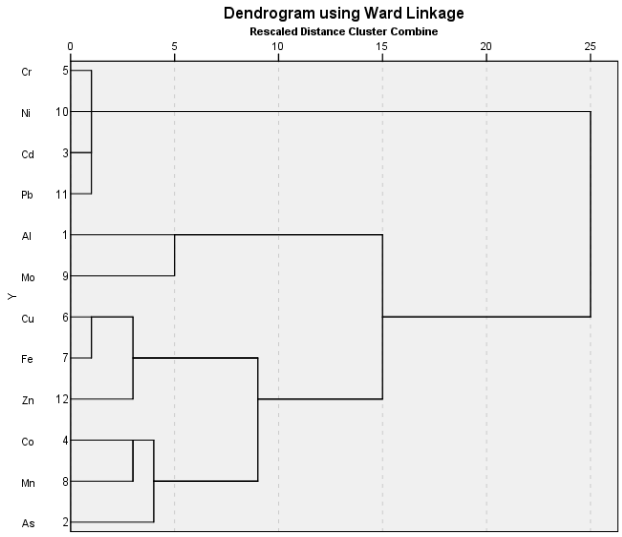

FIGURE 2. PCA analysis of Ms in the lake sediment

TABLE 8. PCA Rotated Component Matrix

	1	2	3
Al	.534	.039	.806
As	.521	.651	-.028
Cd	.969	-.024	.039
Co	.300	.569	-.704
Cr	.966	.074	-.221
Cu	-.463	.812	.095
Fe	-.736	.671	.042
Mn	.152	.800	-.242
Mo	-.414	.064	.836
Ni	.976	.066	-.188
Pb	.994	-.040	-.006
Zn	-.053	.945	.065

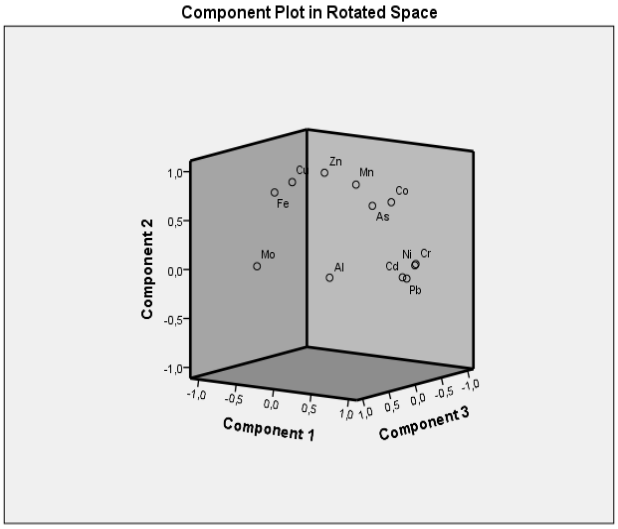

FIGURE 3. Cluster analysis of Ms in the lake sediment

4. CONCLUSIONS

The accumulation profile of metalloids in the sediment of Boraboy Lake has been investigated. The results have shown that there is a very high enrichment in the lake in terms of As, Cd, Co, Cr, Cu, Mn, Ni, Pb and Zn. Additionally, As, Ni and Cu have been determined to be the ones with the highest potential to have a possible toxic effect for the lake. Despite all these results, it would not be correct to speak of any accumulation in the lake. Therefore, it is very important to control the lake regularly in order to prevent the accumulation that this enrichment will create.

Acknowledgment. I am grateful to Prof. Dr. Ahmet Altındağ (Ankara University, Türkiye) for his valuable contributions.

Declaration of Competing Interests The authors declare no conflict of interest.

REFERENCES

[1] Shafie, N.A., Aris, A.Z., Zakaria, M.P., Haris, H., Lim, W.Y., Isa, N.M., Application of geoaccumulation index and enrichment factors on the assessment of heavy metal pollution in the sediments. *Journal of Environmental Science and Health, Part A*, 48 (2013), 182–190. https://doi.org/10.1080/10934529.2012.717810.

[2] Looi, L.J., Aris, A.Z., Yusoff, F.M., Isa, N.M., Haris, H., Application of enrichment factor, geoaccumulation index, and ecological risk index in assessing the elemental pollution status of surface sediments. *Environmental Geochemistry and Health,* 41(1) (2019), 27-42. https://doi.org/10.1007/s10653-018-0149-1.

[3] Şimşek, A., Özkoç, H.B., Bakan, G., Environmental, ecological and human health risk assessment of heavy metals in sediments at Samsun-Tekkeköy, North of Turkey. *Environmental Science and Pollution Research,* 29(2) (2022), 2009-2023. https://doi.org/10.1007/s11356-021-15746-w.

[4] Cüce, H., Kalipci, E., Ustaoğlu, F., Dereli, M.A., Türkmen, A., Integrated spatial distribution and multivariate statistical analysis for assessment of ecotoxicological and health risks of sediment metal contamination, Ömerli Dam (Istanbul, Turkey). *Water, Air, & Soil Pollution,* 233(6) (2022), 1-21. https://doi.org/10.1016/j.ijsrc.2022.06.004

[5] Fikirdeşici-Ergen, Ş., Tekatlı, Ç., Gürbüzer, P., Üçüncü-Tunca, E., Türe, H., Biltekin, D., Kurtuluş, B., Tunca, E., Elemental accumulation in the surficial sediment of Kesikköprü, Çubuk II and Asartepe Dam Lakes (Ankara) and potential sediment toxicity. *Chemistry and Ecology*, 37(6) (2021), 552-572. https://doi.org/10.1080/02757540.2021.1902509.

[6] Barbieri, M., The importance of enrichment factor (EF) and geoaccumulation index (Igeo) to evaluate the soil contamination. *Geology & Geophysics,* 5(1) (2016), 1–4. http://dx.doi.org/10.4172/2381-8719.1000237.

[7] Şenol, E., Boraboy Lake (Amasya) and around's major problems based from recreational use. *Doğu Coğrafya Dergisi*, 23(39) (2018), 95-112. https://doi.org/10.17295/ataunidcd.412503.

[8] Turekian, K.K., Wedepohl, K.H., Distribution of the elements in some major units of the earth's crust. *Geological Society of America Bulletin,* 72 (1961), 175-192. https://doi.org/10.1130/0016-7606(1961)72[175:DOTEIS]2.0.CO;2.

[9] Hakanson, L., An ecological risk index for aquatic pollution control - a sedimentological approach. *Water Research,* 14(8) (1980), 975–1001. https://doi.org/10.1016/0043-1354(80)90143-8.

[10] Abrahim, G.M.S., Parker, R.J., Nichol, S.L., Distribution and assessment of sediment toxicity in Tamaki Estuary, Auckland, New Zealand. *Environmental Geology*, 52(7) (2007), 1315-1323. https://doi.org/10.1007/s00254-006-0570-0.

[11] Tomlinson, D.L., Wilson, J.G., Harris C.R., Jeffrey, D.W., Problems in the assessment of heavy-metal levels in estuaries and the formation of a pollution index. *Helgoländer Meeresuntersuchungen*, 33(1-4) (1980), 566-575. https://doi.org/10.1007/BF02414780.

[12] Hasan, A.B., Kabir, S., Reza, A.S., Zaman, M.N., Ahsan, A., Rashid, M., Enrichment factor and geo-accumulation index of trace metals in sediments of the ship breaking area of Sitakund Upazilla (Bhatiary-Kumira), Chittagong, Bangladesh. *Journal of Geochemical Exploration*, 125 (2013), 130-137. https://doi.org/10.1016/j.gexplo.2012.12.002.

[13] Müller, G., Index of geoaccumulation in sediments of the Rhine River. *GeoJournal,* 2 (1969), 108-118.

[14] Carr, S.R., Chapman, D.C., Long, E.R., Windom, H.L., Thursby, G., Sloane, G.M., Wolfe, D.A., Sediment quality assessment studies of Tampa Bay, Florida. *Environmental Toxicology and Chemistry: An International Journal*, 15(7) (1996), 1218-1231. https://doi.org/10.1002/etc.5620150730.

[15] Oldham, V.E., Mucci, A., Tebo, B.M., Luther, G.W., Soluble Mn(III)–L complexes are abundant in oxygenated waters and stabilised by humic ligands. *Geochimica et Cosmochimica Acta*, 199 (2017), 238–246. https://doi.org/10.1016/j.gca.2016.11.043.
[16] Delfino, J.J., Bortleson, G.C., Lee, G.F., Distribution of Mn, Fe, Mg P, K, Na, and Ca in the surface sediments of Lake Mendota, Wisconsin. *Environmental Science & Technology*, 3 (1969), 1189–1192. https://doi.org/10.1021/es60034a006.
[17] Neubauer, E., Kohler, S.J., von der Kammer, F., Laudon, H., Hofmann, T., Effect of pH and stream order on iron and arsenic speciation in Boreal Catchments. *Environmental Science & Technology*, 47(13) (2013), 7120–7128. https://doi.org/10.1021/es401193j.
[18] Boyle, J.F., Inorganic geochemical methods in palaeolimnology. In: *Tracking environmental change using lake sediments*, Springer, Dordrecht, (2002) 83-141.
[19] Davison, W., Iron and manganese in lakes. *Earth-Science Reviews*, 34(2) (1993), 119-163. https://doi.org/10.1016/0012-8252(93)90029-7.
[20] Kotowski, M., Saczuk, M., Aluminium in water and soil environment. *Ekoinzynieria*, 2 (1997), 22–29.
[21] Wetzel, R.G., Limnology, Lake and River Ecosystems. Academic Press: London, UK, 2001.
[22] John, S.G., Park, J.G., Zhang, Z., Boyle, E.A., The isotopic composition of some common forms of anthropogenic zinc. *Chemical Geology*, 245(1-2), (2007), 61-69. https://doi.org/10.1016/j.chemgeo.2007.07.024.
[23] Bojakowska, B., Krasuska, J., Copper and other trace elements in sediments of lakes near Konin (Poland). *Journal of Elementology*, 19(1) (2014), 31-40. https://doi.org/10.5601/jelem.2014.19.1.589.
[24] Varol, M., Şen, B., Assessment of nutrient and heavy metal contamination in surface water and sediments of the upper Tigris River, Turkey. *Catena*, 92 (2012), 1-10. https://doi.org/10.1016/j.catena.2011.11.011.
[25] Rahman, M.S., Ahmed, Z., Seefat, S.M., Alam, R., Islam, A.R.M.T., Choudhury, T.R., Begum, B.A., Idris, A.M., Assessment of heavy metal contamination in sediment at the newly established tannery industrial estate in Bangladesh: a case study. *Environmental Chemistry and Ecotoxicology*, 4 (2022), 1-12. https://doi.org/10.1016/j.enceco.2021.10.001.
[26] Kastratović, V., Jaćimović, Ž., Bigović, M., Đurović, D., Krivokapić, S., The distribution and accumulation of chromium in the water, sediment and macrophytes of Skadar lake. *Kragujevac Journal of Science*, 38 (2016), 125-134. https://doi.org/10.5937/KgJSci1638125K.
[27] Alkan, A., Alkan, N., Aktaş, M., Comparison of Ni enrichment and background concentrations in the Southeastern Black Sea sediments. *Environmental Forensics*, 22(3-4) (2021), 364-371. https://doi.org/10.1080/15275922.2020.1850559.
[28] Hamilton, E.I., The geobiochemistry of cobalt. *Science of The Total Environment*, 150(1-3) (1994), 7-39. https://doi.org/10.1016/0048-9697(94)90126-0.
[29] Todorović, Z., Polić, P., Đorđević, D., & Antonijević, S., Lead distribution in water and its association with sediment constituents of the" Barje" lake (Leskovac, Yugoslavia). *Journal of The Serbian Chemical Society*, 66(10) (2001), 697-708.
[30] Rahman, Z., Singh, V.P., The relative impact of toxic heavy metals (THMs) (arsenic (As), cadmium (Cd), chromium (Cr) (VI), mercury (Hg), and lead (Pb)) on the total environment: an overview. *Environmental Monitoring and Assessment*, 191(7) (2019), 419. https://doi.org/10.1007/s10661-019-7528-7

[31] Masuda, H., Arsenic cycling in the Earth's crust and hydrosphere: interaction between naturally occurring arsenic and human activities. *Progress in Earth and Planetary Science,* 5(1) (2018), 1-11. https://doi.org/10.1186/s40645-018-0224-3.

[32] Kabata –Pendias, A., Mukherjee, A., Trace Elements from Soil to Human. Springer-Verlag Berlin, Heidelberg, 2007.

[33] Fu, J., Hu, X., Tao, X., Yu, H., Zhang, X., Risk and toxicity assessments of heavy metals in sediments and fishes from the Yangtze River and Taihu Lake, China. *Chemosphere*, 93 (2013), 1887–95. https://doi.org/10.1016/j.chemosphere.2013.06.061.

[34] Rzętała, M.A., Cadmium contamination of sediments in the water reservoirs in Silesian Upland (Southern Poland). *Journal of Soils and Sediments,* 16(10) (2016), 2458-2470. https://doi.org/10.1007/s11368-016-1477-3

[35] Enuneku, A., Omoruyi, O., Tongo, I., Ogbomida, E., Ogbeide, O., Ezemonye, L., Evaluating the potential health risks of heavy metal pollution in sediment and selected benthic fauna of Benin River, Southern Nigeria. *Applied Water Science,* 8(8) (2018), 1-13. https://doi.org/10.1007/s13201-018-0873-9.

[36] Tunca, E., Aydın, M., Şahin, Ü.A., An ecological risk investigation of marine sediment from the northern Mediterranean coasts (Aegean Sea) using multiple methods of pollution determination. *Environmental Science and Pollution Research,* 25(8) (2018), 7487-7503. https://doi.org/10.1007/s11356-017-0984-0.

[37] Ali, M.M., Ali, M.L., Islam, M.S., Rahman, M.Z., Preliminary assessment of heavy metals in water and sediment of Karnaphuli River, Bangladesh. *Environmental Nanotechnology, Monitoring & Management,* 5 (2016), 27–35. https://doi.org/10.1016/j.enmm.2016.01.002.

[38] Gülşen-Rothmund, H.İ., Avşar, Ö., Avşar, U., Kurtuluş, B., Tunca, E., Spatial distribution of some elements and elemental contamination in the sediments of Köyceğiz Lake (SW Turkey). *Environmental Earth Sciences,* 77(14) (2018), 1-24. https://doi.org/10.1007/s12665-018-7724-8.

[39] Saha, N., Rahman, M.S., Jolly, Y.N., Rahman, A., Sattar, M.A., Hai, M.A., Spatial distribution and contamination assessment of six heavy metals in soils and their transfer into mature tobacco plants in Kushtia district, Bangladesh. *Environmental Science and Pollution Research,* 23(4) (2016), 3414–3426. https://doi.org/10.1007/s11356-015-5575-3.

[40] Withanachchi, S.S., Ghambashidze, G., Kunchulia, I., Urushadze, T., Ploeger, A., Water quality in surface water: a preliminary assessment of heavy metal contamination of the Mashavera River, Georgia. *International Journal of Environmental Research and Public Health,* 15(4) (2018), 621. https://doi.org/10.3390/ijerph15040621.

[41] Seifi, M., Mahvi, A.H., Hashemi, S.Y., Arfaeinia, H., Pasalari, H., Zarei, A., Changani, F., Spatial distribution, enrichment and geo-accumulation of heavy metals in surface sediments near urban and industrial areas in the Persian Gulf. *Desalination and Water Treatment,* 158 (2019), 130-139.

[42] Caeiro, S., Costa, M.H., Ramos, T.B., Assessing heavy metal contamination in sado estuary sediment: an index analysis approach. *Ecological Indicators*, 5 (2005), 151–169. https://doi.org/10.1016/j.ecolind.2005.02.001.

[43] Islam, M.A., Romic, M.A., and Romic, M., Trace metals Accumulation in soil irrigated with polluted water and assessment of human health risk from vegetable consumption in Bangladesh. *Environmental Geochemistry and Health,* 40 (2017), 59–85. https://doi.org/10.1007/s10653-017-9907-8.

[44] Yüksel, B., Ustaoğlu, F., Tokatli, C., Islam, M.S., Ecotoxicological risk assessment for sediments of Çavuşlu Stream in Giresun, Turkey: association between garbage disposal facility and metallic accumulation. *Environmental Science and Pollution Research,* 29(12) (2022), 17223-17240. https://doi.org/10.1007/s11356-021-17023-2.

[45] Algül, F., Beyhan, M., Concentrations and sources of heavy metals in shallow sediments in Lake Bafa, Turkey. *Scientific Reports*, 10(1) (2020), 1-12. https://doi.org/10.1038/s41598-020-68833-2.

[46] Varol, M., Assessment of heavy metal contamination in sediments of the Tigris River (Turkey) using pollution indices and multivariate statistical techniques. *Journal of Hazardous Materials*, 195 (2011), 355- 364. https://doi.org/10.1016/j.jhazmat.2011.08.051.

[47] Sojka, M., Jaskuła, J., Barabach, J., Ptak, M., Zhu, S., Heavy metals in lake surface sediments in protected areas in Poland: concentration, pollution, ecological risk, sources and spatial distribution. *Scientific Reports,* 12(1) (2022), 1-16. https://doi.org/10.1038/s41598-022-19298-y.

[48] Redwan, M., Elhaddad, E., Heavy metal pollution in Manzala Lake sediments, Egypt: sources, variability, and assessment. *Environmental Monitoring and Assessment,* 194(6) (2022), 1-16. https://doi.org/10.1007/s10661-022-10081-0.

[49] Singh, H., Pandey, R., Singh, S.K., Shukla, D.N., Assessment of heavy metal contamination in the sediment of the River Ghaghara, a major tributary of the River Ganga in Northern India. *Applied Water Science*, 7(7) (2017), 4133-4149. https://doi.org/10.1007/s13201-017-0572-y.

http://communications.science.ankara.edu.tr

Commun.Fac.Sci.Univ.Ank.Ser. C Biology
Volume 32, Number 2, Pages 105-118 (2023)
ISSN 1303-6025 E-ISSN 2651-3749
DOI: 10.53447/communc.1281221

Research Article; Received: April 13, 2023; Accepted: June 24, 2023

THE MICROBIOTA OF LONG-LIVING AND CANCER-FREE BLIND MOLERAT (*Nannospalax xanthodon*) FROM THE EDGE OF ITS DISTRIBUTION IN NORTHERN ANATOLIA

HALİL MERT SOLAK[1], EFE SEZGİN[2], DAGMAR ČÍŽKOVÁ[3], JAKUB KREISINGER[4], FARUK ÇOLAK[1], ORTAÇ ÇETİNTAŞ[1] AND ALEXEY YANCHUKOV[1]

[1] Department of Biology, Faculty of Science, Zonguldak Bülent Ecevit University, Zonguldak, TÜRKİYE.
[2] Department of Food Engineering, Izmir Institute of Technology, Izmir, TÜRKİYE.
[3] Institute of Vertebrate Biology, Czech Academy of Sciences, Brno, CZECH REPUBLIC.
[4] Department of Zoology, Charles University, Prague, CZECH REPUBLIC.

ABSTRACT. The mammalian gut is colonized by microorganisms that affect development, immune system, energy metabolism, and reproduction. The majority of studies focused on laboratory or domestic animals in artificial setups, leaving the research focused on wild species underrepresented. The Anatolian Blind Molerat (hereafter ABMR), *Nannospalax xanthodon*, is a subterranean rodent that receives much attention due to its unique traits, such as tolerance to extreme hypoxic stress, resistance to cancer, and longer lifespan compared to similarly sized rodents. In this study, we characterize the gut microbiota of ABMR from its northernmost geographic distribution using 16S rRNA metabarcoding and compare our results with the microbiome characteristics of a few other ABMR populations studied previously, as well as other rodent species. The 16S rRNA barcode dataset revealed that approximately 90% of the ABMR gut microbiota comprises Firmicutes and Bacteriodota bacterial phyla, typical of most mammals. In addition, the ABMR gut microbiota has a high abundance of performance- and longevity-linked bacterial families. Overall, our results generally align well with the previous studies on blind molerats and emphasize the importance of studying the microbiome of natural populations.

1. INTRODUCTION

Microbial communities are integral to organism functioning in all mammals [1]. In animal-associated microbiota, the number of bacterial cells is more or less the same as the cell count of the host body [2]. Therefore, the effect of the gut microbiome, i.e. the microbial community occupying the gastrointestinal system, has a crucial role in the digestion, development, immunity, energetics, and fitness of animals [3–6].

The impact of gut microbiota on humans is a widely studied topic due to its association with various metabolic, autoimmune, and even psychological

Keywords. 16S rRNA, metabarcoding, microbiota, wild, rodent, molerats

mr.solak@hotmail.com- Corresponding author; 0000-0001-6877-9274
efeszgn0@gmail.com- 0000-0002-8000-7485
dejsha@seznam.cz- 0000-0001-5031-7792
jakubkreisinger@seznam.cz- 0000-0001-9375-9814
farukcolak@gmail.com- 0000-0003-3985-7864
ortaccetintas@gmail.com- 0000-0001-7601-2540
yawa33@gmail.com- 0000-0002-9613-8770

disorders [1,7,8]. The laboratory and domestic mammalian species serve as a good proxy model for this research, and there are many studies on their microbiota [9,10]. While studying captive animals is convenient, the effect of captivity conditions on microbiota composition cannot be ignored [11–14]. Besides the effect of captivity, the laboratory animal models often lack heterogeneity compared to their wild equivalents. Moving wild mice into a captive facility for a year dramatically changed the composition of the microbiota and made it more homogenous compared to the more diverse microbiota profiles observed in the wild [15]. Another study compared wild-caught with wild-derived, inbred strains of the house mouse (*M. musculus*) and found that approximately 16% of the bacteria differ between the wild and the inbred mice [16]. Therefore, using wild animals is crucial for understanding the ecological importance of the gut microbiome and revealing the details of the interactions among the host, the microbiome, and the environment that have been shaped by evolution during the course of their mutual coexistence [17–19].

The cause of differences in gut microbiota among individuals, groups, populations, and species is a topic of much interest. While the overall difference in microbiota is the largest at the species level [19], there is still a big room for questioning the within-species variation of microbiota [20] [15,20,21]. The Anatolian Blind Molerat (ABMR) *Nannospalax xanthodon* is a species of murid rodent that possesses many unique adaptations to obligate subterranean lifestyle. The AMBR is successful ecologically, as it is found from the sea level in the Aegean (warm Mediterranean climate) to the highlands of Taurus and Eastern Anatolian mountains (harsh cold alpine climate). The ABMR is in fact a taxonomic complex of multiple, cytogenetically distinct, and potentially genetically isolated geographic populations [22]. With its wide distribution range and potentially genetically isolated geographic populations living in different ecological conditions, the AMBR is a suitable model to study the within-species variation of microbiome composition. Besides its wide distribution range, the Blind Molerats have unique physiological traits such as resistance to extreme hypoxia and hypercapnia underground [23], resistance to cancer [24,25], and longer life span (~20 years) compared to similar sized rat [26]. These traits highlight the importance of intensive biomedical and ecophysiological research on Blind Molerats, including the microbiome.

In this pilot study, we aim to characterise the gut microbiome of wild ABMR in its two northernmost populations in Türkiye using 16S rRNA amplicon sequencing. Since the *Nannospalax* superspecies has a complex evolutionary history and is represented by multiple, cytogenetically distinct, and potentially genetically isolated geographic populations, studying the microbiota can help to understand the ecological difference between these species. Therefore, we aim to compare our results with a few previous studies on the Blind Molerat microbiome.

2. MATERIALS AND METHODS

2.1. Sampling

We captured three ABMR individuals: two in Ağlı and one in Taşköprü, Northern Türkiye, in July 2020 (Figure 1 and Table 1). The distance between the two populations is ~50 km. The genus *Nannospalax* is known for its complex taxonomy with numerous cytogenetic (=chromosomal) races distributed parapatrically in Anatolia. The Ağlı population studied here belongs to the "Kastamonu" cytotype (2N=60) and the Taşköprü population was designated as the "Taşköprü" cytotype (2N=58) in [22, 27]. Animals were captured alive by the hoe technique as described in [28]. We recorded the body mass and sex of the animals. We then dissected the animals, collected the caecum tissue, stored it in EtOh, and placed the sample to -80°C freezer next day. The procedure was approved by the Animal Ethics committee of Bülent Ecevit University (#91330202).

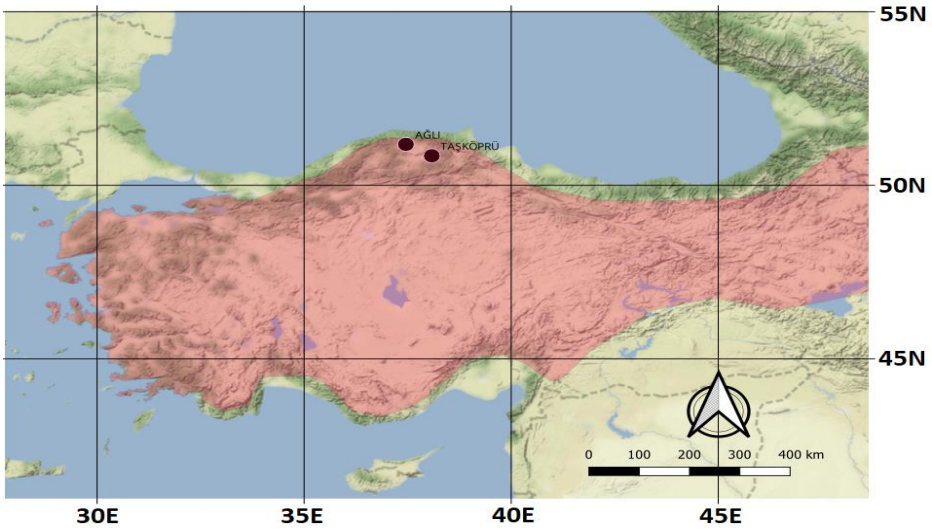

FIGURE 1. The distribution of ABMR and sampling locations. The red-shaded area represents the distribution range of *Nannospalax xanthodon* superspecies.

TABLE 1. List of frozen gut samples used in the study.

Sample	Population	Sex	Mass (gr)	Date of Collection	Latitude	Longitude
AGL1	Ağlı	female	161	03.07.2020	41.7139	33.6529
AGL2	Ağlı	female	212	03.07.2020	41.7139	33.6529
TAS1	Taşköprü	female	229	04.07.2020	41.4922	34.2147

2.2. DNA preparation and amplification

A small piece at the terminal end of the caecum (~5 g) was cut from the frozen sample with a flame-sterilised scalpel and used for DNA extraction. Whole metagenomic DNA was extracted from the caecum samples using DNEasy PowerSoil Kit (Qiagen, Cat No:47014).

The V3–V4 variable region in the bacterial 16S rRNA gene was amplified using the universal primers S-D-Bact-0341-b-S-17 (5'-CCTACGGGNGGCWGCAG-3') and S-D-Bact-0785-a-A-21 (5'-GACTACHVGGGTATCTAATCC-3') [29]. We used Q5 High Fidelity DNA polymerase (NEB, Cat No: M0491S) to perform the PCR in 20 ul reaction volumes, with the following cycling conditions: initial denaturation at 98 °C for 5 min, 30 cycles of 98 °C (15 s), 55 °C for 20 s and 72 °C for 40 s and a final extension at 72 °C for 5 min. The PCR products were run in 1.5% agarose gel to evaluate the product quality and successfully amplified bands were purified using MiniElute Gel Extraction Kit (Qiagen, Cat No:28604). Then, PCR products were pooled according to the equimolar concentrations of each sample. The final pool was loaded on Pippin Prep automatic size selection system (Sage Science) targeting the amplicon size window of 350 - 550 bp.

Each sample was amplified and genotyped twice (in duplicates) to account for the effect of possible amplification stochasticity. In the following analyses, the data from duplicates are treated as individual samples. After that, the dual-indexed sequencing adaptors were ligated using a TruSeq nano DNA library preparation kit (Illumina), and the resulting amplicon libraries were outsourced for sequencing using the Illumina MiSeq instrument, Reagent Kit v2 (2 x 300 bp) at CEITEC Genomics Core Facility (Brno, Czech Republic).

2.3. Bioinformatics analysis

The raw sequencing data were trimmed and demultiplexed using Skewer and reads with low quality were eliminated by setting the expected error rate per paired-end read >1 [30]. The bacterial 16s rRNA haplotypes (Amplicon Sequence Variants, hereafter ASVs) were quality checked, identified, and analyzed using the software DADA2 [31]. Software UCHIME [32] was used for the identification and removal of sequence chimeras. The gold.fna (available at: https://drive5.com/uchime/gold.fa) database is used as a reference for chimera filtering. Silva database version 138.1 (updated in March 2021, [33] was used as a reference in DADA2 software [31]. Finally, *phyloseq* [34] package in R (version 4.2) was used to create a database that contains the OTU table, OTU sequences, taxonomic annotations, and phylogeny of bacterial OTUs.

2.4. Statistical analysis

The microbiome database comprised 61274 high-quality sequences grouped in 4841 non-chimeric OTUs. PROTEST (Procrustes Rotation of Two

Configurations in R package *vegan*) was used to compare duplicates. We used the observed number of OTUs, the Shannon index, and the Simpson index to estimate alpha diversity via the estimate_richness command in the phyloseq package in R. Because Taşköprü population was represented by only one sample, we used duplicates of each sample as pseudo-samples to calculate beta diversity. The Bray-Curtis dissimilarity index was used to calculate the divergence in microbiota composition between samples. Then, we applied PERMANOVA (adonis2 function from the *vegan* R package) to test the difference between the gut microbiota composition of samples.

3. RESULTS

We successfully genotyped the 16S rRNA amplicons from three ABMR caecum samples. After quality filtering, the numbers of reads per sample were 20421, 20426, and 20427 in samples TAS1, AGL2, and AGL1, respectively. PROTEST showed no significant difference between duplicates (number of permutations= 999; p-value=0.001).

The bacteriome database was dominated by Firmicutes (50% of all reads), Bacteriodota (39%), and Desulfobacterota (2%) (Figures 2 and 3A). At the family level, the data was dominated by Muribaculaceae (35%), Lacnospiraceae (28%), Oscillospiraceae (12%), Ruminococcaceae (7%), Desulfovibrionaceae (3%), Christensenellaceae (1%), and Rikenellaceae (1%) (Figure 3B). The bacterial phyla or families with less than 1% abundance were grouped into a "remainder" category.

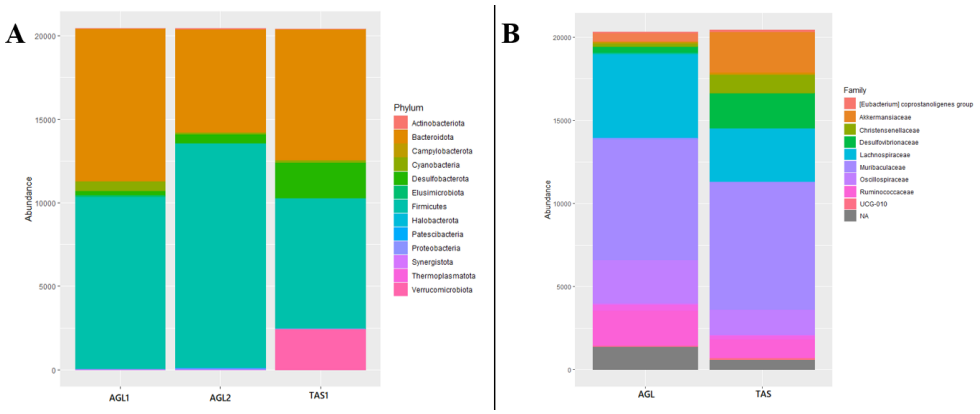

FIGURE 2. Relative abundance of bacterial phyla by sample.

We observed higher relative abundances of Bacteroidota, Firmicutes, and Cyanobacteria in Ağlı compared to Taşköprü. Conversely, Taşköprü exhibited higher relative abundances of Desulfobacterota and Verrucomicrobiota (Figure 2). At the bacterial family level, the relative abundances of Lachnospiraceae, UCG-010, and Ruminococcaceae were higher in Ağlı, while the relative

abundances of Akkermansiaceae, Christensenellaceae, Desulfovibrionaceae, and Muribaculaceae were higher in Taşköprü (Figure 2B).

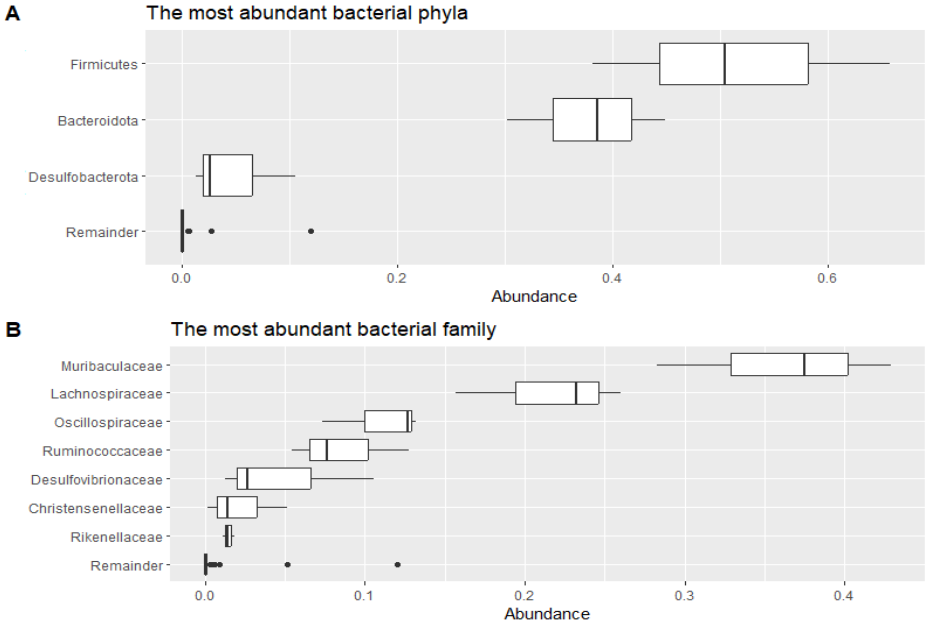

FIGURE 3. **A:** The most abundant bacterial phyla and **B:** The most abundant bacterial families for all samples together (X-axis represents % of the abundance of all read and "remainder" represents the taxa with <1% abundance).

We estimated the alpha diversity by using (i) the exact number of observed OTUs, (ii) the Shannon index, and (iii) the Simpson index. With a higher number of observed OTUs and higher values of Shannon and Simpson index values, all the alpha diversity indexes showed that samples from Ağlı have more diverse microbiota compared to the Taşköprü (Table 2). The relative abundance-based Bray-Curtis index values are used to calculate the difference in gut microbiota difference. On the PCoA plot based on the Bray-Curtis index, the first axis showed a clear separation of populations (Figure 4), however, the PERMANOVA test p-value was only marginally significant (permutation: 999 and p-value: 0.06).

TABLE 2. Variation in gut bacteriome diversity between samples.

Sample ID	Observed number of OTUs	Shannon index	Simpson index
AGL1	232	4.772	0.986
AGL2	235	4.834	0.985
TAS1	191	4.271	0.967

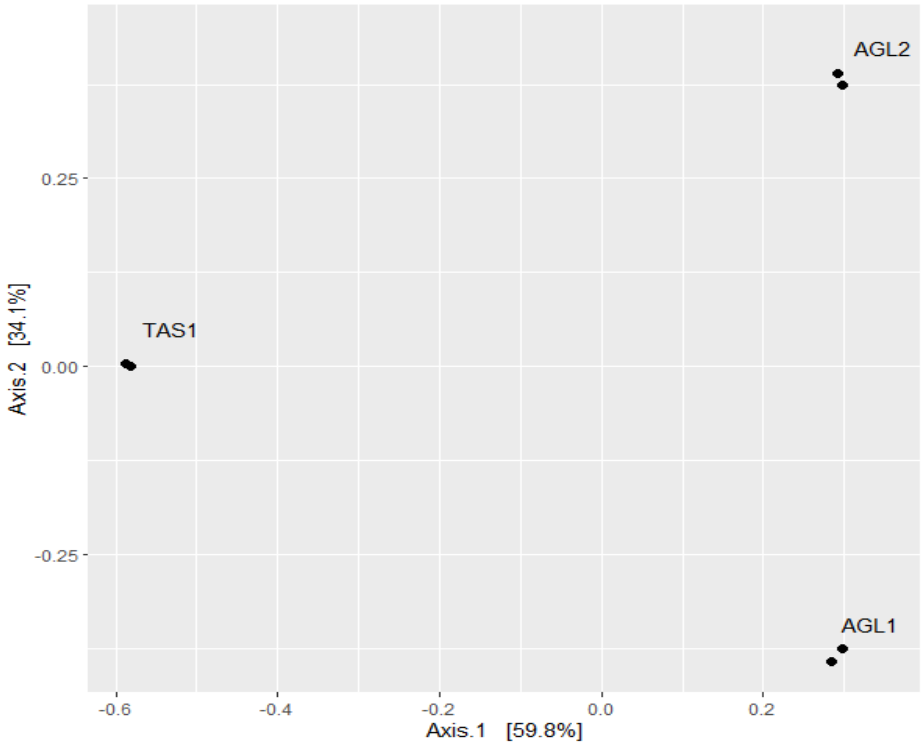

FIGURE 4. Principal Coordinate Analysis (PCoA) ordination of gut microbiota composition divergence between samples (based on the Bray-Curtis index).

4. DISCUSSION

In this study, we characterised the gut microbiota of wild-caught ABMRs from two populations in North Anatolia. We investigated the bacterial diversity of the ABMR microbiota at the class, phylum, and family levels. Taxonomic assignment of the 16S rRNA sequences revealed the most abundant bacterial classes: Clostridia (50%), Bacteroidia (38%), and Desulfovibrionia (2%). At the level of phyla, approximately 90% of the ABMR gut microbiota was dominated by Firmicutes and Bacteriodota (Figure 3A). These are typical components of mammalian microbiota and play a role in various processes, such as immune regulation, metabolism, and storage of fat [35–39].

The Desulfobacterota was the third most abundant phylum in our dataset, more abundant (~12%) in Taşköprü compared to Ağlı (~5%). While the Taşköprü population is represented by only one sample, we used duplicates as pseudo-samples and calculated dissimilarity using the relative abundance-based Bray-Curtis index. The difference in the gut microbiome composition between populations was only marginally above the significance level, which may be attributed to reduced test power caused by the small sample size. The differences between the locations (ie. relative abundances of bacterial phyla and alpha

diversity) could have been caused by differences in soil, climate, diet, vegetation, or host genetics. The effect of these factors on the animal microbiome has been discussed in many studies [40–43]. Further investigations are necessary to explore the intriguing variations in the relative abundances of bacterial taxa observed between populations. To gain a better understanding of these changes, it is important to conduct more extensive sampling across a broader range of geographical areas and consider the influence of multiple environmental factors. Additional efforts in these areas could shed light on the potential explanations for these observed differences.

TABLE 3. Comparison of the relative abundance of bacterial phyla between studies (Desulfobacterota is a synonym for Proteobacteria). N represents the sample size for each study. C (=caecal), F (=fecal), and GI (=gastrointestinal) represent the source of microbiota. *The study by Sibai et al. (2020) documented the change in fecal microbiome composition over a 1–2-month period, therefore the results are presented as a range of % values.

Study	Species	*N*	source	Relative abundance of most abundant bacterial phyla (%)			
				Firmicutes	Bacteriodota	Desulfobacterota	Actinobacteria
This study	*N. xanthodon*	3	C	50	39	2	>1
Kuang et al. 2022	*N. ehrenbergi*	12	C	59.6	10.7	17.4	7.6
Sibai et al. 2020 *	*N. xanthodon*	34	F	~31-32	~50-65	~12	>1
Weldon et al. 2015	*M. musculus*	39	C	68	22	1	NA
Kreisinger et al. 2015	*A. flavicollis*	15	GI	67	27	4	>1
Debebe et al. 2017	*H. glaber*	35	F	40.8	38.8	2.6	2.7

Previously, Sibai et al. [44] examined faecal and skin microbiomes of AMBR sourced from geographically close populations 140 km SW of Ağlı and Taşköprü (Gerede, Bolu province). Regardless of the distance between sampling locations, our samples belong to the "Kastamonu" (2N=60) and the "Taşköprü" (2N=58) cytotypes, while they used another chromosomal race of *N. xanthodon* named "Abant" cytotype (2N=52) by [22]. In addition, the animals used in Sibai et al. [44] were housed in captivity for several weeks prior to metabarcoding, and even then showed a progressive temporal change of microbiome composition in a series of samples taken over the course of 1-2 months. In our study, the sampling of gut content was performed on the same day the animals were captured, therefore our results represent a snapshot of the actual microbiome composition in the wild. A comparison of our results with the above-mentioned study showed that the three main bacterial phyla (Firmicutes, Bacteriodota, and Desulfobacterota) were always the most abundant. Even though Sibai et al. used the same species (*N. xanthodon*) with different chromosomal races, Bacteriodota was more abundant in their study compared to Firmicutes. Rather than a different evolutionary history of the hosts, different sampling seasons may also explain the differences in the relative abundance of the phyla. Another study of closely

related Blind Molerat species (*N. ehrenbergi*) showed the exact same order of the most abundant phyla, while the relative abundances of the phyla are slightly different [45] (Table 3). The same three bacterial phyla dominate the microbiota of other rodents, such as house mice [17,46], rats [47], and naked molerats [18,48].

At the family level, Muribaculaceae (phylum Bacteriodota) and Lachnospiraceae (phylum Firmicutes) were the most common bacterial families in all samples, 35% and 28% respectively (Figure 3B). While bacteria from the Lachnospiraceae family have numerous functions, they share a few common roles in the maintenance of gut health, act as active degraders of plant material in the gut [49], and take a role in butyrate production [50]. The Muribaculaceae family contributes to propionate, succinate, and acetate production [51,52]. Interestingly, the possible role of the Muribaculaceae family on extended life span was discussed by [44]. It should be noted, however, that Muribaculaceae also has a high abundance in short-living rodents [47,53,54] and other (possibly long-living) members of the family Spalacidae [55]. The association of this family with the host longevity thus deserves a more thorough and focused study.

The bacterial phyla Oscillospiraceae (phylum Firmicutes) and Ruminococcus (phyla Firmicutes) were the third and fourth most abundant phyla with 12% and 7% abundance, respectively. While [44] reported that these bacterial families comprised >5% of their data too (Oscillospiraceae used to categorise under Ruminococcus), [45] did not mention the abundance of bacterial families in their study. Together with the second most abundant bacterial family Lachnospiraceae, Oscillospiraceae, and Ruminococcus were found to be abundant in performance-associated hosts such as human athletes and racehorses [56,57]. Overall, the ABMR caecum microbiome is comparable to that of several other terrestrial rodents (Table 3).

A deeper investigation of the multiple functions of ABMR microbiome could provide better insight into its role in the extreme physiology of this unique animal species.

In conclusion, this study investigated the gut microbiome of ABMRs in two populations from the edge of its distribution in Northern Anatolia. The results revealed that the ABMR gut microbiota is dominated by Firmicutes, Bacteroidota, and Desulfobacterota, which aligns well with previous studies on closely related species and other rodent species, albeit with slight differences in the relative abundances of bacterial taxa. Alpha diversity analysis indicated that the microbiota of the Ağlı population is more diverse than that of Taşköprü. However, the differences in microbiota composition between populations were only marginally significant, possibly due to the small sample size. Therefore, further research with larger sample sizes and consideration of environmental factors is necessary to gain a better understanding of the factors influencing the variations in the ABMR gut microbiome. The findings of this study contribute to the knowledge of within-species variation of microbiota and underscore the

importance of using wild animal models to study the ecological significance of the gut microbiome.

Acknowledgment This study was supported by TÜBİTAK grant 220Z032, and the collection of samples was funded by TUBITAK 119Z400. DC and JK were supported by Czech Science Foundation (19-19307S). The numerical calculations reported in this paper were partially performed at TÜBİTAK ULAKBİM, High Performance and Grid Computing Center (TRUBA resources). This study is a part of the Ph.D. dissertation by HMS, supervised by AY and JK.

Author Contribution Statements HMS, AY, and ES designed the study, and HMS drafted the manuscript. FÇ and AY performed the sampling. HMS, JK, DC, and OÇ performed laboratory analyses and HMS, JK, and DC performed data analyses. AY, ES, JK, and DC secured the funding. All authors provided helpful comments and recommendations and approved the final version of the manuscript.

Declaration of Competing Interests The authors declare no conflict of interest.

Data availability The bacteriome 16S rRNA dataset is available at the European Nucleotide Archive under the accession number of the study PRJEB61312 and the accession numbers for the samples are ERS14903192-ERS14903197.

REFERENCES

[1] Lin, L., Zhang, J., Role of intestinal microbiota and metabolites on gut homeostasis and human diseases. *BMC Immunology*, 18 (1) (2017), 2. https://doi.org/10.1186/s12865-016-0187-3.

[2] Sender, R., Fuchs, S., Milo, R., Revised estimates for the number of human and bacteria cells in the body. *PLoS Biology*, 14 (8) (2016), e1002533. https://doi.org/10.1371/journal.pbio.1002533.

[3] Knight, R., Callewaert, C., Marotz, C., Hyde, E.R., Debelius, J.W., McDonald, D., Sogin, M.L., The microbiome and human biology. *Annual Review of Genomics and Human Genetics*, 18 (2017), 65–86. https://doi.org/10.1146/annurev-genom-083115-022438.

[4] Lindsay, E.C., Metcalfe, N.B., Llewellyn, M.S., The potential role of the gut microbiota in shaping host energetics and metabolic rate. *The Journal of Animal Ecology*, 89 (11) (2020), 2415–2426. https://doi.org/10.1111/1365-2656.13327.

[5] McFall-Ngai, M., Hadfield, M.G., Bosch, T.C.G., Carey, H.V., Domazet-Lošo, T., Douglas, A.E., Dubilier, N., Eberl, G., Fukami, T., Gilbert, S.F., Hentschel, U., King, N., Kjelleberg, S., Knoll, A.H., Kremer, N., Mazmanian, S.K., Metcalf, J.L., Nealson, K., Pierce, N.E., Rawls, J.F., Reid, A., Ruby, E.G., Rumpho, M., Sanders, J.G., Tautz, D., Wernegreen, J.J., Animals in a bacterial world, a new imperative for the life sciences. *Proceedings of the National Academy of Sciences of the United States of America*, 110 (9) (2013), 3229–3236. https://doi.org/10.1073/pnas.1218525110.

[6] Suzuki, T.A., Links between Natural Variation in the Microbiome and Host Fitness in Wild Mammals. *Integrative and Comparative Biology*, 57 (4) (2017), 756–769. https://doi.org/10.1093/icb/icx104.

[7] Lynch, S.V., Pedersen, O., The human intestinal microbiome in health and disease. *The New England Journal of Medicine*, 375 (24) (2016), 2369–2379. https://doi.org/10.1056/NEJMra1600266.

[8] Thursby, E., Juge, N., Introduction to the human gut microbiota. *The Biochemical Journal*, 474 (11) (2017), 1823–1836. https://doi.org/10.1042/BCJ20160510.

[9] Wang, J., Lang, T., Shen, J., Dai, J., Tian, L., Wang, X., Core gut bacteria analysis of healthy mice. *Frontiers in Microbiology*, 10 (2019), 887. https://doi.org/10.3389/fmicb.2019.00887.

[10] Bäckhed, F., Manchester, J.K., Semenkovich, C.F., Gordon, J.I., Mechanisms underlying the resistance to diet-induced obesity in germ-free mice. *Proceedings of the National Academy of Sciences of the United States of America*, 104 (3) (2007), 979–984. https://doi.org/10.1073/pnas.0605374104.

[11] Rogers, G.B., Kozlowska, J., Keeble, J., Metcalfe, K., Fao, M., Dowd, S.E., Mason, A.J., McGuckin, M.A., Bruce, K.D., Functional divergence in gastrointestinal microbiota in physically-separated genetically identical mice. *Scientific Reports*, 4 (2014), 5437. https://doi.org/10.1038/srep05437.

[12] Roeselers, G., Mittge, E.K., Stephens, W.Z., Parichy, D.M., Cavanaugh, C.M., Guillemin, K., Rawls, J.F., Evidence for a core gut microbiota in the zebrafish. *The ISME Journal*, 5 (10) (2011), 1595–1608. https://doi.org/10.1038/ismej.2011.38.

[13] van Leeuwen, P., Mykytczuk, N., Mastromonaco, G.F., Schulte-Hostedde, A.I., Effects of captivity, diet, and relocation on the gut bacterial communities of white-footed mice. *Ecology and Evolution*, 10 (11) (2020), 4677–4690. https://doi.org/10.1002/ece3.6221.

[14] Belheouane, M., Vallier, M., Čepić, A., Chung, C.J., Ibrahim, S., Baines, J.F., Assessing similarities and disparities in the skin microbiota between wild and laboratory populations of house mice. *The ISME Journal*, 14 (10) (2020), 2367–2380. https://doi.org/10.1038/s41396-020-0690-7.

[15] Wang, J., Linnenbrink, M., Künzel, S., Fernandes, R., Nadeau, M.-J., Rosenstiel, P., Baines, J.F., Dietary history contributes to enterotype-like clustering and functional metagenomic content in the intestinal microbiome of wild mice. *Proceedings of the National Academy of Sciences of the United States of America*, 111 (26) (2014), E2703-10. https://doi.org/10.1073/pnas.1402342111.

[16] Kreisinger, J., Cížková, D., Vohánka, J., Piálek, J., Gastrointestinal microbiota of wild and inbred individuals of two house mouse subspecies assessed using high-throughput parallel pyrosequencing. *Molecular Ecology*, 23 (20) (2014), 5048–5060. https://doi.org/10.1111/mec.12909.

[17] Weldon, L., Abolins, S., Lenzi, L., Bourne, C., Riley, E.M., Viney, M., The gut microbiota of wild mice. *Plos One*, 10 (8) (2015), e0134643. https://doi.org/10.1371/journal.pone.0134643.

[18] Debebe, T., Biagi, E., Soverini, M., Holtze, S., Hildebrandt, T.B., Birkemeyer, C., Wyohannis, D., Lemma, A., Brigidi, P., Savkovic, V., König, B., Candela, M., Birkenmeier, G., Unraveling the gut microbiome of the long-lived naked mole-rat. *Scientific Reports*, 7 (1) (2017), 9590. https://doi.org/10.1038/s41598-017-10287-0.

[19] Ley, R.E., Hamady, M., Lozupone, C., Turnbaugh, P.J., Ramey, R.R., Bircher, J.S., Schlegel, M.L., Tucker, T.A., Schrenzel, M.D., Knight, R., Gordon, J.I., Evolution of mammals and their gut microbes. *Science*, 320 (5883) (2008), 1647–1651. https://doi.org/10.1126/science.1155725.

[20] Zhou, T., Liu, S., Jiang, A., Comparison of gut microbiota between immigrant and native populations of the Silver-eared Mesia (Leiothrix argentauris) living in mining area. *Frontiers in Microbiology*, 14 (2023), 1076523. https://doi.org/10.3389/fmicb.2023.1076523.

[21] Linnenbrink, M., Wang, J., Hardouin, E.A., Künzel, S., Metzler, D., Baines, J.F., The role of biogeography in shaping diversity of the intestinal microbiota in house mice. *Molecular Ecology*, 22 (7) (2013), 1904–1916. https://doi.org/10.1111/mec.12206.

[22] Arslan, A., Kryštufek, B., Matur, F., Zima, J., Review of chromosome races in blind molerats (*Spalax* and *Nannospalax*). *Folia Zoologica*, 65 (4) (2016), 249–301. https://doi.org/10.25225/fozo.v65.i4.a1.2016.

[23] Shams, I., Avivi, A., Nevo, E., Oxygen and carbon dioxide fluctuations in burrows of subterranean blind molerats indicate tolerance to hypoxic-hypercapnic stresses. *Comparative Biochemistry and Physiology. Part A, Molecular & Integrative Physiology*, 142 (3) (2005), 376–382. https://doi.org/10.1016/j.cbpa.2005.09.003.

[24] Altwasser, R., Paz, A., Korol, A., Manov, I., Avivi, A., Shams, I., The transcriptome landscape of the carcinogenic treatment response in the blind molerat: insights into cancer resistance mechanisms. *BMC Genomics*, 20 (1) (2019), 17. https://doi.org/10.1186/s12864-018-5417-z.

[25] Lagunas-Rangel, F.A., Cancer-free aging: Insights from Spalax ehrenbergi superspecies. *Ageing Research Reviews*, 47 (2018), 18–23. https://doi.org/10.1016/j.arr.2018.06.004.

[26] Schmidt, H., Malik, A., Bicker, A., Poetzsch, G., Avivi, A., Shams, I., Hankeln, T., Hypoxia tolerance, longevity and cancer-resistance in the molerat Spalax - a liver transcriptomics approach. *Scientific Reports*, 7 (1) (2017), 14348. https://doi.org/10.1038/s41598-017-13905-z.

[27] Sözen, M., Sevindik, M., Matur, F., Karyological and some morphological characteristics of *Spalax leucodon* Nordmann, 1840 (Mammalia: Rodentia) superspecies around Kastamonu province, Turkey. *Turkish Journal of Zoology*, 30 (2) (2006), 205–219.

[28] Wertheim, G., Nevo, E., Helminths of birds and mammals from Israel: III. Helminths from chromosomal forms of the mole-rat, *Spalax ehrenbergi*. *Journal of Helminthology*, 45 (2–3) (1971), 161–169. https://doi.org/10.1017/S0022149X00007045.

[29] Klindworth, A., Pruesse, E., Schweer, T., Peplies, J., Quast, C., Horn, M., Glöckner, F.O., Evaluation of general 16S ribosomal RNA gene PCR primers for classical and next-generation sequencing-based diversity studies. *Nucleic Acids Research*, 41 (1) (2013), e1. https://doi.org/10.1093/nar/gks808.

[30] Jiang, H., Lei, R., Ding, S.-W., Zhu, S., Skewer: a fast and accurate adapter trimmer for next-generation sequencing paired-end reads. *BMC Bioinformatics*, 15 (2014), 182. https://doi.org/10.1186/1471-2105-15-182.

[31] Callahan, B.J., McMurdie, P.J., Rosen, M.J., Han, A.W., Johnson, A.J.A., Holmes, S.P., DADA2: High-resolution sample inference from Illumina amplicon data. *Nature Methods*, 13 (7) (2016), 581–583. https://doi.org/10.1038/nmeth.3869.

[32] Edgar, R.C., Haas, B.J., Clemente, J.C., Quince, C., Knight, R., UCHIME improves sensitivity and speed of chimera detection. *Bioinformatics*, 27 (16) (2011), 2194–2200. https://doi.org/10.1093/bioinformatics/btr381.

[33] Quast, C., Pruesse, E., Yilmaz, P., Gerken, J., Schweer, T., Yarza, P., Peplies, J., Glöckner, F.O., The SILVA ribosomal RNA gene database project: improved data processing and web-based tools. *Nucleic Acids Research*, 41 (Database issue) (2013), D590-6. https://doi.org/10.1093/nar/gks1219.

[34] McMurdie, P.J., Holmes, S., phyloseq: an R package for reproducible interactive analysis and graphics of microbiome census data. *Plos One*, 8 (4) (2013), e61217. https://doi.org/10.1371/journal.pone.0061217.

[35] Chung, H., Kasper, D.L., Microbiota-stimulated immune mechanisms to maintain gut homeostasis. *Current Opinion in Immunology*, 22 (4) (2010), 455–460. https://doi.org/10.1016/j.coi.2010.06.008.

[36] Stappenbeck, T.S., Hooper, L.V., Gordon, J.I., Developmental regulation of intestinal angiogenesis by indigenous microbes via Paneth cells. *Proceedings of the National Academy of Sciences of the United States of America*, 99 (24) (2002), 15451–15455. https://doi.org/10.1073/pnas.202604299.

[37] Semova, I., Carten, J.D., Stombaugh, J., Mackey, L.C., Knight, R., Farber, S.A., Rawls, J.F., Microbiota regulate intestinal absorption and metabolism of fatty acids in the zebrafish. *Cell Host & Microbe*, 12 (3) (2012), 277–288. https://doi.org/10.1016/j.chom.2012.08.003.

[38] Vaikunthanathan, T., Safinia, N., Lombardi, G., Lechler, R.I., Microbiota, immunity and the liver. *Immunology Letters*, 171 (2016), 36–49. https://doi.org/10.1016/j.imlet.2016.01.008.

[39] Kotzampassi, K., Giamarellos-Bourboulis, E.J., Stavrou, G., Obesity as a consequence of gut bacteria and diet interactions. *ISRN Obesity*, 2014 (2014), 651895. https://doi.org/10.1155/2014/651895.

[40] van Leeuwen, P.M.L., Schulte-Hostedde, A.I., Fournier-Chambrillon, C., Fournier, P., Pigneur, L.-M., Aranda, C.M., Urra-Maya, F., Michaux, J.R., A microbial tale of farming, invasion and conservation: on the gut bacteria of European and American mink in Western Europe. *Biological Invasions*, (2023), https://doi.org/10.1007/s10530-023-03007-5.

[41] Wang, X.-W., Liu, Y.-Y., Origins of scaling laws in microbial dynamics. *Physical Review Research*, 5 (1) (2023), 013004. https://doi.org/10.1103/PhysRevResearch.5.013004.

[42] Nielsen, D.P., Harrison, J.G., Byer, N.W., Faske, T.M., Parchman, T.L., Simison, W.B., Matocq, M.D., The gut microbiome reflects ancestry despite dietary shifts across a hybrid zone. *Ecology Letters*, 26 (1) (2023), 63–75. https://doi.org/10.1111/ele.14135.

[43] Wang, Z., Zhang, C., Li, G., Yi, X., The influence of species identity and geographic locations on gut microbiota of small rodents. *Frontiers in Microbiology*, 13 (2022), 983660. https://doi.org/10.3389/fmicb.2022.983660.

[44] Sibai, M., Altuntaş, E., Yıldırım, B., Öztürk, G., Yıldırım, S., Demircan, T., Microbiome and longevity: High abundance of longevity-linked Muribaculaceae in the gut of the long-living rodent *Spalax leucodon*. *Omics : A Journal of Integrative Biology*, 24 (10) (2020), 592–601. https://doi.org/10.1089/omi.2020.0116.

[45] Kuang, Z., Li, F., Duan, Q., Tian, C., Nevo, E., Li, K., Host diet shapes functionally differentiated gut microbiomes in sympatric speciation of blind molerats in Upper Galilee, Israel. *Frontiers in Microbiology*, 13 (2022), 1062763. https://doi.org/10.3389/fmicb.2022.1062763.

[46] Bendová, B., Piálek, J., Ďureje, Ľ., Schmiedová, L., Čížková, D., Martin, J.-F., Kreisinger, J., How being synanthropic affects the gut bacteriome and mycobiome: comparison of two mouse species with contrasting ecologies. *BMC Microbiology*, 20 (1) (2020), 194. https://doi.org/10.1186/s12866-020-01859-8.

[47] Kreisinger, J., Bastien, G., Hauffe, H.C., Marchesi, J., Perkins, S.E., Interactions between multiple helminths and the gut microbiota in wild rodents. *Philosophical Transactions of the Royal Society of London. Series B, Biological Sciences*, 370 (1675) (2015). https://doi.org/10.1098/rstb.2014.0295.

[48] Cong, W., Xing, J., Feng, Y., Wang, J., Fu, R., Yue, B., He, Z., Lin, L., Yang, W., Cheng, J., Sun, W., Cui, S., The microbiota in the intestinal and respiratory tracts of naked mole-rats revealed by high-throughput sequencing. *BMC Microbiology*, 18 (1) (2018), 89. https://doi.org/10.1186/s12866-018-1226-4.

[49] Biddle, A., Stewart, L., Blanchard, J., Leschine, S., Untangling the genetic basis of fibrolytic specialization by lachnospiraceae and ruminococcaceae in diverse gut communities. *Diversity*, 5 (3) (2013), 627–640. https://doi.org/10.3390/d5030627.

[50] Rinninella, E., Raoul, P., Cintoni, M., Franceschi, F., Miggiano, G.A.D., Gasbarrini, A., Mele, M.C., What is the healthy gut microbiota composition? A changing ecosystem across age, environment, diet, and diseases. *Microorganisms*, 7 (1) (2019). https://doi.org/10.3390/microorganisms7010014.

[51] Smith, B.J., Miller, R.A., Ericsson, A.C., Harrison, D.C., Strong, R., Schmidt, T.M., Changes in the gut microbiome and fermentation products concurrent with enhanced longevity in acarbose-treated mice. *BMC Microbiology*, 19 (1) (2019), 130. https://doi.org/10.1186/s12866-019-1494-7.

[52] Ormerod, K.L., Wood, D.L.A., Lachner, N., Gellatly, S.L., Daly, J.N., Parsons, J.D., Dal'Molin, C.G.O., Palfreyman, R.W., Nielsen, L.K., Cooper, M.A., Morrison, M., Hansbro, P.M., Hugenholtz, P., Genomic characterization of the uncultured Bacteroidales family S24-7 inhabiting the guts of homeothermic animals. *Microbiome*, 4 (1) (2016), 36. https://doi.org/10.1186/s40168-016-0181-2.

[53] Zhao, N., Zhao, M., Jin, H., Microplastic-induced gut microbiota and serum metabolic disruption in Sprague-Dawley rats. *Environmental Pollution*, 320 (2023), 121071. https://doi.org/10.1016/j.envpol.2023.121071.

[54] Siddiqui, R., Qaisar, R., Khan, N.A., Alharbi, A.M., Alfahemi, H., Elmoselhi, A., Effect of microgravity on the gut microbiota bacterial composition in a hindlimb unloading model. *Life (Basel, Switzerland)*, 12 (11) (2022). https://doi.org/10.3390/life12111865.

[55] Zou, Y., Liang, N., Zhang, X., Han, C., Nan, X., Functional differentiation related to decomposing complex carbohydrates of intestinal microbes between two wild zokor species based on 16SrRNA sequences. *BMC Veterinary Research*, 17 (1) (2021), 216. https://doi.org/10.1186/s12917-021-02911-z.

[56] Li, C., Li, X., Guo, R., Ni, W., Liu, K., Liu, Z., Dai, J., Xu, Y., Abduriyim, S., Wu, Z., Zeng, Y., Lei, B., Zhang, Y., Wang, Y., Zeng, W., Zhang, Q., Chen, C., Qiao, J., Liu, C., Hu, S., Expanded catalogue of metagenome-assembled genomes reveals resistome characteristics and athletic performance-associated microbes in horse. *Microbiome*, 11 (1) (2023), 7. https://doi.org/10.1186/s40168-022-01448-z.

[57] Han, M., Yang, K., Yang, P., Zhong, C., Chen, C., Wang, S., Lu, Q., Ning, K., Stratification of athletes' gut microbiota: the multifaceted hubs associated with dietary factors, physical characteristics and performance. *Gut Microbes*, 12 (1) (2020), 1–18. https://doi.org/10.1080/19490976.2020.1842991.

http://communications.science.ankara.edu.tr

Commun.Fac.Sci.Univ.Ank.Ser. C Biology
Volume 32, Number 2, Pages 119-136 (2023)
ISSN 1303-6025 E-ISSN 2651-3749
DOI: 10.53447/communc.1272043

Research Article; Received: March 28, 2023; Accepted: July 06, 2023

THE CYTOTOXIC AND APOPTOTIC EFFECTS OF *Abies nordmanniana* subsp. *bornmülleriana Mattf* RESIN EXTRACT ON PROSTATE CANCER CELLS

MUHAMMET BURAK BATIR[1], SEVİNÇ BATIR[1], FEYZAN ÖZDAL KURT[1], FETHİ SIRRI ÇAM[2]

[1] Faculty of Arts and Sciences, Department of Biology, Manisa Celal Bayar University, Manisa, TÜRKİYE
[2] Faculty of Medicine, Department of Medical Genetics, Manisa Celal Bayar University, Manisa, TÜRKİYE

ABSTRACT. Cancer has become one of the most critical health issues, with an increasing incidence and mortality in recent years. Meanwhile, many studies are carried out on discovering new compounds which reflects effective results on cancer cells. Therefore, this study aimed to examine the cytotoxic, anti-proliferative and apoptotic effects on cancer cell lines by using the extract obtained from Uludağ Fir (*Abies nordmanniana* subsp. *bornmülleriana Mattf*) resin. Uludağ Fir resin extract was obtained by applying the methanol extraction method. In our study, fibroblast cell L-929, human metastatic prostate cancer PC-3 and human metastatic prostate cancer DU-145 cell lines were cultured in RPMI-1640 medium. The effects of the resin extract concentrations on the viability of the cells were determined with the Muse™ Cell Count & Viability test. In addition, apoptosis and cell cycle phases of the cells were determined using the Muse™ cell analyzer. Finally, RT-qPCR analysis was performed to determine the resin extract effect on pro-apoptotic and anti-apoptotic gene expression. The apoptotic effect of Uludağ Fir resin extract on cancer cell lines was significantly higher in contrast to the healthy normal cells. In addition, it was determined that Uludağ Fir extract caused G0/G1 cell cycle arrest in cancer cells. In RT-qPCR analysis, the pro-apoptotic gene expression levels were apparently increased in cancer cells, which was followed by a decrease in the anti-apoptotic gene expression levels. All taken together, these results indicate that Uludağ Fir resin extract exerts two prong effects as it induces a cell cycle arrest and apoptotic pathway activation on human prostate cancer cell lines.

1. INTRODUCTION

Cancer, caused by the uncontrolled proliferation of cells, is one of our age's most important health problems, and the mortality rate among patients is relatively high [1]. One of these cancer type is prostate cancer and it is a type of cancer that develops in the prostate gland, which is a small walnut-shaped gland that produces seminal fluid in males. It is one of the most common types of cancer in men, and its incidence increases with age [2]. Also, In underdeveloped countries, the problem is more severe due to the lack of diagnostic techniques, standard

Keywords. Prostate cancer, Uludağ Fir, cell viability, apoptosis, cell cycle arrest

buraks1@hotmail.com- Corresponding author; 0000-0002-8722-5055
soylevsevinc@gmail.com- 0000-0003-1817-3113
feyzanozdalkurt@yahoo.com- 0000-0001-6070-3742
sirricam@gmail.com- 0000-0002-0972-8896

treatment methods and higher treatment costs [3]. These countries, which have problems in the diagnosis and treatment of cancer, overcome these problems using synthetic drugs. These drugs target the rapidly growing and dividing cells of various tumors [4]. However, although these synthetic drugs can cause some acute and irreversible side effects also effect rapidly dividing normal cells in our body [5]. In addition, it has been reported by various studies that chemotherapeutic drugs used in cancer treatment cause multi-drug resistance [6,7]. For this reason, the high cost, increasing drug resistance, and side effects of current therapeutic approaches are forcing scientists to explore alternative medicines known as conventional medicine as an option to find new chemicals for cancer treatment.

Herbal agents are currently being researched for different uses in many laboratories worldwide. For example, from the point of view of cancer treatment, many researchers worldwide are working on treatment by testing extract samples obtained from different species, such as algae and plants, by different methods in different cancer cell types [8-10]. In some recent studies, it has been determined that essential oils obtained from some Pinus, Citrus, Lavandula and Melaleuca species have cytotoxic effects against cervical (HeLa), breast (MCF-7), kidney (HEK-293), colon (HT-29), livers (HepG2, BEL-7402) and many other cancer cell lines [11-14]. In addition, it has been reported that resin extract obtained from Abies balsamea (L.) Mill. (Canadian Fir) has anti-cancer effects in studies on various cancer cell lines. Also, it was observed that healthy cells were affected less than cancer cells [15]. In a study on the determination of the cytotoxic activity of the resin obtained from Taurus Fir, the resin extract exhibited cytotoxic activity on cancer cells [16]. Also, a compound derived from Abies sibirica was able to inhibit the growth of cancer cells. The researchers suggested that this effect may be due to the compound's ability to induce cell death in the cancer cells [17]. However, there is some evidence to suggest that Fir resin may have an effect on cancer cells, but the research is still in the early stages and more studies are needed to fully understand its potential benefits.

As mentioned above, many different species of Fir resins were experimentally tested on different cancer cell lines. However, the different species of Fir resins' extracts constituents could differ. One of these species is Uludağ Fir (Abies nordmanniana subsp. bornmülleriana Mattf), an endemic species for Turkey and the subject of our study. This species locates in the Western Black Sea Region, between Kızılırmak and Uludağ [18]. Therefore, this study aimed to unveil the cytotoxic, anti-proliferative and apoptotic effects of Uludağ Fir resin extract on the mouse fibroblast cell line L-929 and prostate cancer cell lines (PC-3 and DU-145).

2. MATERIALS AND METHODS

2.1. Preparation and application of Uludağ Fir resin extract

1 g of Uludağ Fir resin was initially dissolved in 4 ml pure methanol in a 15 ml centrifuge tube. The resin solution dissolved in methanol was passed through a 40 µm nylon filter to remove plant residues from it and passed through a 20 µm polyethersulfone (PES) filter to prevent bacterial contamination. Then, the cap of the tube containing the extract solution was loosened and incubated at 37 °C for two days to evaporate the methanol in the tube. As a result, 700 mg of pure resin was obtained after all operations and dissolved in 7 ml of Dimethyl sulfoxide (DMSO). Thus, a resin extract solution was obtained with a final concentration of 100 mg/ml. The extract obtained at the end of all processes was stored at -20 °C for further processing. Then, different amounts as 1500, 1000, 750, 500, 300, and 100 µg/ml, doses of resin extract from prepared stock solution were simultaneously applied to healthy normal cells and cancer cell lines for treatment.

2.2. Cell line and culture conditions

Mouse fibroblast cell line L-929, human prostate cancer cell lines PC-3 and DU-145 were purchased from ATCC (American Type Cell Culture). L-929, PC-3 and DU-145 cells were cultured in a medium containing RPMI 1640 (Gibco, 11875093), 10% fetal bovine serum (FBS) (Gibco, 10270098), %1 penicillin/streptomycin (Gibco, 15070063) and %1 L-Glutamine (Gibco, 25030081) at 37° C in a 5% CO_2 incubator. The medium was changed in every second day. When the cells became confluent, they were passaged to ensure growth. Cells (45000 cells/ml/well) were cultured in 24-well plates for 24 hours, then were incubated with the extracts at different dilutions for 24 and 48hours. All experiments were performed in triplicate for each extract. After the last incubation time, the cells were collected for viability and proliferation assays.

2.3. Cell viability analysis in cell lines treated with Uludağ Fir resin extract

Cell viability assays were carried out with flow cytometry analysis. Flow cytometry analysis, the attached cells in the 24 well plates were washed with Dulbecco's phosphate-buffered saline 1X (DPBS) (Gibco, 14190144), and washed cells were then trypsinized (Gibco, 25200056). Following trypsinization, centrifuged cells were suspended and diluted in a related complete medium. After dilution of the cells, the total cell concentrations and viability of the cells were determined with Muse Count & Viability reagent (Merck Millipore, Billerica, MA, USA, MCH100102) by following the manufacturer's instructions with using the automated Muse® Cell Analyzer (Merck Millipore, Billerica, MA, USA) which stains viable and dead cells based on their permeability to two different DNA binding dyes.

2.4. Apoptosis analysis in cell lines treated with Uludağ Fir resin extract

The apoptotic effects in L-929, PC-3 and DU-145 cells, which were grown in 6-well plates and then applied Uludağ Fir resin extract for 24 and 48 hours at IC_{50} and IC_{25} values, was determined using the Muse Annexin V and Dead Cell kit. For this reason, the viability and cell number of the cells were determined in the MUSE device with the Merck Muse® Count & Viability Assay kit. After cell counting, 250.000 cells in 2 ml RPMI-1640 complete medium were divided into groups of 3 for each cell type (as control, IC_{50} and IC_{25}) added into 6-well culture plate for 24 and 48 hours extract applications. In addition, three 6-well culture plate were used for these analyses. Cells transferred to 6-well culture plate were placed in a humidified incubator at 37°C and 5% CO_2 for 16-18 hours to ensure 70-80% cell confluency in the wells before applying the extract. After the incubation process, Uludağ Fir resin extract concentrations determined for IC_{50} and IC_{25} values in 2 ml RPMI-1640 complete medium were added to the wells, excluding the control well, respectively the culture plate were placed to the incubator at 37°C and 5% CO_2 humidified environment. At the end of 24 hours, the first group cells were taken from the incubator and the cells removed from the wells by trypsinization as centrifuged at 1000 rpm for 5 minutes in 15 ml tubes. At the end of centrifugation, the supernatant was removed, and the cells at the bottom of the tube were suspended with 1 ml of culture medium. The suspended cells were transferred to different 1.5 ml centrifuge tubes as 100 µl and then 100 µl of Muse Annexin V and Dead Cell solution was added into each tube. After incubating the cells for at least 60 minutes at room temperature in the dark, the cells were analyzed on the Muse flow cytometry instrument to determine the apoptosis rate. Similar procedures were performed within the 48-hour experiment group [19].

2.5. RT-qPCR analysis of mRNA expression levels of anti-apoptotic Bcl-2, Bcl-xL and pro-apoptotic Caspase-3, Bax and Cytochrome C target genes in cell lines treated with Uludağ Fir resin extract

Isolation of RNA from L-929, PC-3 and DU-145 cells, which were grown in 6-well plates and Uludağ Fir resin extract applied for 24 and 48 hours at IC_{50} and IC_{25} values, was carried out with PureLink™ RNA Mini (Thermo Fischer Scientific) according to the manufacturer's procedure. cDNA synthesis was performed with a High-Capacity cDNA Reverse Transcription kit from the samples isolated total RNAs in the SensoQuest thermal cycler according to the manufacturer's procedure. After this, to perform mRNA expression analyses of target genes on cDNAs Bcl-2 (BCL2F1 5'-CTTCGCCGAGATGTCCAGC-3', BCL2R1 5'-CTCTCCACACACATGACCCC-3'), Bcl-xL (BCLxLF1 5'-TCCCCATGGCAGCAGTAAAG-3', BCLxLR1 5'-TCCCCATGGCAGCAGTAAAG-3') Caspase-3 (CASP3F15'-TGAGATCAAGCCCCACGATG-3', CASP3R1 5'-ACAGCAGATGAAGCAGTCCA-3'), Bax (BAXF1 5'-ACGGCAACTTCAACTGGGG-3', BAXRCATGTCAGCCCAAT-3') and

Cytochrome C (COX1F1 5'-CCTCTTCGTCTGATCCGTCC-3', COX1R1 5'-TGAGGGTTGCGGTCTGTTAGT-3') primer pairs were designed. Also, expression analysis of target genes was performed with a 25 µl total reaction mixture of 2 µl cDNA, 1.25 µl EvaGreen, 0.3 µl 10 pmol Primer Forward, 0.3 µl 10 pmol Primary Reverse, 12.5 µl 2X Hot-start master mix and 8.65 µl ddH2O in a Rotor-Gene Real-Time PCR (Qiagen, USA) device. Normalization of target genes was carried out according to the most stable expression values of the Hypoxanthine-guanine phosphoribosyltransferase 1 (HPRT1) housekeeping gene. Quantification of normalized expression values of target genes was determined according to the $2^{-\Delta\Delta Ct}$ method [20].

2.6. Analysis of cell cycle state in cell lines treated with Uludağ Fir resin extract

Cell cycle analysis of L-929, PC-3 and DU-145 cells, which were grown in 6-well plates and then applied Uludağ Fir resin extract for 24 and 48 hours at IC_{50} and IC_{25} values, was carried out in the MUSE device with the Merck Muse® Muse Cell Cycle Kit. Cell cycle analysis of L-929, PC-3 and DU-145 cells, which were grown in 6-well plates and then Uludağ Fir resin extract applied for 24 and 48 hours at IC_{50} and IC_{25} values and carried out in the MUSE device with the Merck Muse® Cell Cycle Assay kit. First, the incubated cells at 37°C in 95% humidity and 5% CO_2 environment were fixed in 70% ethanol (EtOH) and incubated at -20°C for 3 hours. Then, the fixed cells were washed with cold PBS and collected by centrifugation at 1000 rpm for 5 minutes. Finally, the cells were analyzed in the MUSE flow cytometry device after staining with the Muse Cell Cycle Kit (Millipore, Germany) in the dark for 30 minutes.

2.7. Statistical analysis

The SPSS (statistical package software, Windows 23.0) was used to analyze the significances of differences observed between the groups. The obtained data were tested by performing One-way ANOVA and Tukey post hoc test. The p-values smaller than 0.05 were considered and all data represented the triplicate experiments. Finally, the data were presented as a mean ± standard deviation (SD).

3. RESULTS

3.1. Detection of IC_{50} and IC_{25} values for Uludağ Fir resin extract

In vitro anti-cancer activity of the extract of Uludağ Fir resin extract was assessed through the MUSE flow cytometry assays against prostate cancer cell lines. Uludağ Fir resin extract was added onto L-929, PC-3 and DU-145 cells at concentrations of 1500, 1000, 750, 500, 300, and 100 µg/mL for 24 and 48 hours. Cell viability analyses performed with the MUSE flow cytometry device; comparative data were obtained in cell viability increases in accordance with the decreasing extract concentration. The analysis performed with MUSE flow

cytometry determined that the cell viability value was 49.0% in L-929 cells at a concentration of 1500 µg/mL for 24 hours (Figure 1). Cell viability values for PC-3 and DU-145 cells were determined as 4.9% and 5.8%, respectively. The 24 hours IC_{50} values of L-929, PC-3, and DU-145 cells, obtained from the flow cytometry analysis were found as 1520 µg/mL, 1040 µg/mL, and 1065 µg/mL, respectively. IC_{25} values of L-929, PC-3, and DU-145 cells were 750 µg/mL, 500 µg/mL, and 520 µg/mL, respectively.

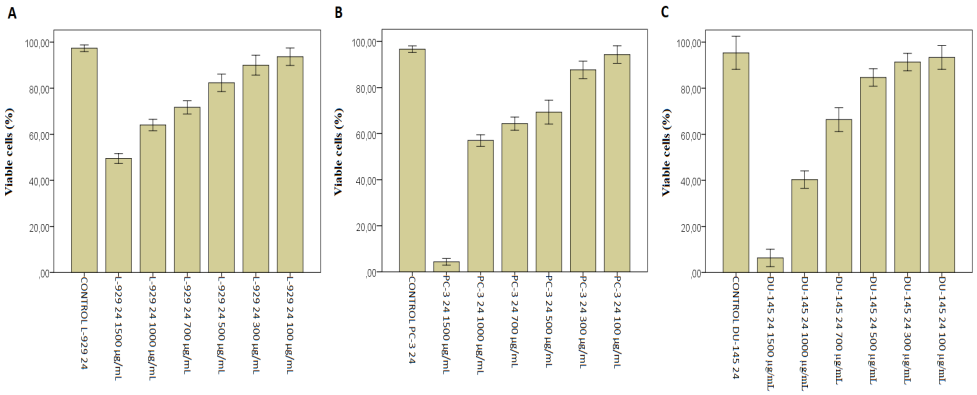

FIGURE 1. Muse cell viability analysis of 24-hours Uludağ Fir resin extracts treated. A L-929, B PC-3, C DU-145 cell lines.

As a result of 48 hours of extract applications at 1500 µg/mL concentration, it was determined that the viability decreased below 7.0% in all cell line groups (Figure 2). Also, IC_{50} and IC_{25} values of the cell lines were determined according to the timeline due to detection of the longitude effect of Uludağ Fir resin extract. The IC_{50} values of L-929, PC-3, and DU-145 cells, obtained from the flow cytometry analysis were found as 1110 µg/mL, 930 µg/mL, and 940 µg/mL, respectively. IC_{25} values of L-929, PC-3, and DU-145 cells were 550 µg/mL, 450 µg/mL, and 460 µg/mL, respectively.

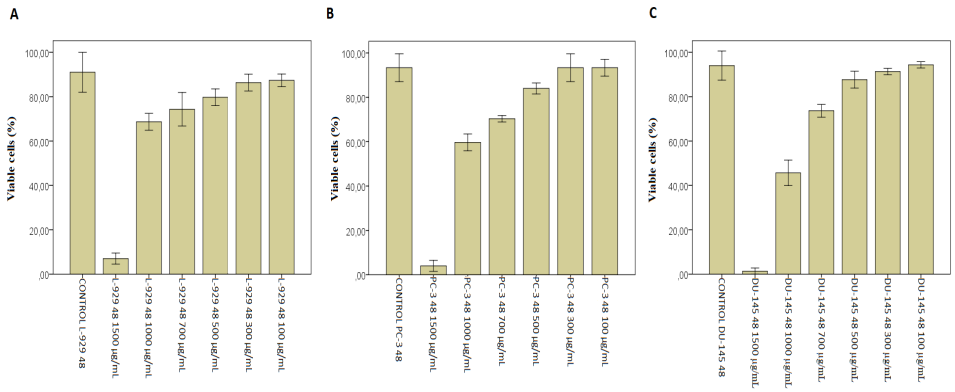

FIGURE 2. Muse cell viability analysis of 48-hours Uludağ Fir resin extracts treated. A L-929, B PC-3, C DU-145 cell lines.

3.2. Evaluation of the antitumor activity of Uludağ Fir resin

The apoptotic potential of the Uludağ Fir resin extract was measured by flow cytometry, which allows the identification of viable (AnnV-/PI-), early apoptotic (AnnV+/PI-), late apoptotic (AnnV+/PI+) and necrotic (AnnV-/PI+) cells. According to the data obtained from cell viability, IC_{50} and IC_{25} extract ratios were applied to L-929, PC-3, and DU-145 cell lines in 6-well cell culture dishes for 24 and 48 hours, respectively. In addition, the apoptotic process occurring in the cell lines was determined in the Muse flow cytometry device, using the Muse Annexin V and Dead Cell kit (Figure 3).

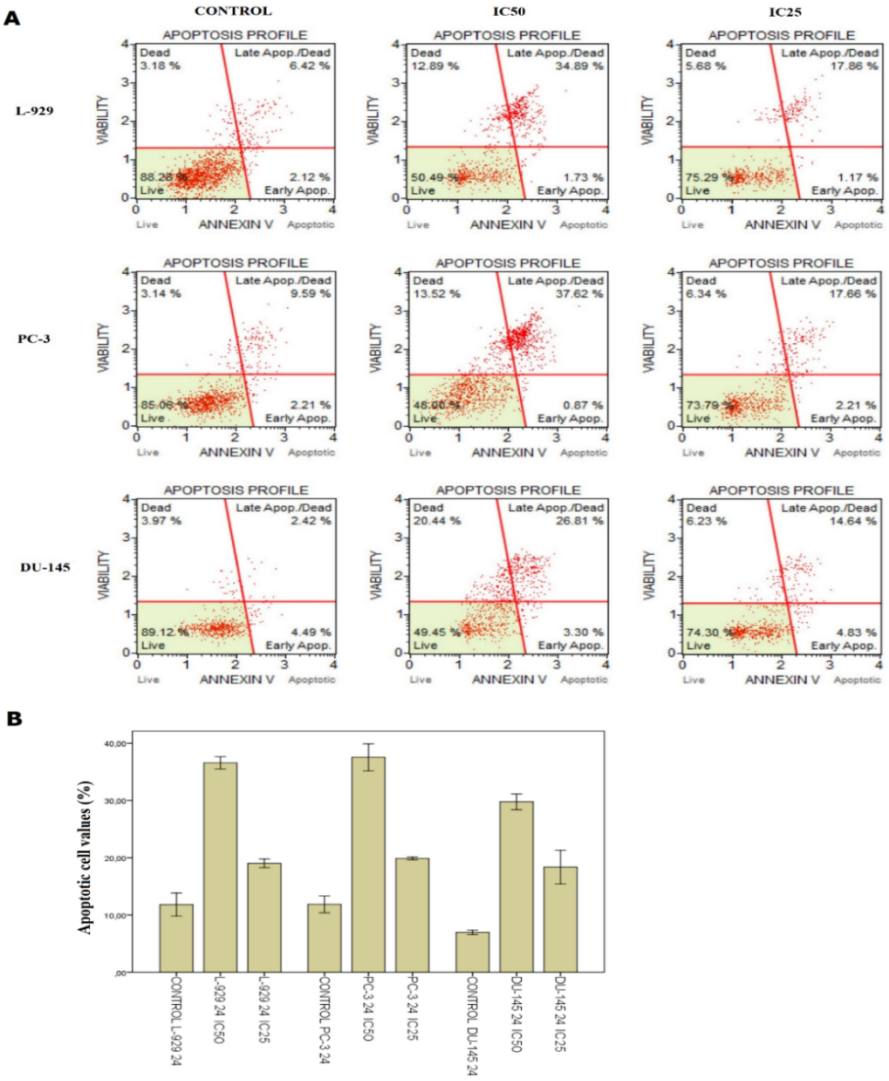

FIGURE 3. 24-hours apoptosis values of L-929, PC-3, DU-145 cell lines treated with IC_{50} and IC_{25} Uludağ Fir resin extract. A graphic of flow cytometry analysis, B % ratio of apoptotic cell values of control and treated cell lines.

Cells were treated with IC_{25} (concentration causing 25% growth inhibition) and IC_{50} (concentration causing 50% growth inhibition) of Uludağ Fir resin extract to demonstrate the concentration-dependent apoptotic effect. All cancer cell lines tested with IC_{25} and IC_{50} concentrations, consistent with flow cytometry cell viability analysis (p=0.001), showed reduced viability and markedly increased apoptotic cells at lower concentrations than healthy normal cells.

As shown in Figure 3, the total number of apoptotic (early and late apoptosis) cells at 24 hours in the control group of L-929 cells was 11.86±0.60%. In L-929 cell groups, which were applied extract during 24 hours at concentrations of 550 µg/mL (IC_{25}) and 1110 µg/mL (IC_{50}), the total number of apoptotic cells increased by 19.03±0.30% ($p<0.0001$) and 36.62±0.50% ($p<0.0001$) according to the control group, respectively. Compared to PC-3 control cells with a total apoptotic cell count of 11.86±0.60% at 24 hours, the application of the extract at concentrations of 450 µg/ml (IC_{25}) and 930 µg/ml (IC_{50}) resulted in the increasing number of total PC-3 apoptotic cell count as a 19.87±0.10% (p=0.0001) and 37.58±0.90% (p=0.0001), respectively. Compared to DU-145 control cells with a total apoptotic cell count of 6.97±0.11% at 24 hours, the application of the extract at concentrations of 460 µg/mL (IC_{25}) and 940 µg/mL (IC_{50}) resulted in the increasing number of total DU-145 apoptotic cell count as an 18.87±1.21% (p=0.0001) and 29.77±0.58% (p=0.0001), respectively. These results showed that Uludağ Fir resin extract could induce apoptosis in all tested cancer cells to a significant extent in a concentration-dependent manner.

As shown in Figure 4, the total number of apoptotic (early and late apoptosis) cells at 48 hours in the control group of L-929 cells was 6.24±0.30%. In L-929 cell groups, which were applied extract for 48 hours at concentrations of 550 µg/mL (IC_{25}) and 1110 µg/mL (IC_{50}), the total number of apoptotic cells increased by 28.89±0.70% ($p<0.0001$) and 41.48±1.2% ($p<0.0001$) according to the control group, respectively. Compared to untreated PC-3 control cells with a total apoptotic cell count of %6.22±0.51 at 48 hours, the application of the extract at concentrations of 450 µg/mL (IC_{25}) and 930 µg/mL (IC_{50}) resulted in the increasing number of total PC-3 apoptotic cell count as a %29.80±0.61 (p=0.0001) and %48.64±0.51 (p=0.0001), respectively. Also, compared to DU-145 control cells with a total apoptotic cell count of %4.88±1.65 at 48 hours, the application of the extract at concentrations of 460 µg/mL (IC_{25}) and 940 µg/mL (IC_{50}) resulted in the increasing number of total DU-145 apoptotic cell count as an %12.27±0.40 (p=0.0001) and %40.41±1.10 (p=0.0001), respectively. Unlike the 24-hour applications, the early apoptosis rate in L-929 cells was higher in contrast to PC-3 and DU-145 cancer cells in 48-hour applications. In comparison, the late apoptotic or dead cell rate was found to be higher in PC-3 and DU-145 cancer cells according to the healthy normal L-929 cells in 48-hour applications.

These results show that healthy normal L-929 cells that survived 24 hours of extract application were affected much later in contrast to PC-3 and DU-145 cancer cells. The cell viability and apoptosis studies revealed that the **extract** has minor effects on normal cell lines and can be qualified for additional applications.

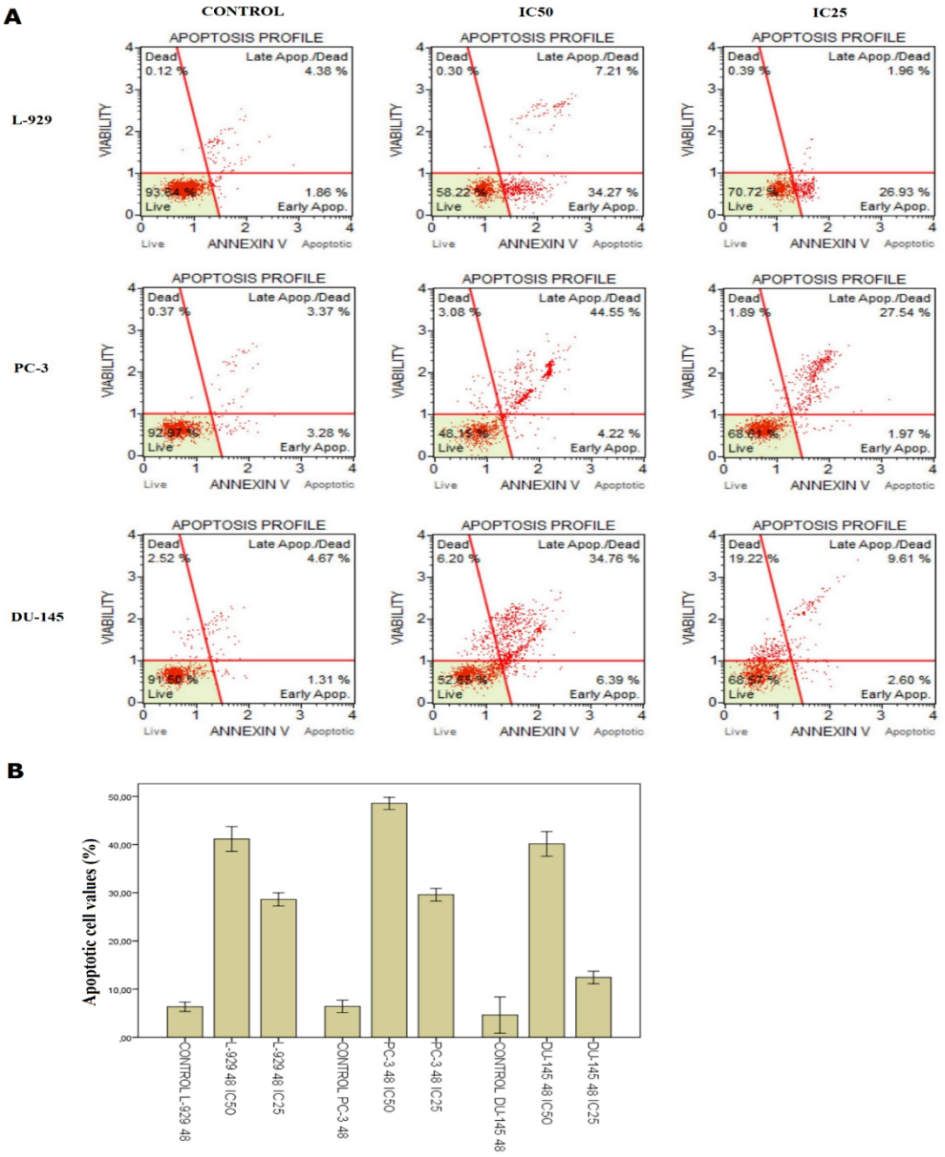

FIGURE 4. 48-hours apoptosis values of L-929, PC-3, DU-145 cell lines treated with IC_{50} and IC_{25} Uludağ Fir resin extract. A graphic of flow cytometry analysis, B % ratio of apoptotic cell values of control and treated cell lines.

3.3. Evaluation of cell cycle status of Uludağ Fir resin extract treated cells

Cell viability analysis revealed that Fir resin extract had a significant cytotoxic effect on all tested cancer cell lines. For this reason, the effect of extract on cell distribution in different phases of the cell cycle was also investigated. Therefore, cancer cells were treated with the calculated IC_{25}, and IC_{50} values of Uludağ Fir resin extract for 24 and 48 hours and analyzed by flow cytometry. According to the analysis results, the extract caused an increase in cell populations that remained in the G0/G1 stage. In contrast, this increase was accompanied by a decrease in the cell population in the G2/M stage. As shown in Figure 5, the following data were obtained according to cell cycle analyses from 24-hour extract applications. There was no significant difference between the G0/G1 population (61.7±0.57) of the L-929 IC_{25} treatment group ($p=0.507$) and the G0/G1 population (59.3±0.36%) of the untreated L-929 control group. However, a significant difference was found between the G0/G1 population 66.9±1.53% of the L-929 IC_{50} treatment group ($p=0.001$) and the G0/G1 population (59.3±0.36%) of the untreated L-929 control group. Furthermore, a major difference was found between the G0/G1 population of the PC-3 IC_{25} treatment group (73.30±0.85%) ($p<0.0001$) and the G0/G1 population of the PC-3 IC_{50} treatment group (78.70±1.44%) ($p<0.0001$) compared to the G0/G1 population (%64.56±1.28) of untreated PC-3 control cells. Meanwhile, there was a significant difference between the G0/G1 population of the IC_{25} treatment group (53.23±2.05%) ($p<0.0001$) and the G0/G1 population of the IC_{50} treatment group (55.73%±1.04%) ($p<0.0001$) compared to the G0/G1 population (44.30±0.50) of DU-145 control cells.

As shown in Figure 6, the following data were obtained according to cell cycle analyses resulting from 48-hour extract applications. Although, there was a slight difference between the G0/G1 population of the untreated L-929 control group (51.70±0.26%) and the G0/G1 population of the IC_{25} treatment group (55.20±1.25%), which was significant ($p=0.041$). However, a significant difference was also found between the G0/G1 population of the IC_{50} treatment group (62.23±0.51) compared to the G0/G1 population of the L-929 control group ($p=0.001$). On the other hand, a significant difference was found between the G0/G1 population of the PC-3 IC_{25} treatment group (78.30±0.60%) ($p<0.0001$) and the G0/G1 population of the PC-3 IC_{50} treatment group (82.10±0.87) ($p<0.0001$) compared to the G0/G1 population of the untreated PC-3 control group (55.17±1.02%). Also, there was a major difference between the G0/G1 population of the IC_{25} treatment group (%65.03±0.61) ($p<0.0001$) and the G0/G1 population of the IC_{50} treatment group (%67.86±0.72) ($p<0.0001$) compared to the G0/G1 population of the DU-145 control group (%52.80±0.75).

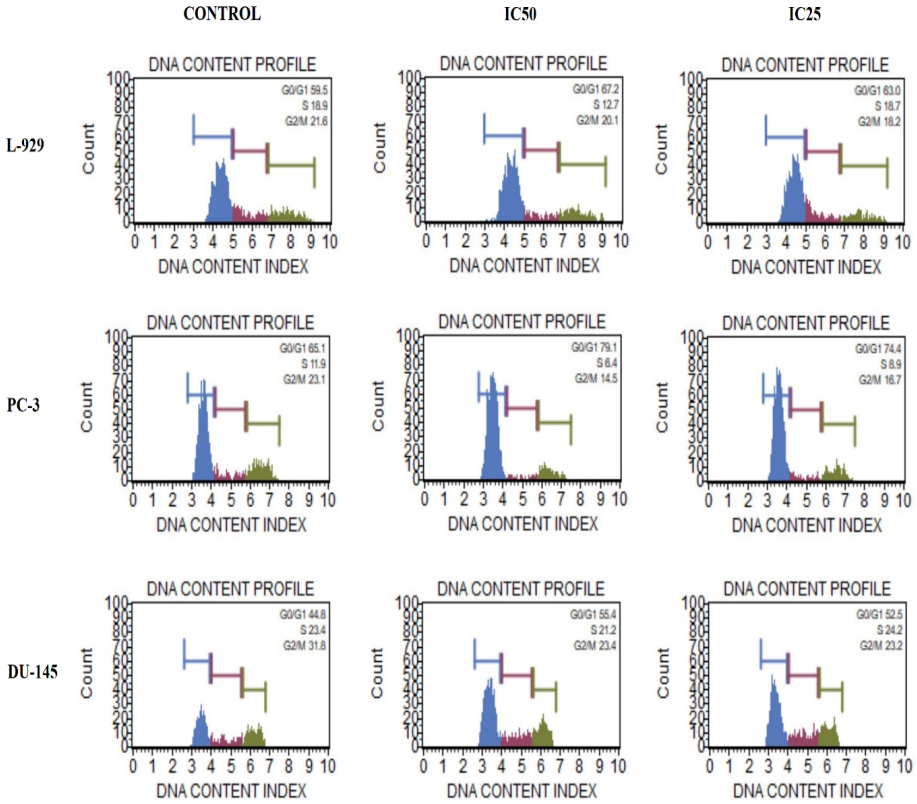

FIGURE 5. 24-hours cell cycle analysis values of L-929, PC-3, DU-145 cell lines treated with IC_{50} and IC_{25} Uludağ Fir resin extract

3.4 RT-qPCR analysis of mRNA expression levels of anti-apoptotic and pro-apoptotic target genes in cell lines treated with Uludağ Fir extract

The data on the changes in the expression levels of target genes were obtained according to the RT-qPCR analysis of Anti-apoptotic Bcl-2, Bcl-xL and Pro-apoptotic Caspase-3, Bax and Cytochrome C genes in cells treated with Uludağ Fir resin extract for 24 and 48 hours. Figure 7 shows an important decrease in the Bcl-2 gene mRNA expression level of all cell types treated with extract at IC_{50} value for 24 hours compared to untreated controls ($p<0.0001$). However, the decrease in Bcl-2 gene expression in L-929 cells was lesser than in other cancer cells. In addition, there was no valuable distinction between the decrease in the Bcl-xL gene expression level of the IC_{50} treated group of L-929 cells according to the untreated control group ($p=0.295$). On the other hand, a significant difference was observed between the decrease in Bcl-xL gene expression level of all other cancer cell IC_{50} extract treated groups and untreated controls ($p<0.0001$).

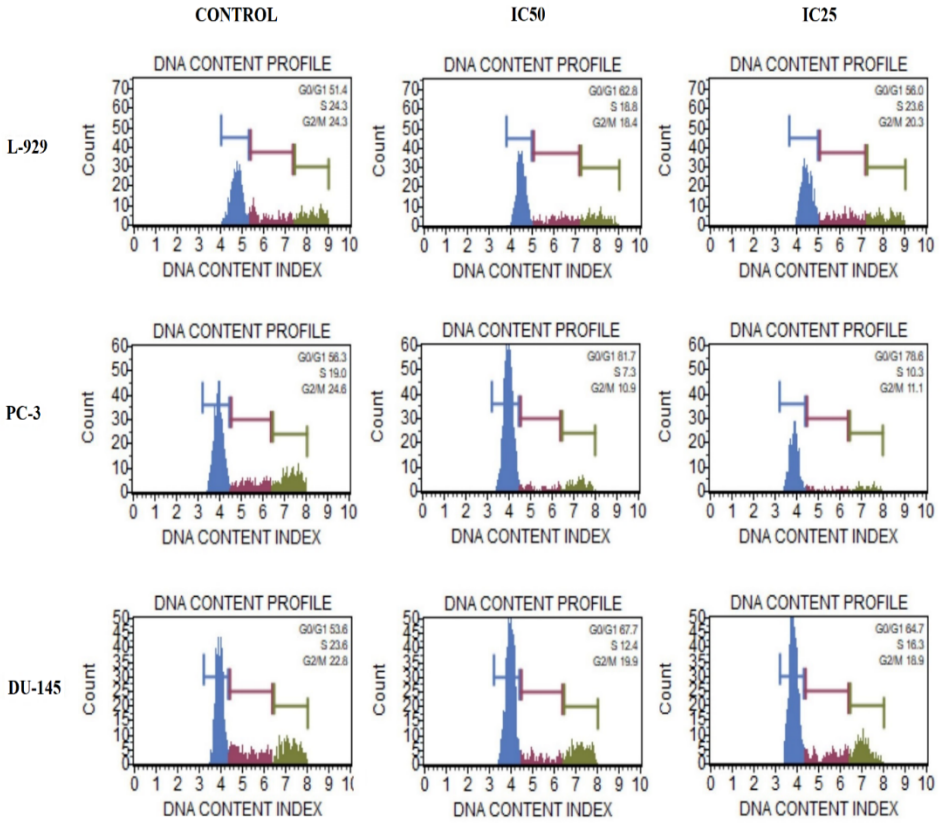

FIGURE 6. 48-hour cell cycle analysis values of L-929, PC-3, DU-145 cell lines treated with IC_{50} and IC_{25} Uludağ Fir resin extract

In addition, there was a significant increase in Caspase-3 and Cytochrome C gene expression levels of L-929, PC-3 and DU-145 treated at IC_{50} value for 24 hours compared to controls ($p<0.0001$). There was no significant difference between the increase in the Bax gene expression level of the IC_{50} extract treated group of L-929 cells and the Bax gene expression level of the control group ($p=0.060$). However, there was an significant difference between the increase in the Bax gene expression level of all IC_{50} extract treated cancer cell groups according to the untreated controls ($p<0.0001$).

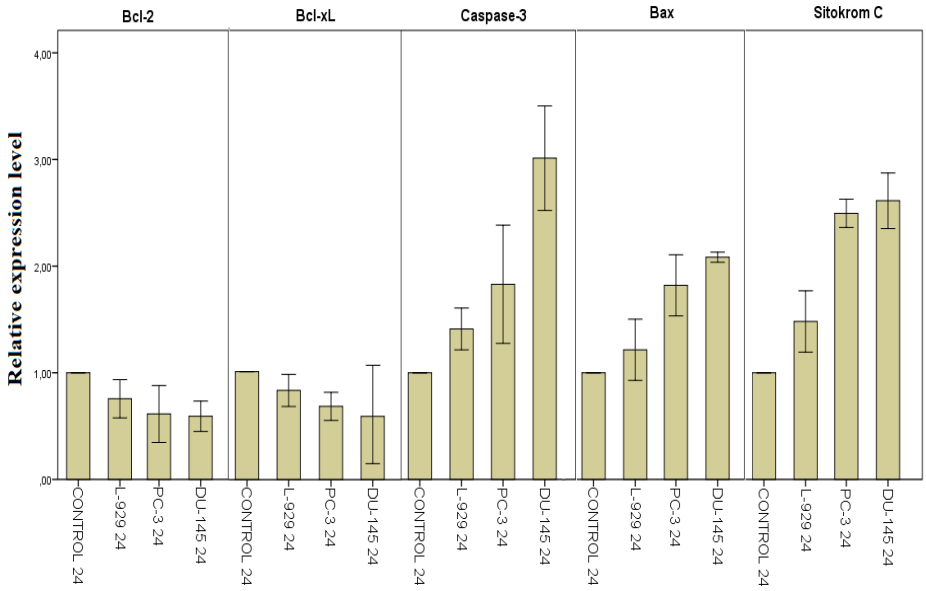

FIGURE 7. 24-hour relative gene expression values of L-929, PC-3, DU-145 cell lines treated with IC_{50} Uludağ Fir resin extract

Figure 8 shows a main decrease in mRNA expression levels of Bcl-2 and Bcl-xL genes in all cell types treated with extract at an IC_{50} value for 48 hours compared to untreated controls ($p<0.0001$), depending on the increased application time. Conversely, there was a significant increase in Caspase-3, Bcl-xL and Cytochrome C gene expression levels of all cell types treated with extract at IC_{50} value for 48 hours compared to untreated controls ($p<0.0001$). However, this increase in Caspase-3, Bcl-xL, and Cytochrome C genes of L-929 cells was more limited compared to PC-3 and DU-145 cancer cells.

Fir resins revealed high variation in composition even in closely related species, which agrees with previous reports on Balsam Fir and Cilician Fir [15,16]. In the current study, Uludağ Fir resin extract exhibited chemo preventive activities, such as inducing apoptosis and cell cycle arrest. Interestingly, Uludağ Fir resin extract revealed a less toxic effect on healthy normal L-929 control cells in contrast to PC-3 and DU-145 prostate cancer cells. Also, there are few studies about to anti-cancer effect of Fir resins extract.

Compared to the earlier studies, their findings revealed differences in means of IC_{50} values on healthy normal and cancer cells. Furthermore, according to Legault et al., the study on the cytotoxic activity of Balsam Fir resin extract was evaluated against different cancer and healthy normal cell lines.

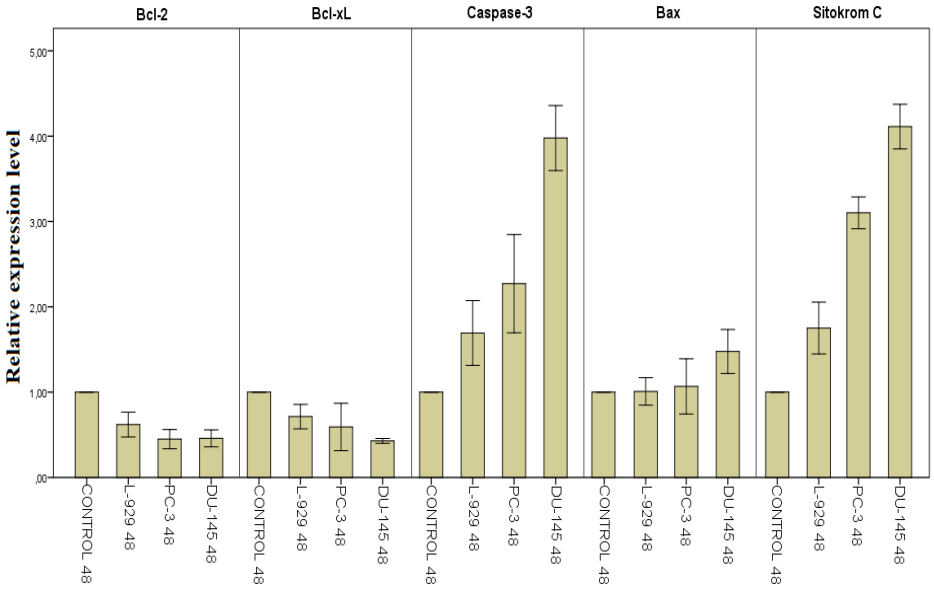

FIGURE 8. 48-hour relative gene expression values of L-929, PC-3, DU-145 cell lines treated with IC_{50} Uludağ Fir resin extract

As a result, they found a less toxic effect on L-929 fibroblast healthy normal cells (IC_{50}, 3100 µg/mL) and a higher toxic effect according to the IC_{50} level on different kinds of cancer cell lines ranging from 760 to 1700 µg/mL during the 24 hours experimental timeline [15]. On the other hand, the other study about the cytotoxicity of Cilician Fir resin extract revealed different results according to the above-mentioned study. They found a higher cytotoxic activity of the resin on WI-38 fibroblast healthy normal cells with lower concentration (IC_{50}, 18.32 µg/mL) and a lower toxic effect according to the IC_{50} level on different cancer cell lines ranging from 23 to 430.1 µg/mL during the 48 hours experimental timeline [16]. Meanwhile, our study results for Uludağ Fir resin extract exhibited lower cytotoxic activity on L-929 healthy normal cells (IC_{50}, 1110 µg/mL) and a higher toxic effect according to the IC_{50} level on different kinds of prostate cancer cell lines ranging from 930 to 940 µg/mL during the 48 hours experimental timeline, which is similar to the Legault et al. study results.

Determining the different types of programmed cell death (PCD) in the agent-treated cell group is essential [21]. PCD includes death mechanisms such as apoptosis, autophagy, necroptosis, and pyroptosis [22,23]. Therefore, determining the different types of cell death mechanisms in the agent-treated cell group is essential. In agent applications, the most common death mechanism is apoptosis. Furthermore, the mechanism of apoptosis was first investigated in cells to which Uludağ Fir resin extract was applied. Also, there are no reports about PCD type of Fir resin-treated cancer cells. According to this study result, apoptosis-related cell death mechanism was apparently determined in the Uludağ

Fir resin extract-treated cell lines during the 24 and 48 hours of extract treatment. Apoptosis detection occurred at higher concentrations in healthy normal cells, while it was observed in prostate cancer cell lines at lower concentrations, which can be clearly seen in Figures 3 and 4. On the other hand, cell cycle arrest is closely associated with apoptosis; that is, cell cycle arrest guides apoptosis via outcomes on different signaling molecules and regulatory proteins. There are many studies on cell cycle arrest and herbal extracts treatment association. Most of the herbal extract treatments on cancer cells result in the G0/G1 cell cycle arrest of cancer cells [24-26]. Similarly, our results demonstrated that Uludağ Fir resin extract induces cell cycle arrest at the G0/G1 phase in human prostate cancer cell lines. Besides, in both 24 and 48 hours IC_{50} and IC_{25} extract applications, the increase in the cell populations that arrested in the G0/G1 stage in healthy normal L-929 cells was found to be significantly less than in all other prostate cancer cell lines ($p<0.0001$).

The capacity of an agent to induce apoptosis in cancer cells demonstrates its potential for use as an anti-cancer agent. Therefore, the apoptosis-inducing potential of Uludağ Fir resin extracts was analyzed by examining the mRNA expression profile of apoptosis-related genes. Furthermore, determining the programmed cell death type makes it necessary to determine which gene-related signaling pathway effectively participates in the cell death process. Previous studies demonstrated that Compounds α/β-pinene and limonene revealed high in Fir resin in previous studies, are promising anticancer agents in recent years due to their ability to induce apoptosis and modulate various signaling pathways [15,16]. In addition, many studies have reported anti-cancer activity for α/β-pinene and limonene against various cancer types [27-30]. The apoptotic level is raised after the induction of nucleases, while the induction of caspase-3 is essential for heterochromatin aggregation and DNA fragmentation in apoptotic cells. Hence, to identify the involvement of caspase-3 in Uludağ Fir resin extract-mediated apoptosis, caspase-3 activity was estimated at the mRNA level. In the previous study, the activity of caspase-3 was found to be enhanced in α-pinene-treated human ovarian cancer cells (PA-1) [31]. Similarly, the result of this study revealed an increased level of caspase-3 expression in parallel with the increasing level of cytochrome-C and Bax expressions. Also, this increases in the expression level of pro-apoptotic caspase-3, cytochrome-C and Bax genes was accompanied by a decrease in the expression level of anti-apoptotic Bcl-2 and Bcl-xL genes. However, the pro-apoptotic and anti-apoptotic mRNA expression changes were lesser in healthy normal L-929 cells according to the human prostate cancer cell lines. According to this, to identify the involvement of caspase-3 in Uludağ Fir resin extract-mediated apoptosis, caspase-3 activity was estimated at the mRNA level.

4. CONCLUSION

Overall, in this study, the anti-cancer effect of the Uludağ Fir resin was analyzed by using flow cytometry and RT-qPCR. The tested resin extract demonstrates

anti-cancer effects in different prostate cancer cell lines by promoting cytotoxicity, halting cell cycle progression and the activation of apoptotic cell death. All these from the present study suggest that the extract of Uludağ Fir resin has the potential for cancer prevention.

Acknowledgment This research was financially supported by the Scientific Investigation Department of Manisa Celal Bayar University (project number 2021-080).

Author Contribution Statements MBB- conceptualization. MBB and FSÇ- data collection, management, and manuscript writing. SB and FÖK- project development, data analysis, manuscript editing, manuscript writing. All authors have read and approved the manuscript.

Declaration of Competing Interests The authors declare no conflict of interest.

REFERENCES

[1] Blagosklonny, M.V., Hallmarks of cancer and hallmarks of aging. *Aging*, 14 (9) (2022), 4176-4187. https://doi.org/10.18632/aging.204082.

[2] Chang, A.J., Autio, K.A., Roach, M., Scher, H.I., High-risk prostate cancer-classification and therapy. *Nature Reviews Clinical Oncology*, 11 (6) (2014), 308–323. https://doi.org/10.1038/nrclinonc.2014.68.

[3] Di Martile, M., Garzoli, S., Ragno, R., Del Bufalo, D., Essential oils and their main chemical components: The past 20 years of preclinical studies in melanoma. *Cancers*, 12 (9) (2020), 2650. https://doi.org/10.3390/cancers12092650.

[4] Cao, Y., Li, H., Harmony between humanity and nature: natural vs. synthetic drug preference in Chinese atheists and taoists. *Journal of Religion and Health*, 61 (4) (2022), 2743–2752. https://doi.org/10.1007/s10943-021-01314-6.

[5] Luethi, D., Liechti, M.E., Designer drugs: mechanism of action and adverse effects. *Archives of Toxicology*, 94 (4) (2020), 1085–1133. https://doi.org/10.1007/s00204-020-02693-7.

[6] Vaghari-Tabari, M., Hassanpour, P., Sadeghsoltani, F., Malakoti, F., Alemi, F., Qujeq, D., Asemi, Z., Yousefi, B., CRISPR/Cas9 gene editing: a new approach for overcoming drug resistance in cancer. *Cellular & Molecular Biology Letters*, 27 (1) (2022), 49. https://doi.org/10.1186/s11658-022-00348-2.

[7] Xavier, C.P.R., Caires, H.R., Barbosa, M.A.G., Bergantim, R., Guimarães, J.E., & Vasconcelos, M.H., The role of extracellular vesicles in the hallmarks of cancer and drug resistance. *Cells*, 9 (5) (2020), 1141. https://doi.org/10.3390/cells9051141.

[8] Martínez Andrade, K. A., Lauritano, C., Romano, G., Ianora, A., Marine microalgae with anti-cancer properties. *Marine Drugs*, 16 (5) (2018), 165. https://doi.org/10.3390/md16050165.

[9] Saadaoui, I., Rasheed, R., Abdulrahman, N., Bounnit, T., Cherif, M., Al Jabri, H., Mraiche, F., Algae-derived bioactive compounds with anti-lung cancer potential. *Marine Drugs*, 18 (4) (2020), 197. https://doi.org/10.3390/md18040197.

[10] Fitsiou, E., Pappa, A., Anticancer activity of essential oils and other extracts from aromatic plants grown in Greece. *Antioxidants*, 8 (8) (2019), 290. https://doi.org/10.3390/antiox8080290.

[11] Elansary, H. O., Abdelgaleil, S. A. M., Mahmoud, E. A., Yessoufou, K., Elhindi, K., El-Hendawy, S., Effective antioxidant, antimicrobial and anticancer activities of essential oils of horticultural aromatic crops in northern Egypt. *BMC Complementary and Alternative Medicine*, 18 (1) (2018), 214. https://doi.org/10.1186/s12906-018-2262-1.

[12] Zuzarte, M., Francisco, V., Neves, B., Liberal, J., Cavaleiro, C., Canhoto, J., Salgueiro, L., Cruz, M.T., *Lavandula viridis* L´Hér. Essential oil inhibits the inflammatory response in macrophages through blockade of NF-KB signaling cascade. *Frontiers in Pharmacology*, 12 (2022), 695911. https://doi.org/10.3389/fphar.2021.695911.

[13] Walia, M., Mann, T.S., Kumar, D., Agnihotri, V.K., Singh, B., Chemical composition and in vitro cytotoxic activity of essential oil of leaves of *Malus domestica* growing in Western Himalaya (India). *Evidence-based Complementary and Alternative Medicine*, eCAM, 2012, 649727. https://doi.org/10.1155/2012/649727.

[14] Thalappil, M.A., Butturini, E., Carcereri de Prati, A., Bettin, I., Antonini, L., Sapienza, F.U., Garzoli, S., Ragno, R., Mariotto, S., *Pinus mugo* essential oil impairs STAT3 activation through oxidative stress and induces apoptosis in prostate cancer cells. *Molecules*, 27 (15) (2022), 4834. https://doi.org/10.3390/molecules27154834.

[15] Legault, J., Dahl, W., Debiton, E., Pichette, A., Madelmont, J.C., Antitumor activity of balsam fir oil: production of reactive oxygen species induced by alpha-humulene as possible mechanism of action. *Planta Medica*, 69 (5) (2003), 402–407. https://doi.org/10.1055/s-2003-39695.

[16] Uçar, S.E, Şahin, B.S., Ulu, M., Akpolat, A., The determination of in vitro antioxidant and cytotoxic activities of resin obtained from Cilician Fir (Abies cilicica (Antoine & Kotschy) Carrière). *Kahramanmaraş Sütçü İmam Üniversitesi Tarım ve Doğa Dergisi,* 23 (6) (2020), 1503-1509. https://doi.org/10.18016/ksutarimdoga.vi.720675.

[17] Kudryavtseva, A., Krasnov, G., Lipatova, A., Alekseev, B., Maganova, F., Shaposhnikov, M., Fedorova, M., Snezhkina, A., Moskalev, A., Effects of *Abies sibirica* terpenes on cancer- and aging-associated pathways in human cells. *Oncotarget*, 7 (50) (2016), 83744–83754. https://doi.org/10.18632/oncotarget.13467.

[18] Anşin, R., Özkan, Z., Abies Mill. Göknarlar, Tohumlu Bitkiler (Spermatophyta), Odunsu Taksonlar, Karadeniz Teknik Üniversitesi, Orman Fakültesi. Trabzon. 167, 19 (1997), 66-72.

[19] Oztatlici, H., Oztatlici, M., Daglı, S. N., Karadeniz Saygili, S., Bir sefalosporin olan sefepim, nb2a nöroblastoma hücrelerinde apoptozu ve oksidatif stresi indükler. *Euroasia Journal of Mathematics, Engineering, Natural & Medical Sciences*, 9 (21) (2022), 79–86. https://doi.org/10.38065/euroasiaorg.962.

[20] Livak, K. J., Schmittgen, T. D., Analysis of relative gene expression data using real-time quantitative PCR and the 2(-Delta Delta C(T)) Method. *Methods*, 25 (4) (2001), 402–408. https://doi.org/10.1006/meth.2001.1262.

[21] Lin, L., Zhang, M. X., Zhang, L., Zhang, D., Li, C., Li, Y. L., Autophagy, pyroptosis, and ferroptosis: New regulatory mechanisms for atherosclerosis. *Frontiers in Cell and Developmental Biology*, 9 (2022), 809955. https://doi.org/10.3389/fcell.2021.809955.

[22] Zhao, J., Jiang, P., Guo, S., Schrodi, S. J., He, D., Apoptosis, autophagy, NETosis, necroptosis, and pyroptosis mediated programmed cell death as targets for innovative therapy in Rheumatoid Arthritis. *Frontiers in Immunology*, 12 (2021), 809806. https://doi.org/10.3389/fimmu.2021.809806.

[23] Bertheloot, D., Latz, E., Franklin, B.S., Necroptosis, pyroptosis and apoptosis: an intricate game of cell death. *Cellular & Molecular Immunology*, 18 (5) (2021), 106-1121. https://doi.org/10.1038/s41423-020-00630-3.

[24] Trang, D.T., Hoang, T.K.V., Nguyen, T.T.M., Van Cuong, P., Dang, N.H., Dang, H.D., Nguyen Quang, T., Dat, N.T., Essential oils of lemongrass (Cymbopogon citratus Stapf) induces apoptosis and cell cycle arrest in A549 lung cancer cells. *BioMed research international*, (2020), 5924856. https://doi.org/10.1155/2020/5924856.

[25] Chung, K. S., Hong, J. Y., Lee, J. H., Lee, H. J., Park, J. Y., Choi, J. H., Park, H. J., Hong, J., Lee, K. T., β-Caryophyllene in the essential oil from Chrysanthemum Boreale induces G1 phase cell cycle arrest in human lung cancer cells. *Molecules*, 24 (20) (2019), 3754. https://doi.org/10.3390/molecules24203754.

[26] Seal, S., Chatterjee, P., Bhattacharya, S., Pal, D., Dasgupta, S., Kundu, R., Mukherjee, S., Bhattacharya, S., Bhuyan, M., Bhattacharyya, P. R., Baishya, G., Barua, N. C., Baruah, P. K., Rao, P. G., Bhattacharya, S., Vapor of volatile oils from Litsea cubeba seed induces apoptosis and causes cell cycle arrest in lung cancer cells. *PloS One*, 7 (10) (2012), e47014.4 https://doi.org/10.1371/journal.pone.0047014.

[27] Salehi, B., Upadhyay, S., Erdogan Orhan, I., Kumar Jugran, A., L D Jayaweera, S., A Dias, D., Sharopov, F., Taheri, Y., Martins, N., Baghalpour, N., Cho, W. C., Sharifi-Rad, J., Therapeutic potential of α- and β-Pinene: A miracle gift of nature. *Biomolecules*, 9 (11) (2019), 738. https://doi.org/10.3390/biom9110738.

[28] Li Y, Gao Y, Deng L, Lian H, Guo W, Wu W, Xue B, Li B, Su Y, Zhang H. Volatile profiling and transcriptome sequencing provide insights into the biosynthesis of α-pinene and β-pinene in Liquidambar formosana hance leaves. *Genes*, 14 (1) 163. https://doi.org/10.3390/genes14010163.

[29] Chebet, J. J., Ehiri, J. E., McClelland, D. J., Taren, D., Hakim, I. A., Effect of d-limonene and its derivatives on breast cancer in human trials: a scoping review and narrative synthesis. *BMC cancer*, 21 (1) (2021) 902. https://doi.org/10.1186/s12885-021-08639-1.

[30] Alipanah, H., Farjam, M., Zarenezhad, E., Roozitalab, G., Osanloo, M., Chitosan nanoparticles containing limonene and limonene-rich essential oils: potential phytotherapy agents for the treatment of melanoma and breast cancers. *BMC Complementary Medicine and Therapies*, 21 (1) (2021), 186. https://doi.org/10.1186/s12906-021-03362-7.

[31] Hou, J., Zhang, Y., Zhu, Y., Zhou, B., Ren, C., Liang, S., Guo, Y., α-Pinene induces apoptotic cell death via caspase activation in human ovarian cancer cells. *Medical Science Monitor*, 25 (2019), 6631–6638. https://doi.org/10.12659/MSM.916419.

http://communications.science.ankara.edu.tr

Commun.Fac.Sci.Univ.Ank.Ser. C Biology
Volume 32, Number 2, Pages 137-149 (2023)
ISSN 1303-6025 E-ISSN 2651-3749
DOI: 10.53447/communc.1317798

Research Article; Received: June 21, 2023; Accepted: July 15, 2023

DETECTION TARGET GENES IN COMBATING BIOFILM FORMS IN *SALMONELLA* TYPHIMURIUM 14028

SARAH FARHAD NİHAD[1], NEFİSE AKÇELİK[2], MUSTAFA AKÇELİK[1]

[1]Department of Biology, Faculty of Science, Ankara University, Ankara, TÜRKİYE
[2]Biotechnology Institute, Ankara University, Ankara, TÜRKİYE

ABSTRACT. In this study, the relationship of *hilA, invA, adrA, spiC, otsB* and *csgD* genes, which are known to play critical roles in the pathogenicity and virulence of *Salmonella* strains, with biofilm formation was investigated by examining the changes in the expression levels of these genes during the transition from planktonic form to biofilm form. When the virulence gene expressions between the *S.* Typhimurium 14028 mutant, which lost its ability to form biofilms due to *csgD* gene deletion, and the wild type strain were compared, it was determined that the expression levels of *hilA, invA* and *adrA* genes increased, whereas the expression levels of *spiC, otsB* and *csgD* genes decreased. These data indicate that all examined genes play critical activation or inhibition roles in biofilm regulation as well as pathogenicity and virulence. On the other hand, in the mutant strain; The increase in the expression levels of *hilA, invA* and *adrA* genes shows that inhibitors of the proteins encoded by these genes have the potential to be of practical use in the prevention and control of infections caused by both biofilm-forming and non-biofilm-forming *Salmonella* strains.

1. INTRODUCTION

Salmonella is an important genus of pathogenic bacteria that has many hosts and causes different diseases in these hosts, including different subspecies and serovariates. In addition to the serovariates of species and subspecies of this genus adapted to certain host organisms, serovariates with wide host ranges can also be found. These serovariates can cause local or systemic diseases with very different courses from limited gastroenteritis caused by non-typhoid *Salmonella* (NTS) serovariates to typhoid fever, which can result in fatal intestinal perforation. Although it has been determined that plant material is a serious source of contamination today; animal products, especially poultry products, are identified as the main sources of *Salmonella* sp. [1].

The clinical course and outcome of salmonellosis is characterized by a complex host-bacteria interactions. Efficiency of host response to infection by NTS *Salmonella* serovariates, it varies depending on many factors such as nutritional status, age, gastric pH, genetic predisposition, and both innate and adaptive immunity [2]. Bacterial features that contribute to the severity of the disease can be defined as serotype, infectious dose, physiological state of bacterial cells,

Keywords. Salmonella, biofilm, gene expression, qRT-PCR

sarahfarhad92@gmail.com- 0009-0009-9999-6445
nakcelik@ankara.edu.tr 0000-0001-5541-1681
akcelik@science.ankara.edu.tr- Corresponding author; 0000-0002-1227-2324

antimicrobial resistance (AMR), gene inactivation and virulence factors. It is possible to summarize virulence factors of *Salmonella* as toxins, capsule, flagella, fimbrial structures, effector proteins and their secretion systems. These factors are encoded by *Salmonella* Pathogenicity Islands (SPIs), virulence plasmids or prophages (temperate phages). To date, 24 SPIs have been identified whose functionality has been described at different stages of *Salmonella* infection. Among these SPIs, SPI-1 and SPI-2 are the ones whose genetic and phenotypic features have been studied the most. SPI-1 is common in both *S. enterica* and *S. bongori* and encodes a type three secretion system (T3SS) that allows the displacement of effector molecules involved in the invasion of host cells. SPI-2, found in many subspecies of *S. enterica* but not in *S. bongori*, contains an additional T3SS genes involved in the translocation of effector molecules important for the intracellular survival of these bacteria. Other SPIs are variably present in *S. enterica* subspecies, and some encode other secretion systems such as T1SS and T6SS, other effector molecules and fimbriae [3].

The much higher resistance of biofilm forms of these bacteria to antimicrobial agents compared to planktonic strains increases the likelihood of failures in the prevention and treatment of the spread of *Salmonella* infections and limits therapeutic options in industrial and clinical applications when treatment is required. In addition to their high resistance to adverse environmental conditions, biofilms that develop on equipment and tools used in food industry and medical treatment also constitute reservoirs of pathogenic and food spoilage microorganisms that increase the risk of microbial contamination [4,5,6]. For these reasons, *Salmonella* biofilm infections originating from the food industry and hospitals cause serious health problems and economic losses all over the world [6].

Biofilm structures, which are a multicellular organization-like life form, are the result of genetic and therefore physiological reprogramming of bacteria attached to a surface in solid-air or liquid-air intermediate phases, surrounded by an exopolymeric matrix that functions as a protection against stress conditions and a nutrient store. The formation of functional differentiation in cells of the same species in the biofilm structure is the main reason why these structures are defined as multicellular bacterial life forms [7]. The fact that the resistance of the biofilm structures of bacteria to all known bacterial control agents is much higher than the planktonic forms of the same bacteria has brought about the necessity of determining new control agents against these structures. In this regard, the detection or development of natural or synthetic antibiofilm agents is one of the most commonly used strategies. Here, the fact that the biofilm matrix generally does not allow the penetration of the agents in question or significantly prevents their entry into the biofilm structure is the main reason limiting the chance of combating new agents [8,9,10]. The safest way to overcome this handicap is to determine the genetic expression differences that occur in the transition from the planktonic form to the biofilm form in a bacterium and to develop specific control agents for the gene products to be selected in this direction. In this way,

both the prevention of the formation of biofilm structures and the eradication of the formed biofilms will be possible in a safer way [11].

In this study, the expression levels of *otsB, spiC, adrA, csgD, hilA* and *invA* genes that play a role in virulence and pathogenicity in *S.* Typhimurium 14028 wild-type strain and its mutant with impaired biofilm forming ability (14028*ΔcsgD*) were examined, and the efficacy of these genes in the transition to biofilm form was investigated. Therefore, it is aimed to lay the foundations of an effective antibiofilm strategy that will target both biofilm structures and pathogen-associated molecular patterns (PAMPs).

2. MATERIALS AND METHODS

2.1 Biomaterial

S. Typhimurium 14028 strain was obtained from American Type Culture Collection (ATCC, 10801 University Blvd, Manassas, VA, USA), and the *csgD* gene mutant of this strain, which cannot form biofilm, was obtained from Ankara University Biotechnology Institute. Luria-Bertani (LB) broth and agar (Merck, Rahway, NJ 07065 USA) media were used for the activation and routine production of bacteria from stock cultures. Stock cultures were stored in LB broth media containing 40% glycerol at -80 ^{0}C.

2.2. Formation and measurement of biofilm structures

After single colonies of the bacteria to be tested were suspended in TSB medium, the density of the suspension was standardized by comparison with the 1.0 McFarland standard (ie. 3.0 X 10^8 cfu/mL). Cultures were diluted 1:30 in freshly prepared growth medium to obtain a bacterial concentration of approximately 1.0 X 10^7 cfu/mL in sterile polypropylene or glass tubes. Thereafter, 150 µL volumes of 1/30 dilutions were added to each well of a 96-well microtiter plate (Corning® Thermowell PCR 96 well plates, Merck, Rahway, NJ 07065 USA). After the autoclaved PEGs (Merck, Rahway, NJ 07065 USA) were placed in the growth medium, the microtiter plates were covered with aluminum foil and incubated at 20 ºC for 24, 48 and 72 hours. After the supernatants were removed at the end of the incubation period, the wells were washed three times with phosphate-buffered saline (PBS, pH 7.0±2.0). After washing, 140 µL of 95 % methanol was added to fix the biofilm structures attached to the PEGs and kept at room temperature for 20 minutes. Biofilm structures were stained for 15 minutes using 1% crystal violet. The plates were washed with sterile distilled water, and the microplates were dried at room temperature after removing the dye that did not adhere to the biofilm structures. 140 µL (33%) glacial acetic acid was added to the wells to dissolve the dye bound to the produced biofilm, and the plates were incubated at room temperature for 30 minutes. At the end of the incubation, the amount of dye attached to the biofilm was determined at OD_{595} nm in the ELISA reader (Biorad, USA). The final calculation was performed by subtracting the average of the OD values of the control (wells containing LB-

NaCl broth only) group from the mean of the OD values determined for the strains tested. These trials were carried out in 3 parallel and 2 repetitions [12].

2.3. Quantitative real time PCR (QRT-PCR)

S. Typhimurium 14028 and its mutant obtained by deletion of *csgD* regulator gene were inoculated at 1% in LB broth medium and incubated at 37 ºC under shaking conditions until the optical density (OD_{600}) value reached approximately 0.6 in the growth medium. High Pure RNA Isolation (Promega) kit was used for total RNA detection from bacterial cultures. Purity and quantification of the obtained RNAs were determined using the ND-1000 spectrophotometer (Thermo Scientific / USA) device, and electrophoresis was performed in 2% agarose gel at 100 V constant electric current for 1 hour. RNA gels containing 0.2 µg/mL EtBr were visualized under UV light. Molecular size determination was performed using the GeneRuler 1 kb (kilobase) DNA Ladder (Thermo Scientific / USA).

cDNA synthesis with RNA samples obtained from *S.* Typhimurium 14028 and *csgD g*ene mutant was performed using cDNA synthesis Kit (Roche, Germany). The reaction mixtures used in cDNA synthesis and the applied temperature cycle were given Tables 1, 2 and 3. The resulting cDNAs were stored at -20 °C until qRT-PCR experiments.

TABLE 1. Denaturation solution

Contents	**Concentration**	**Final Concentration**	**Volume (µL)**
RNA	-	1000 ng/µL	-
Random primer	600 pmol/µL	60 µM	2
Water (PCR grade)	-	-	Volume is made up 13 µL

TABLE 2. Reverse transcription solution

Contents	**Concentration**	**Final Concentration**	**Volume (µL)**
Reverse transcription buffer	5X	1X (8 mM $MgCl_2$)	4
RNase inhibitor	40 U/µL	20 U	0.5
dNTP mix	10 mM for each nucleotide	1 mM for every nucleotide	2
Reverse transcriptase	20 U/mL	10 U	0.5
Final volume	-	-	**20**

TABLE 3. Temperature cycle for reverse transcription reactions

Steps	Temperature (°C)	Time (min)	Number of cycle
Elongation 1	25	10	1
Elongation 2	50	60	1
Inactivation	85	5	1

2.4 Determination of gene expression levels

The genes whose expression levels were investigated in QRT-PCR experiments and the primers designed specifically for these genes are given in Table 4. LightCycler 480 (Roche, Germany) device was used for all QRT-PCR experiments performed in this study. 5 X HOT FIREPol EvaGreen QRT-PCR Supermix (Solis BioDyne, Estonia) kit was used as the amplification mix for all the genes given in Table 5. The amplification mix for QRT-PCR is given in Table 6. Amplification reactions were performed in 96-well plates in a total volume of 10 μL. The reaction mixture containing the same volume of ddH2O without the cDNA template was used as a negative control (NK). The program used for amplification in Light Cycler 480 device performed as given in Table 6 [13].

TABLE 4. Genes and primers

Target Genes and Their Functions	Primer	Reference
adrA, Regulator for cellulose production	F: GGCTGGGTCAGCTACCAG R: CGTCGGTTATACACGCCCG	[14]
csgD, Regulator for curli fimbria synthesis	F: ACGCTACTGAAG ACC AGG AAC R: GCATTCGCCACGCAGAATA	[15]
hilA, Virulence regulator	F: CATGGCTGGTCAGTTGGAG R: CGTAATTCATCGCCTAAACG	[16]
spiC, Encodes an efector protein. For host cell invasion	F: CTGTGGCTTTCAGTGGTCAG R: TGCGTTGTCCGGTAGTATTTC	[16]
invA, Host cell invasion	F: CACGCTCTTTCGTCTGGCA R: TACGGTTCCTTTGACGGTGCGA	[17]
otsB, stress response, trehalose production	F: TTAACCGTATCCCCCGAACTC R: CCGCGAGACGGTCTAACAAC	[18]

TABLE 5. Amplification mixture for QRT-PCR

Contents	Final Concentration	Volume (µL)
EvaGreen qPCR supermix (5X)	1X	2
Forward primer	10 pmol / µL	0.5
Reverse primer	10 pmol / µL	0.5
cDNA (1:10)	10 ng /µL	1
ddH_2O	-	6
Final volume	-	10

TABLE 6. qRT-PCR programme for LightCycler 480

Steps	Process	Temperature (^{0}C)	Time
First denaturation	First denaturation	95	15 dk
Amplification (40 cycles)	Denaturation	95	15 sn
	Annealing	58*	20 sn
	Elongation	72	20 sn
Melting curve	Denaturation	95	30 sn
	Annealing	60	30 sn
	Elongation	99	30 sn
Cooling	Cooling	40	30 sn

*Primer binding Temperature™ was determined as 58 ºC for all tested genes and 55 ºC for the reference gene 16S rDNA.

2.5 Statistical analyses

Statistical analyzes of the data obtained from the study were performed using Graph Pad Prism Version 5.10 (Graph Pad Software Inc., San Diego, CA, USA). In this program, the data were first subjected to Dunnett post hoc and then one-way ANOVA analysis. The normalization of the data obtained from the live cell counts was performed on the basis of log10 [19]. In the interpretation of all statistical studies, the threshold P value was taken as <0.05.

3. RESULTS AND DISCUSSION

3.1. Biofilm formation characteristics of wild type strain and its *csgD* gene deleted mutant

In the study conducted to determine the biofilm production capacities of *S.* Typhimurium 14028 wild type and its *csgD* mutant strain, the highest amount of biofilm production was determined at 72 hours in the incubation periods tried. The amount of biofilm production of the *csgD* gene mutant strain was reduced by approximately 90-95% ($p<0.05$) compared to the wild type at all incubation times tried (Figure 1). These measurement values in the mutant are within the definition of the strain that does not have the ability to produce biofilms [20,21,22].

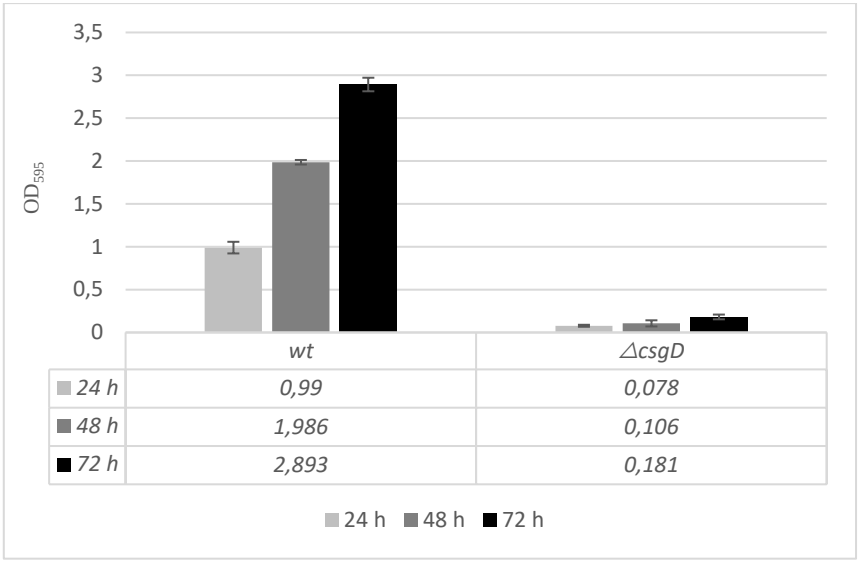

FIGURE 1. Biofilm production capacities of *S.* Typhimurium 14028 wild type strain and its *csgD* mutant.

3.2. Changes in expression levels of virulence and pathogenicity-related genes in *S.* Typhimurium 14028 wild type strain and its non-biofilm forming mutant (14028*ΔcsgD*)

In order to determine the changes in virulence and pathogenicity between *S.* Typhimurium 14028 wild type strain and its biofilm-forming mutant (14028*ΔcsgD*), expression levels of *otsB*, *spiC*, *adrA*, *csgD*, *hilA* and *invA* genes were investigated. For the qRT-PCR experiments carried out in this direction, total RNA isolations from all strains were performed in the first step and the purity of the isolated RNA samples were checked on agarose gels (Figure 2).

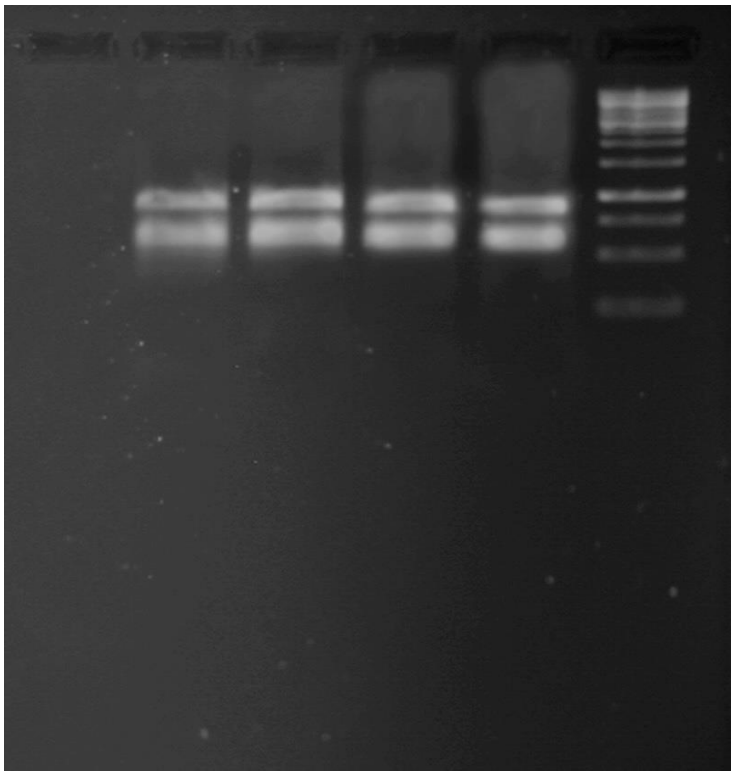

FIGURE 2. Agarose gel image of total RNAs isolated from *S.* Typhimurium 14028 and *ΔcsgD* mutant.

In the next step, cDNA synthesis was performed from the RNA samples determined to be of sufficient purity and concentration, and the obtained cDNA samples were used in qRT-PCR experiments. In order to analyze the qRT-PCR data obtained from the experiments, the amplification efficiencies of the primers were added to the normalization calculations as a variable. In summary, Ct values obtained for each primer pair using serial dilutions prepared with cDNA samples obtained from *S.* Typhimurium 14028 wild type strain were used as calibrators. Expression level of 16S rRNA gene, which is a housekeeing gene, was used as qRT-PCR control (Table 7 and Figure 3).

TABLE 7. Ct values of genes whose expression levels were investigated in wild type and mutant strains

CT Values	*otsB*	*spiC*	*adrA*	*csgD*	*hilA*	*invA*	*16S RNA*
14028 WT	24,56	24,47	24,49	25,22	24,54	24,47	30,22
	24,51	24,44	24,44	25,16	24,56	24,51	30,57
	24,54	24,36	24,33	25,24	24,64	24,48	32,14
14028*ΔcsgD*	28,31	28,57	21,01	28,18	20,71	21,34	31,145
	28,13	28,06	20,99	27,02	20,61	21,48	30,87
	28,14	28,3	20,99	27,74	20,65	21,49	31,81

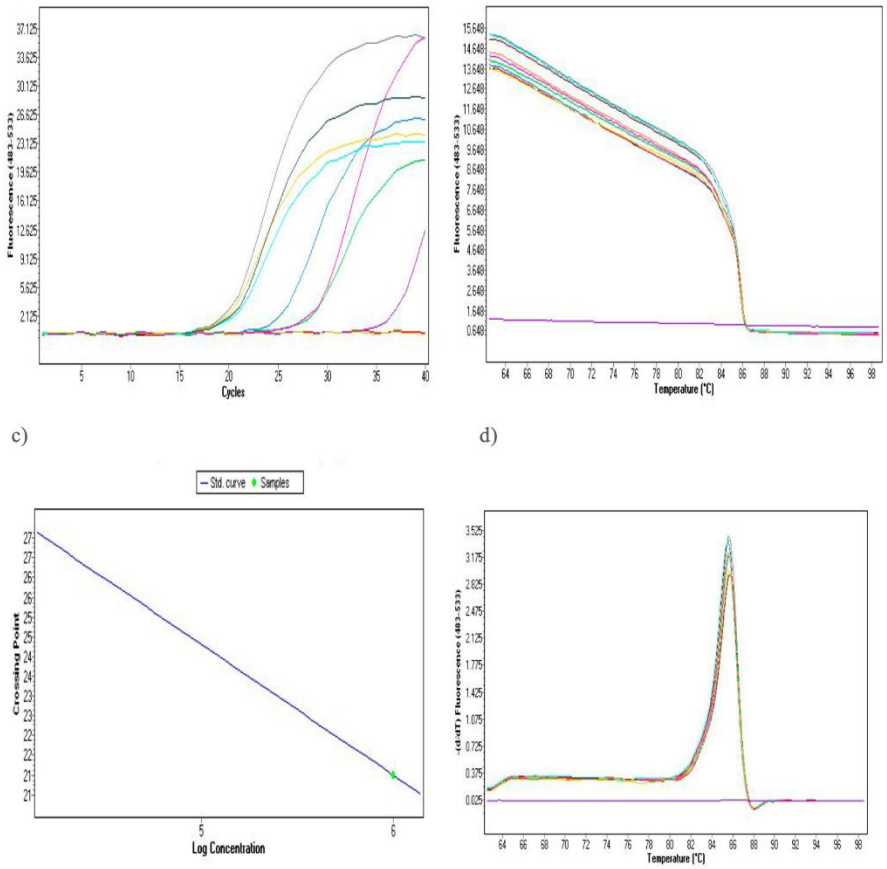

FIGURE 3. Results of the standardization process performed in qRT-PCR experiments. a) amplification curves, b) melting curves, c) standard curve, d) melting peaks.

After these standardization and normalization measurements, fold changes in the expression levels of the genes investigated using the Livak method were determined. As a result of these studies, the expression levels of the investigated genes in *S*. Typhimurium 14028 wild-type strain and its biofilm deficient mutant (14028*ΔcsgD*) were defined comparatively. According to these data, the expression levels of *spiC, otsB* and *csgD* genes were decreased by 12.25, 10.26 and 4.41 folds (*p≤0.05), and the expression levels of *adrA, hilA* and *invA* genes increased by 13.19, 18.66 and 10.18 folds, respectively, in mutant strain (Figure 4).

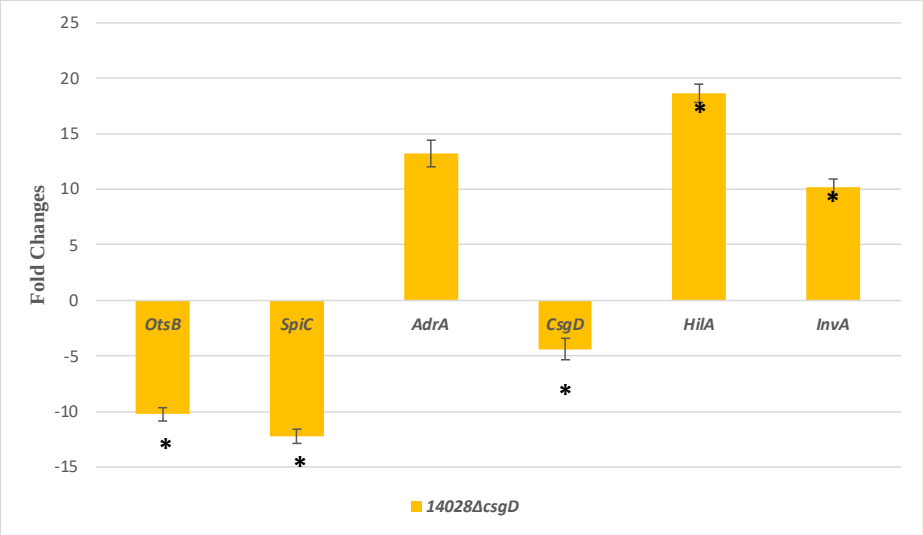

FIGURE 4. Fold changes of normalized gene expression levels in *S.* Typhimurim 14028 *csgD* mutant compared to wild-type strain.

When the data obtained from these trials were examined; The *hilA* gene, which is a member of the Ompr/ToxR family and acts as a transcriptional activator of genes related to host cell invasion in *S.* Typhimurium [23], the *invA* gene, which is the positive regulator of the Type 3 Secretory System (T3SS) [24] and the *adrA* gene, which encodes an enzyme that participates in cyclic di ganosyl monophosphate (c-di-GMP) metabolism in *Salmonella*, and which in this way is active in the biosynthesis of cellulose[25], expression levels were found to increase. This indicates that environmental adaptation is achieved by increasing host cell invasion functions in mutants whose environmental persistence has decreased due to loss of biofilm formation ability. These findings may shed light on the evolution of *Salmonella* pathogenicity, with expression levels of genes involved in whole cell invasion generalized by comparative analysis. These findings also show that inhibitors of the proteins encoded by these genes have the potential to be of practical use in the prevention and control of infections caused by both biofilm-forming and non-biofilm-forming *Salmonella* strains.

On the other hand, the decrease in the expression level of the *spiC* gene [26], which encodes a translocator protein in *Salmonella* and whose role in pathogenicity is controversial, but which is claimed to be involved in traffic blocking in cases where cell trafficking is disrupted, indicates that the gene in question has functions different from those suggested in the literature. In addition, the decrease in the expression of the *otsB* gene [27], which encodes the acid stress and low water activity resistance protein in the mutant that has lost the ability to form biofilm, is a new evidence supporting the relationship of these functions with biofilm structures. Finally, the detection of decreased expression levels of the *csgD* gene [28], which is the transcriptional regulator of the coiled fimbria, which is an important component of the biofilm matrix in *Salmonella* serovariates, is evidence that the target function of the mutant used is impaired.

4. CONCLUSIONS

In our study, differences in the expression levels of certain virulence genes were investigated between the *S.* Typhimrium 14028 wild strain and its biofilm-deficient mutant (14028*ΔcsgD*) to identify pathogen-associated molecular patterns (PAMP) to be targeted to combat *Salmonella* biofilm forms. These expression differences clearly showed that the expression levels of three important genes known to play a role in *Salmonella* pathogenicity and virulence (*invA*, *hilA* and *adrA*) were increased in the biofilm-producing mutant of *S.* Typhimurium 14028 strain. This indicates that these genes play important roles not only in pathogenicity and virulence, but also in the transition from the planktonic form to the biofilm form. In the light of these data, it is possible to say that choosing and testing natural or synthetic compounds with strong inhibitory activity against the products of *invA*, *hilA* and *adrA* genes as antibiofilm agents has a strong potential to combat biofilm structures.

Author Contribution Statements SFN- data collection and analysis, interpretation of results and draft manuscript preparation. NA-study conception and design, data analysis, interpretation of results, manuscript editing. MA-study conception and design, interpretation of results, manuscript editing. All authors reviewed the results and approved the final version of the manuscript.

Declaration of Competing Interests The authors declare no conflict of interest.

REFERENCES

[1] Brasil, A. Agência Nacional de Vigilância Sanitária., Programa Nacional de Monitoramento de Prevalência e da Resistência Bacteriana em Frangos - PREBAF. Monitoramento de prevalência e do perfil de susceptibilidade aos antimicrobianos em enterococos e salmonelas isolados de carcaças de frango congeladas comercializadas no Brasil. Brasília, DF, *ANVISA*, (2013), p.1-171.

[2] Cheng, R.A., Eade, C.R., Wiedmann, M., Embracing diversity: differences in virulence mechanisms, disease severity, and host adaptations contribute to the success of nontyphoidal *Salmonella* as a foodborne pathogen. *Frontiers in Microbiology*, 10 (2019), 1368-1378. https://doi.org/10.3389/fmicb.2019.01368.

[3] Scallan, E., Hoekstra, R.M., Angulo. F.J., Tauxe, R.V., Widdowson, M.A., Roy, S.L., Jones, J.L., Griffin, P.M., Foodborne illness acquired in the United States--major pathogens. *Emerging Infectious Diseases*. 17 (2011), 7-15. doi: 10.3201/eid1701.P11101.

[4] Xu, H., Lee, H.Y., Ahn, J., Growth and virulence properties of biofilm-forming *Salmonella enterica* serovar. Typhimurium under different acidic conditions. *Applied Environmental Microbiology*, 76 (2010), 910-917. doi: 10.1128/AEM.01508-10.

[5] Hasegawa, A., Hara-Kudo, Y., Kumagai, S., Survival of *Salmonella* strains differing in their biofilm-formation capability upon exposure to hydrochloric and acetic acid and to high salt. *Journal of Veterinary Medical Science*, 73 (2011), 1163-1168. doi: 10.1292/jvms.11-0090.

[6] Yang, Y. C., Lii, C. K., Wei, Y. L., Li, C. C., Lu, C. Y., Liu, K. L., Docosahexaenoic acid inhibition of inflammation is partially via cross-talk between Nrf2/heme oxygenase 1 and IKK/NFkappaB pathways. *The Journal of Nutritional Biochemistry*. 24 (2013), 204–212. doi: 10.1016/j.jnutbio.2012.05.003.

[7] Akçelik, M., Akçelik, N., What makes another life possible in bacteria? Global regulators as architecs of bacterial biofilms. *World Journal of Microbiology and Biotechneology*, 28 (2023), 26-36. doi: 10.1007/s11274-022-03376-4.

[8] Allen, N. E., From vancomycin to oritavancin: the discovery and development of a novel lipoglycopeptide antibiotic. *Anti-Infective Agents in Medicinal Chemistry*. 9 (2010), 23–47. doi: 10.2174/187152110790886745.

[9] Barraud, N., Kelso, M. J., Rice, S. A., Kjelleberg, S., Nitric oxide: a key mediator of biofilm dispersal with applications in infectious diseases. *Current Pharmaceutical Design*. 21 (2015), 31–42. doi: 10.2174/1381612820666140905112822.

[10] Özdemir, C., Akçelik, N., Özdemir, F.N., Evcili, İ., Kahraman, T., Gürsel, İ., Akçelik, M., The role of *bcsE* gene in the pathogenicity of *Salmonella*. *Pathogens and Disease*. 79 (2021),156-165. doi: 10.1093/femspd/ftab037

[11] Özdemir, F.N., Buzrul, S., Özdemir, C. Akçelik, N., Akçelik, M., Determination of an effective agent combination using nisin against *Salmonella* biofilm. *Archives of Microbiology*. 204 (2022), 167-172. doi: 10.1007/s00203-022-02766-4

[12] Kurtz, J.R., Nieves, W., Bauer, D.L., Israel, K.E., Adcox, H.E., Gunn, J.S., Morici, L.A., McLachlan, J.B., *Salmonella* persistence and host immunity are dictated by the anatomical microenvironment. *Infection and Immunity*. 21(2020) 3507-3512. doi: 10.1128/IAI.00026-20

[13] Yoon, B. K., Jackman, J. A., Valle-González, E. R., Cho, N.J., Antibacterial free fatty acids and monoglycerides: biological activities, experimental testing, and therapeutic applications. *International Journal of Molecular Sciences*. 19 (2018), 1114-1121. doi: 10.3390/ijms19041114.

[14] Gualdi, L., Tagliabue, L., Bertagnoli, S., Ierano, T., De Castro, C., Landini, P., Cellulose modulates biofilm formation by counteracting curli-mediated colonization of solid surfaces in *Escherichia coli*. *Microbiology*, 154 (2008). 2017–2024. doi: 10.1099/mic.0.2008/018093-0.

[15] Monteiro, C., Papenfort, K., Hentrich, K., Ahmad, I., Le Guyon, S., Reimann, R., Grantcharova, N., Römling, U., Hfq and Hfq-dependent small RNAs are major contributors to multicellular development in *Salmonella enterica* serovar Typhimurium. *RNA Biology*. 94 (2012), 489-502. doi: 10.4161/rna.19682

[16] Mizusaki, H., Takaya, A., Yamamoto, T., Aizawa, S., Signal pathway in salt-activated expression of the *Salmonella* pathogenicity island 1 type III secretion system in *Salmonella enterica* serovar Typhimurium. *Journal of Bacteriology*, 190 (2008), 4624–4631. doi: 10.1128/JB.01957-07.

[17] D'Souza, D., Critzer, F., Golden, D., Real-time reverse-transcriptase polymerase chain reaction for the rapid detection of *Salmonella* using *invA* primers. *Foodborne Pathogens and Disease*, 6 (2009), 1097–1106. doi: 10.1089/fpd.2009.0322.

[18] Balaji, B., O'Connor, K., Lucas, J., Anderson, J., Csonka, L., Timing of induction of osmotically controlled genes in *Salmonella enterica* Serovar Typhimurium, determined with quantitative real-time reverse transcription-PCR. *Applied and Environmental Microbiology*, 71 (2005), 8273–8283. doi: 10.1128/AEM.71.12.8273-8283.2005.

[19] Appiah, T., Boakye,Y.D., Agyare, C., Antimicrobial activities and time-kill kinetics of extracts of selected Ghanaian mushrooms. *Evidence-based Complementary and Alternative Medicine*, 17 (2017), 1-15. https://doi.org/10.1155/2017/4534350.

[20] Hall-Stoodley, L., Costerton, J.W., Stoodley, P., Bacterial biofilms: From the natural environment to infectious diseases. *Nature Reviews Microbiology*. 2 (2004), 95–108.doi: 10.1038/nrmicro821.

[21] Lee, C.K., De Anda, J., Baker, A.E., Bennett, R.R., Luo, Y., Lee, E.Y., Multigenerational memory and adaptive adhesion in early bacterial biofilm communities. *Proceedings of the National Academy of Sciences*, 115 (2018), 4471–4476. doi: 10.1073/pnas.1720071115.

[22] Krukiewicz, K., Kazek-Kesik, A., Brzychczy-Włoch, M., Los, M.J., Ateba, C.N., Mehrbod, P., Ghavami, S., Shyntum, D.Y., Recent advances in the control of clinically important biofilms. *International Journal of Molecular Sciences*, 23 (2022), 4-26. doi: 10.3390/ijms23179526.

[23] Bajaj, V., Hwang, C., Lee, C.A., *hilA* is a novel *ompR*/*toxR* family member that activates the expression of *Salmonella typhimurium* invasion genes. *Molecular Microbiology*, 18 (1995), 715-727. doi: 10.1111/j.1365-2958.1995.mmi_18040715.x

[24] Kim, S., Jung, U.T., Kim, S.K., Lee, J.H., Choi, H.S., Kim, C.S., Jeong, M.Y., Nanostructured multifunctional surface with antireflective and antimicrobial characteristics. *ACS Applied Materials & Interfaces*, 7 (2015), 326–331. doi: 10.1021/am506254r.

[25] Tsai,M. H., Liang, Y.H., Chen, C.Y., Chiu, C. H., Characterization of *Salmonella* resistance to bile during biofilm formation. *Journal of Microbiology, Immunology and Infection*, 53 (2020), 518-524. doi: 10.1016/j.jmii.2019.06.003.

[26] Wang,Y., Cai, Y., Zhang, J., Liu, D., Gong, X., Pan, Z., Geng, S., Jiao, X., Controvesy surrounding the function of SpiC protein in *Salmonella*. *Frontiers in Microbiology*, 10 (2019), 331-340. https://doi.org/10.3389/fmicb.2019.01784.

[27] Aviles, B., Klotz, C., Eifert, J., Williams, R., Ponder, M., Biofilms promote survival and virulence of *Salmonella enterica* sv. Tennessee during prolonged dry storage and after passage through an in vivo digestion system. *International Journal of Food Microbiology*, 163 (2013), 252-259. doi: 10.1016/j.ijfoodmicro.2013.01.026.

[28] Sokaribo, A. S., Hansen, E. G., McCarthy, M., Desin, T. S., Waldner, L. L., MacKenzie, K. D., Mutwiri, G., Jr, Herman, N. J., Herman, D. J., Wang, Y., White, A. P., Metabolic activation of CsgD in the regulation of *Salmonella* Biofilms. *Microorganisms*, 8 (2020), 964-871. doi: 10.3390/microorganisms8070964

http://communications.science.ankara.edu.tr

Commun.Fac.Sci.Univ.Ank.Ser. C Biology
Volume 32, Number 2, Pages 150-173 (2023)
ISSN 1303-6025 E-ISSN 2651-3749
DOI: 10.53447/communc.1261628

Research Article; Received: March 07, 2023; Accepted: August 05, 2023

NATURAL PLANT DIVERSITY OF THREE FARMS OF ANKARA UNIVERSITY

CANSU DOĞAR[1], GÜL NİLHAN TUĞ[1]

[1]Department of Biology, Faculty of Science, Ankara University, Ankara, TÜRKİYE

ABSTRACT. Natural flora of cultivated or agricultural areas are generally under estimated or accepted as weeds because they compete with agricultural plants and repress their growth. Ankara University has three research and application farms/stations especially for educational purposes. Between the agricultural patches at these farms there are small natural patches possessing important plant diversity but there is not any information about the natural flora of these farms. The aim of this study is to find out the natural plant diversity of these three farms. The field studies conducted between 2016-2018 and 927 specimens were collected totally, and the number of taxa and the farm that were collected from are as follows respectively; 118 taxa from Ayaş Horticulture Reasearch and Application Station, 64 taxa from both Kalecik Viticulture Research and Application Station, and Haymana Research and Application Farm. The families with the highest number of taxa are Asteraceae and Brassicaceae. 4 of these taxa are endemic. Most of the species are cosmopolitan with the ratio of 70% and the distribution of the rest of the taxa in phytogeographical regions are as follows; 15% Irano-Turanian, 8% Euxin and 7% Mediterranean.

1. INTRODUCTION

Natural patches between agricultural areas are refuge for wild life and very important for biodiversity. One of the reason for the increase in attention to biodiversity is its contribution to plant breeding and agricultural processes. The increase in human population together with the expansion of agricultural areas result in loss of natural habitats, and especially in developed countries natural plant cover is stacked in between agricultural areas [1-5]. The biodiversity inside these agricultural areas are generally under estimated grouped the relation of functions of biodiversity with agricultural activities. The biodiversity inside these agricultural areas are generally under estimated and grouped according to the relation of functions of biodiversity with agricultural activities. According to their grouping biodiversity is considered in three main headlines, agricultural biodiversity, para-agricultural biodiversity and extra-agricultural biodiversity [6]. Agricultural biodiversity covers the animal and plant species, subspecies and varieties used in agricultural activities. Para agricultural diversity which is also known as functional biodiversity covers the soil fauna, pollinators, natural plants except for the ones that are not used directly in agricultural activities and in general meaning the ecosystem services. Extra-agricultural diversity is all the

Keywords. Flora, agricultural areas, native plants

cansu.dogar@gmail.com- Corresponding author; 0009-0004-5916-7101
tug@science.ankara.edu.tr- 0000-0002-2702-2387

diversity in production area that are not contributed to the agricultural production. These are generally specific species like the endangered ones [7]. Gurr et al. [8] draw attention to the beneficial effects of biodiversity to agricultural production especially the pest management. These studies reveal the importance of the natural areas between agricultural areas, and also their biodiversity.

In last few decades, the ecosystem services of both agricultural and natural areas draw more attention, other than primary production like the influence of agricultural changes over biodiversity and the abundance of native taxa [5, 9-12]. There are many direct and indirect interaction with weeds and agricultural plants, as crop-weed competition [13], food source for pollinators [14,15], earthworms [16], beetles [17-19], ants [20], birds [14,21], and mammals [22].

Turkey draws attention with both its biological diversity and large agricultural areas. The studies about the function and importance of natural diversity at agricultural areas are under estimated in Turkey, and mainly researches at agricultural areas concentrated on weeds which are the plants competing with agricultural products for all the resources. With this study, it was aimed to determine the natural plant diversity within the borders of research and application farms and stations of Ankara University; Haymana Research and Application Farm, Ayaş Horticulture Research and Application Station and Kalecik Viticulture Research and Application Station.

2. MATERIALS AND METHODS

During the vegetation periods between 2016 and 2018 plant specimens were collected and prepared as herbarium specimen. All the plant material was kept at - 20 °C for three days to avoid for disinfestation. “Flora of Turkey and East Aegean Islands I-XI” [23-25] and “Resimli Türkiye Florası” volumes 1, 2 and 3a [26-28] used for plant identification. All the specimens were prepared as herbarium material and deposited in herbarium ANK.

The valid names of the plant species and their Turkish names were checked from the “Türkiye Bitkileri Listesi-Damarlı Bitkiler” [29] and listed according to the flora order of Turkey and the East Aegean Islands. For each research area a code is produced according to the initials of their names and together with the information about collector number, date of collection, endemism status and chorology were given.

ABBAUİ: Ayaş Horticulture Research and Application Station

It covers an area of 406 decares with an altitude of 685 m within the borders of Ayaş district. The farm produces saplings, vegetables (tomatoes, aubergine, cabagge, bean, pumpkin, corn, lettuce et.), fruits (melon, watermelon, cherry, apricot etc.) and alfalfa and also spices and medicinal plants.

HAUÇ: Haymana Research and Application Farm

Located within the borders of Haymana district, the farm covers an area of 4200 decares at an altitude of 1055 m. Field crops and horticultural crops are cultivated, and it provides seeds to the surrounding farmers, especially with wheat improvement studies. Cherry, plum, apple and apricot trees cover about 100 decares of the area. In addition, herd cattle, beef cattle, ovine breeding, beekeeping and feed production are carried out.

KBAUİ: Kalecik Viticulture Research and Application Station

It was established on an area of 175 decares at an altitude of 700 m in Kalecik district. Viticulture activities are carried out within the scope of the area.

The locations of the studied farms and stations in Ankara province can be seen from Figure 1.

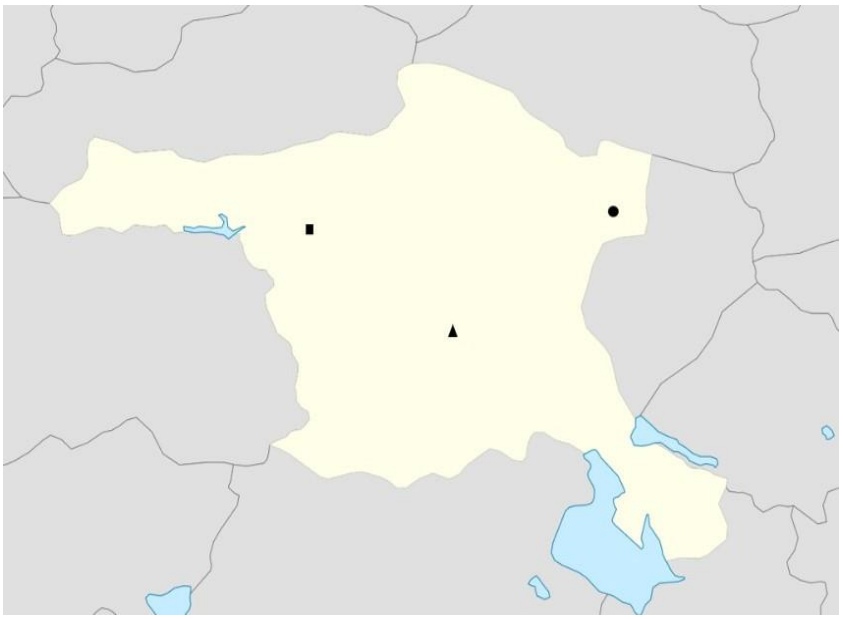

FIGURE 1. The locations of the studied farms and application stations in Ankara. ■: Ayaş Horticulture Research and Application Station ●: Kalecik Viticulture Research and Application Station ▲: Haymana Research and Application Farm

The biometeorological analysis of the study area is done by using 94 years data of Ankara station taken from Turkish State Meteorological Service, and evaluated according to Emberger [30]. The meteorological stations at Ayaş, Kalecik and Haymana are very newly established and their data are not cover the 30 years of observations which is the minimum duration for suitable climatic evaluation.

3. RESULTS

Bioclimate: All the values used for bioclimatological evaluation of Ankara can be seen from Table 1. According to the s value, which is below 5, Ankara is under the influence of Mediterranean climate. With the evaluation of m, Q and P values the bioclimate of the area is very cold sub-arid Mediterranean bioclimate and the precipitation regime is included in east Mediterranean precipitation regime type 2. The hottest and coldest months are august and january respectively. The duration of arid period is about 4 to 5 months between june and october. (Figure 2). All the values about bioclimate can be seen from Table 1.

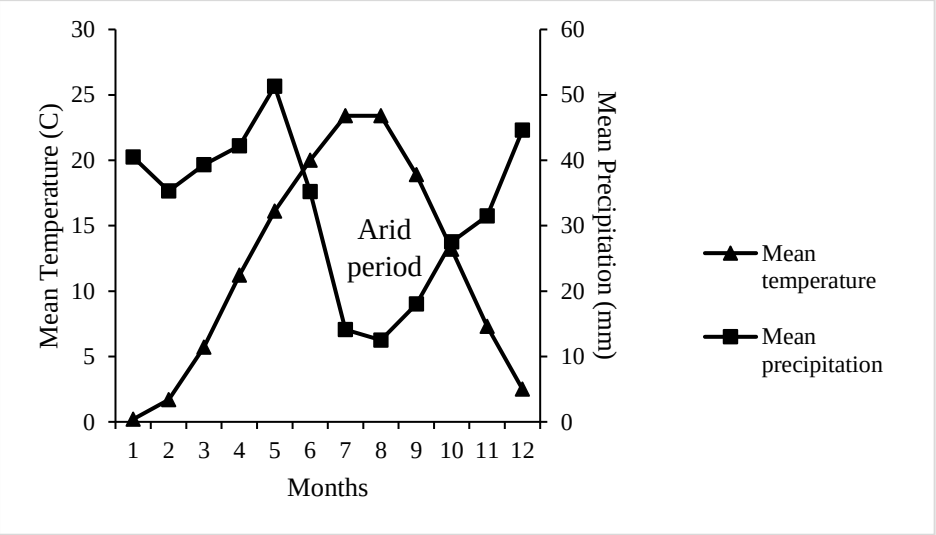

FIGURE 2. Ombrothermical Climate Diagram of Ankara Meteorological Station

TABLE 1. Bioclimatological synthesis of Ankara

S: aridity index, PE=summer precipitation, Q=Precipitation-Temperature index, M=max temperature of the hottest month, m=min temperature of the coldest month, P=mean annual total precipitation, Sp= Spring, W= Winter, F= Fall, Su=Summer.

Station	s	PE	Q	M (°C)	m (°C)	P (mm)	Precipitaton regime	Bioclimatology
Ankara	2,02	61,8	41	30,5	-3,2	392	SpWFSu-East mediterranean precipitation regime type 2.	Very cold sub-arid Mediterranean bioclimate

During the field works between 2016 and 2018 totally 927 plant specimen were collected. Identified specimens were belong to 40 different families. The highest number of taxa was collected from Ayaş Horticulture Research and Application Station with 118 taxa from 35 families. The number of taxa from Kalecik Viticulture Research and Application Station and Haymana Research and Application Farm were 64 taxa from 24 families and 64 taxa from 23 families respectively (Table 2).

TABLE 2. The number of families, genera and species from each station

Station	Number of families	Number of genera	Number of taxa
Haymana	23	56	64
Ayaş	35	89	118
Kalecik	24	57	64

According to our results the highest plant diversity was determined at Ayaş Horticulture Research and Application Station with 118 species which can be related with the different types of agricultural products grown at this station. The distribution of number of taxa within the families from each farm can be seen from Figures 3,4 and 5.

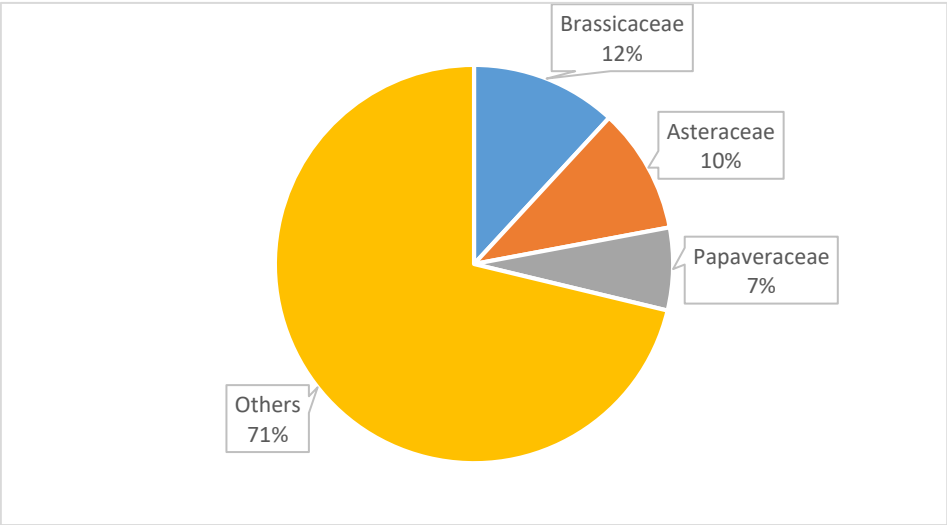

FIGURE 3. The families with the highest number of taxa at Ayaş Horticulture Research and Application Station

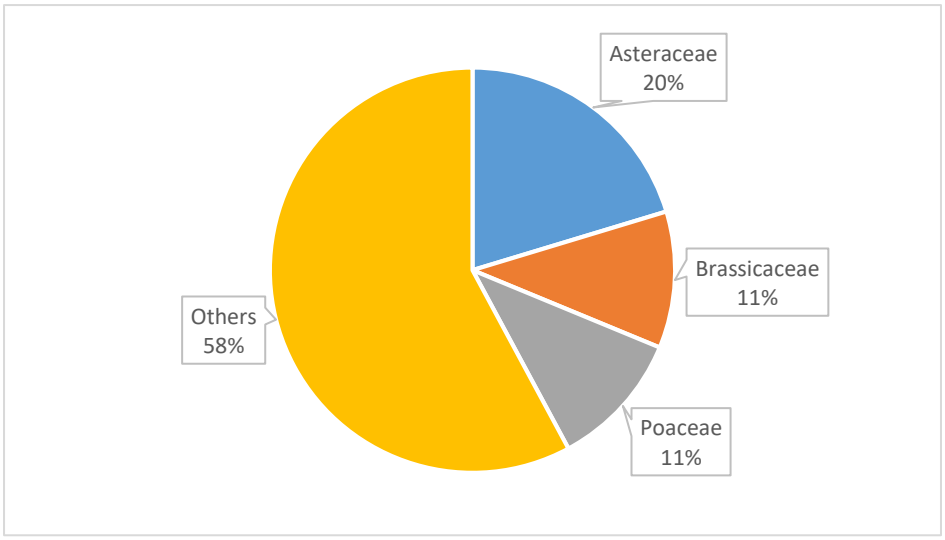

FIGURE 4. The families with the highest number of taxa at Haymana Research and Application Farm

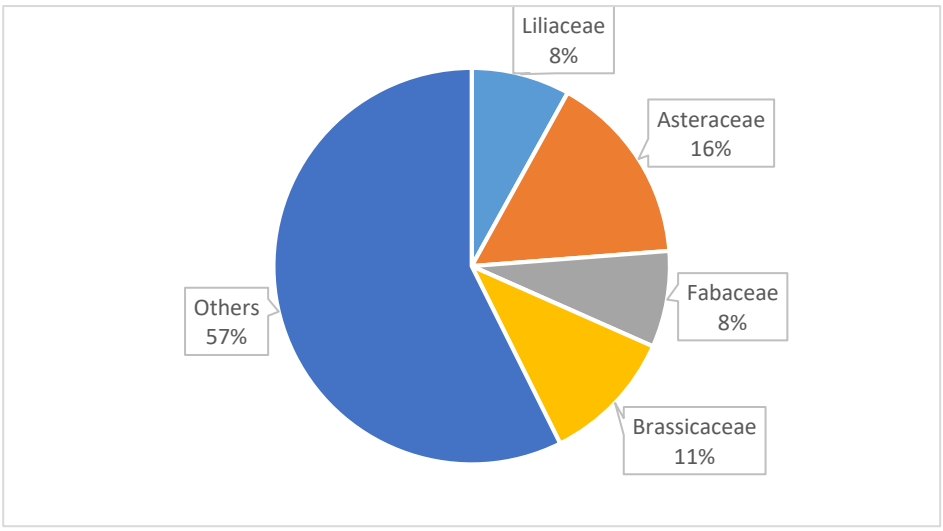

FIGURE 5. The families with the highest number of taxa at Kalecik Viticulture Research and Application Station

All the stations are surrounded by Central Anatolian steppe vegetation but because of agricultural activities for long period of time, they lost their natural structure. The endemism ratio is very low and only 4 endemic taxa determined from these three farmlands; *Delphinium venulosum* Boiss., *Verbascum ancyritanum* Bornm., *Stachys cretica* L. subsp. *anatolica* Rech. Fil. and *Crocus danfordiae* subsp. *danfordiae* Maw.

Phytogeograhically the area belongs to Irano Turanian phytogeogrephical region but cosmopolitan species dominates the area. The phytogeographic distribution of the recorded taxa from the area is as follows; Irano Turanian 15,25%, Mediterranean 6,68%, Euxine 8,48% and Cosmopolitan and unknown 69,49% (Figure 6).

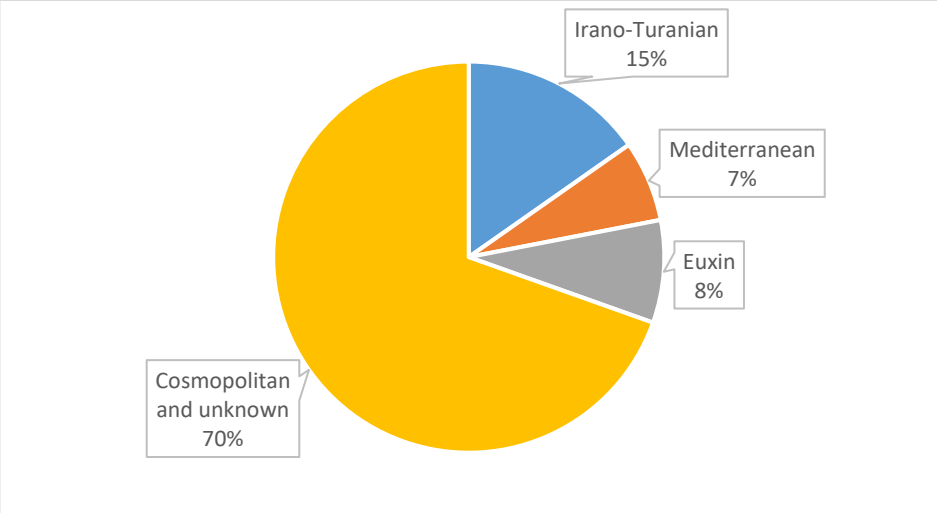

FIGURE 6. The distribution of plant taxa in phytogeographical regions

The life span of the species collected from each farmland were determined from the Flora of Turkey and East Aegean Islands and related publication and can be seen from table 3. According to the table 8 it can be seen that mainly annuals dominate all the agricultural areas which may be the result of grazing and the harvesting processes that do not let the perennials to settle.

TABLE 3. The distribution of taxa in study areas with respect to life span.

Code of the farm	Annual	Biennual	Perennial	Annual or biennual	Biennual or perennial	Annual to perennial	Annual or biennual or perennial	Unknown
ABBAUI	60	2	40	6	5	1	1	1
HAUÇ	25	3	27	2	5	1	1	-
KBAUI	31	-	22	5	2	1	2	-

Natural flora at or around agricultural areas are generally accepted as field weeds and agricultural pests and some methods are used to combust them. Weeds have the ability to grow faster and produce more seeds so they retard the growth of agricultural plants [31,32]. Also they increase the fire risk especially at arid season [33]. But even though they are accepted as weed they are important genetic resources for agricultural plants [34]. They have many other benefits like production of animal feed, medicinal and industrial usage and also, they are important for integrity of soil structure and combating erosion [35].

Most of the studies about natural flora of agricultural areas concentrated on the detrimental effects of natural flora over agricultural plants or trees, because they compete with agricultural plants and repress their growth [36]. The species that are defined as pest at orchards and collected from study area are as follows; *Alopecurus myosuroides* Huds., *Setaria viridis* L., *Artemisia vulgaris* L., *Cichorium intybus* L., *Cirsium arvense* (L.) Scop., *Convolvulus arvensis* L., *Geranium tuberosum* L., *Oxalis pes-caprae* L., *Plantago lanceolata* L., *P. major* L., *Rumex crispus* L., *Taraxacum officinale* Wiggers, *Phragmites australis* Steudal, *Ornithogalum umbellatum* L., *Amaranthus retroflexus* L., *Capsella bursa-pastoris* (L.) Medik., *Carduus pycnocephalus* L., *Chenopodium album* L., *Datura stramonium* L., *Erodium cicutarium* (L.) L'Herit, *Euphorbia helioscopia* L., *E. falcata* L., *Fumaria asepala* Boiss., *F. officinalis* L., *Geranium tuberosum* L., *Heliotropium europaeum* L., *Hibiscus trionum* L., *Lactuca serriola* L., *Lamium amplexicaule* L., *L. orientale* (Fisch. & C.A.Mey.) E.H.L.Krause, *Papaver rhoeas* L., *Polygonum bellardii* All., *Senecio vernalis* Walds & Kit, *S. vulgaris* L., *Sinapis arvensis* L., *Sonchus asper* (L.) Hill., *Stellaria media* (L.) Vill., *Xanthium spinosum* L., *X. strumarium* L.

There are similar studies also at grain production fields to define the pest plants. According to Taştan ve Erciş [37] the pest plants determined at our study area are; *Adonis aestivalis* L., *ajuga chamaepitys* L., *Alhagi maurorum*, *Alopecurus myosuroides* Hudson, *Amaranthus retroflexus* L., *anagallis arvensis* L., *Bifora radians* Bieb., *Bromus tectorum* L., *Buglossoides arvense* (L.) Johnst., *Capsella burs-pastoris* (L.) Medik., *Carduus pycnocephalus* L., *Cerastium perfoliatum* L., *Ceratocephalus falcatus* (L.) Pers., *Chondrilla juncea* L., *Cirsium arvense*

(L.) Scop., *Cichorium inthybus* L., *Consolida regalis* S.F.Gray, *Convolvulus arvensis* L., *C. galaticus* Rotsan ex Choisy, *Crepis foetida, Cyanus depressus (*Bieb.) Sojak, *Daucus carota* L., *Descurainia Sophia* (L.) Webb., *Echinophora tenuifolia* L., *Echium italicum* L., *Fumaria officinalis* L., *Galium aparine* L., *Geranium tuberosum* L., *Gladiolus atroviolaceus* Boiss., *Gypsophila pilosa* Hudson, *Hordeum murinum* L., *Hypecoum procumbens* L., *Isatis tinctoria* L., *Lactuca serriola* L., *Lamium amplexicaule* L., *L. orientale* (Fisch. & C.A.Mey.) E.H.L.Krause, *Malva neglecta* Wallr., *Medicago sativa* L., *Melilotus officinalis* (L.) Desr., *Ornithogalum* narbonense L., *Papaver rhoeas* L., *Phragmites autralis, Plantago lanceolate* L., *Polygonum bellardii* All., *Reseda lutea* L., *Senecio vernalis* Waldst & Kitt, *S. vulgaris* L., *Setaria viridis* (L.) P. Beauv, *Sinapis arvensis* L., *Stellaria media* (L.) Vill., *Turgenia latifolia* (L.) Hoffm., *Xanthium strumarium, Vaccaria pyrimidata* Medik, *Veronica hederifolia* L.

As a result of this study the natural flora of three farms and application centers of Ankara University were determined with their influences over agricultural areas and their functions in natural vegetation.

Acknowledgement The authors would like to thank to Prof. Dr. Ahmet Emre Yaprak, Dr. İsa Başköse and S. Tuğrul Körüklü for their scientific support. Also, the authors would like to thank Prof. Dr. Gökhan Söylemezoğlu and the staff of the farms and application centers for their assistance during the field works.

Author Contribution Statements CD-specimen collection and identification, data analysis and manuscript writing. GNT-specimen collection, data analysis and manuscript writing.

Declaration of Competing Interests The authors declare no conflict of interest.

REFERENCES

[1] Bretagnolle, V., Gaba, S., Weeds for bees? A review, *Agronomy for Sustainable Development*, 35(2015), 891-909, doi:10.1007/s13593-015-0302-5.

[2] Geiger, F., Bengtsson, J., Berendse, F., Weisser, W.W., Emmerson, M., Morales, M.B., Ceryngier, P., Liira, J., Tscharntke, T., Winqvist, C., Eggers, S., Bommarco, R., Pärt, T., Bretagnolle, V., Plantegenest, M., Clement, L.W., Dennis, C., Palmer, C., Oñate, J.J., Guerrero, I., Hawro, V., Aavik, T., Thies, C., Flohre, A., Hänke, S., Fischer, C., Goedhart, P.W., Inchausti, P., Persistent negative effects of pesticides on biodiversity and biological control potential on European farmland, *Basic and Applied Ecology*, 11(2) (2010), 97–105. doi:10.1016/j.baae.2009.12.001.

[3] Robinson, R.A., Sutherland, W.J., Post-war changes in arable farming and biodiversity in Great Britain, *Journal of Applied Ecology*, 39(2002), 157–176. http://dx.doi.org/10.1046/j.1365-2664.2002.00695.x

[4] Kleijn, D., Sutherland, W.J., How effective are European agrienvironment schemes on conserving and promoting biodiversity? *Journal of Applied Ecology*, 40(2003), 947–970. doi:10.1111/j.1365-2664.2003.00868.x

[5] Tscharntke, T., Klein, A.M., Kruess, A., Steffan-Dewenter, I., Thies, C., Landscape perspectives on agricultural intensification and biodiversity - ecosystem service management, *Ecology Letters*, 8(2005), 857–874. https://doi.org/10.1111/j.1461-0248.2005.00782.x

[6] Peeters, A., Janssens, F., Agriculture et nature, concilier la biodiversité et une production agricole performante en prairie: est-ce possible? Annales Gembloux, 10(1995), 127–147.

[7] Clergue, B., Amiaud, B., Pervanchon, F., Lasserre-Joulin, F., Plantureux, S., Biodiversity: function and assessment in agricultural areas. A review, *Agronomy for Sustainable Development*, 25(2004), 1-15. doi:10.1007/978-90-481-2666-8_21

[8] Gurr, G.M., Wratten, S.D., Luna, J.M., Multifunction agricultural biodiversity: pest management and other benefits, *Basic and Applied Ecology*, 4(2003), 107–116. doi:10.1078/1439-1791-00122

[9] Petit, S., Firbank, L., Wyatt, B., Howard, D., MIRABEL: Models for Integrated Review and Assessment of Biodiversity in European Landscapes, *Ambio*, 30(2001), 81–88. doi: 10.1579/0044-7447-30.2.81

[10] Petit, S., Boursault, A., Le Guillux, M., Munier-Jolain, N., Reboud, X., Weeds in agricultural landscapes. A review, *Agronomy for Sustainable Development*, 31(2011), 309 317. doi:10.1051/agro/2010020

[11] Benton, T.G., Vickery, J.A., Wilson, J.D., Farmland biodiversity: is habitat heterogeneity the key? *Trends in Ecology & Evolution*, 18 (2003), 182–188. doi:10.1016/S0169-5347(03)00011-9

[12] Cardinale, B.J., Duffy, J.E., Gonzalez, A., Hooper, D.U., Perrings, C., Venail, P., Narwani, A., Mace, G.M., Tilman, D., Wardle, D.A., Kinzig, A.P., Daily, G.C., Loreau, M., Grace, J.B., Larigauderie, A., Srivastava, D.S., Naeem, S., Biodiversity loss and its impact on humanity, *Nature*, 486(7401) (2012): 59–67. doi:10.1038/nature11148.

[13] Bastiaans, L., Kropff, M.J., Goudriaanb, J., Van Laar, H.H., Design of weed management systems with a reduced reliance on herbicides poses new challenges and prerequisites for modeling crop-weed interactions, *Field Crops Research*, 67(2000), 161–179. doi:10.1016/S0378-4290(00)00091-5

[14] Gibbons, D.W., Bohan, D.A., Rothery, P., Weed seed resources for birds in fields with contrasting conventional and genetically modified herbicide-tolerant crops, *Philosophical Transactions of the Royal Society B: Biological Sciences*, 273(2006), 1921–1928. doi:10.1098/rspb.2006.3522

[15] Backman, J.P.C., Tiainen, J., Habitat quality of field margins in a Finnish farmland area for bumblebees (Hymenoptera: *Bombus* and *Psithyrus*), *Agriculture, Ecosystems & Environment*, 88(2002), 53–68. https://doi.org/10.1016/S0167-8809(01)00318-8

[16] Thompson, K., Green, A., Jewels, A.M., Seeds in soil and worm casts from a neutral grassland, *Functional Ecology*, 8(1994), 29–35. doi:10.2307/2390108

[17] Hawes, C., Haughton, A.J., Osborne, J.L., Roy, D.B., Clark, S.J., Perry, J.N., Rothery, P., Bohan, D.A., Brooks, D.R., Champion, G.T., Dewar, A.M., Heard, M.S., Woiwod, I.P., Daniels, R.E., Young, M.W., Parish, A.M., Scott, R.J., Firbank, L.G., Squire, G.R., Responses of plants and invertebrate trophic groups to contrasting herbicide regimes in the Farm Scale Evaluations of genetically modified herbicide-tolerant crops, *Philosophical Transactions of the Royal Society B*, 358(2003), 1899– 1913. doi: 10.1098/rstb.2003.1406 doi: 10.1098/rstb.2003.1406

[18] Biesmeijer, J.C., Roberts, S.P.M., Reemer, M., Ohlemuller, R., Edwards, M., Peeters, T., Schaffers, A.P., Potts, S.G., Kleukers, R., Thomas, C.D., Settele, J., Kunin, W.E., Parallel declines in pollinators and insect-pollinated plants in Britain and the Netherlands, *Science*, 313(5785) (2006), 351–354. doi:10.1126/science.1127863

[19] Marshall, E.J.P., Brown, V.K., Boatman, N.D., Lutman, P.J.W., Squire, G.R., Ward, L.K., The role of weeds in supporting biological diversity within crop fields, *Weed Research*, 43(2003), 77–89. https://doi.org/10.1046/j.1365-3180.2003.00326.x

[20] Jacob, H.S., Minkey, D.M., Gallagher, R.S., Borger, C.P., Variation in postdispersal weed seed predation in a crop field, *Weed science*, 54(2006), 148–155. doi:10.1614/WS-05-075R.1

[21] Wilson, J.D., Morris, A.J., Arroyo, B.E., Clack, S.C., Bradbury, R.B., A review of the abundance and diversity of invertebrate and plant foods of granivorous birds in northern Europe in relation to agricultural change, *Agriculture, Ecosystems & Environment*, 75(1999), 13–30. doi:10.1016/S0167-8809(99)00064-X

[22] Manson, R.H., Stiles, E.W., Links between microhabitat preferences and seed predation by small mammals in old fields, Oikos, 82(1) (1998), 37– 50. https://doi.org/10.2307/3546915

[23] Davis, P.H., Flora Of Turkey And The East Aegean Islands. Volume 1-9, University Press., Edinburgh, 1965-1985.

[24] Davis, P.H., Mill, R.R., Tan, K., Flora Of Turkey And The East Aegean Islands (Supplement). Volume 10, University Press., Edinburgh, 1988.

[25] Güner, A., Özhatay, N., Ekim, T., Başer,K.H.C., Flora of Turkey and the East Aegean Islands.Volume 11, Edinburgh at the university press, Edinburg, 2000.

[26] Güner, A., Ekim, T. (eds), Resimli Türkiye Florası, cilt 1. NGBB Yayınları Flora Dizisi 2, Flora Araştırmaları Derneği and Türkiye İş Bankası Kültür Yayınları yayını, İstanbul, 2014.

[27] Güner, A., Kandemir, A., Menemen, Y., Yıldırım, H., Aslan, S., Ekşi, G., Güner, I., Çimen, A.Ö. (eds), Resimli Türkiye Florası (lllustrated Flora of Turkey), Vol. 2 ANG Vakfı Nezahat Gökyiğit Botanik Bahçesi Yayınları, İstanbul, 2018.

[28] Güner, A., Kandemir, A., Menemen, Y., Yıldırım, H., Aslan, S., Çimen, A.Ö., Güner, I., Ekşi Bona, G., Şen Gökmen, F. (eds), Resimli Türkiye Florası (lllustrated Flora of Turkey), ANG Vakfı Nezahat Gökyiğit Botanik Bahçesi Yayınları. İstanbul, 2022.

[29] Güner, A., Aslan, S., Ekim, T., Vural, M., Babaç, M.T. (eds), Türkiye Bitkileri Listesi (Damarlı Bitkiler). Nezahat Gökyiğit Botanik Bahçesi ve Flora Araştırmaları Derneği Yayını, İstanbul, 2012.

[30] Akman, Y., İklim ve Biyoiklim, Palme Yayinevi, Ankara, 1999.

[31] Liebman, M., Weed management: a need for ecological approaches, In: Ecological Management in Agricultural Weeds, Cambridge University Press, Cambridge, 2001. https://doi.org/10.1017/CBO9780511541810

[32] Fried,G., Norton, L.R., Rebound, X., Environmental and management factors determining weed species composition and diversity in France, *Agriculture, Ecosystems & Environment*, 128(2008), 68-76. doi:10.1016/j.agee.2008.05.003

[33] James, R., Lockwood, M., Economics of blackberries: current data and rapid valuation techniques, *Plant Protection Quaterly*, 13 (4) (1988), 175-179.

[34] Spahillari, M., Hammer, K., Gladis, T., Diederichsen, A., Weeds as part of agriculture, *Outlook Agric*, 28(1999), 227–232. https://doi.org/10.1177/003072709902800405
[35] Ekwealor, K.U., Echereme, C.B., Ofobeze, T.N., Okereke, C.N., Economic importance of weeds: A review, *Asian Plant Research Journal*, 3(2) (2019), 1-11. doi:10.9734/APRJ/2019/v3i230063
[36] Jaric, S.V., Karadzic, B.D., Vrbnicanin, S.P., Mitrovic, M.M., Kostic, O.A., Pavlovic, P.Z., Floristic and phytocoenological research of segetal plant communities in cultivated areas of southern Srem, *Archives of Biological Sciences*, 67(2) (2015), 591- 609. https://doi.org/10.2298/ABS141017021J
[37] Taştan, B., Erciş, A., Orta Anadolu Bölgesi buğday ekim alanlarında gözlenen yabancı otların yayılış ve yoğunlukları üzerine araştırmalar, *Bitki Koruma Bülteni*, 31(1991), 39-60.

Plant List

Divisio: PTERIDOPHYTA
Ordo: FILICALES
1. EQUISETACEAE
1. EQUISETUM L.
E. ramosissimum Desf. (Kırkboğum)
ABBAUİ, 18.05.2018, C. Doğar 1330, 1361.
Divisio: SPERMATOPHYTA
Subdivisio: GYMNOSPERMAE
1. PINACEAE
***1. PINUS** L.*
P. nigra J. F. Arnold (Karaçam)
HAUÇ, 27.04.2016, C. Doğar 1003.
ABBAUİ, 18.05.2018, C. Doğar 1422.
2. CUPRESSACEAE
***1. JUNIPERUS** L.*
J. foetidissima Willd. (Kokuluardıç)
ABBAUİ, 18.05.2018, C. Doğar 1423.
Subdivisio: ANGIOSPERMAE
Classis: DICOTYLEDONES
1.RANUNCULACEAE
***1. NIGELLA** L.*
N. arvensis L. subsp. glauca Boiss. (Tarlaçörekotu)
HAUÇ, 25.06.2016, C. Doğar 1189.
***2. DELPHINIUM** L.*
D. venulosum Boiss. (Hezaren)
KBAUİ, 03.09.2016, C. Doğar 1232. Irano-Turanian /Endemic.
***3. CONSOLIDA** Gray*
C. orientalis (J.Gay) Schrödinger. (Morçiçek)
ABBAUİ, 12.05.2016, C. Doğar 1104, K, 724 m., 02.06.2016, C. Doğar 1139, 18.05.2018, C. Doğar 1389.
C. regalis S. F. Gray subsp. paniculata (Host) Soó var. paniculata (Horozkuyruğu)
HAUÇ, 25.06.2016, C. Doğar 1187.
ABBAUİ, 16.08.2016, C. Doğar 1198.
HAUÇ, 28.08.2016, C. Doğar 1209.
ABBAUİ, 01.10.2016, C. Doğar 1239.
***4. ADONIS** L.*
A. aestivalis L. subsp. aestivalis (Kandamlası)
ABBAUİ, 12.05.2016, C. Doğar 1111.

ABBAUİ, 29.04.2017, C. Doğar 1273.
A. flammea Jacq. (Cinlalesi)
HAUÇ, 27.04.2016, C. Doğar 1032.
KBAUİ, 02.06.2016, C. Doğar 1057.
ABBAUİ, 29.04.2016, C. Doğar 1085.
ABBAUİ, 29.04.2017, C. Doğar 1268.
***5. RANUNCULUS** L.*
R. argyreus Boiss. (Çitemik)
ABBAUİ, 29.04.2017, C. Doğar 1269.
***6. CERATOCEPHALUS** Moench.*
C. falcatus (L.) Pers. (Düğünotu)
HAUÇ, 24.02.2018, C. Doğar 1291.
ABBAUİ, 11.03.2018, C. Doğar 1318.
2. PAPAVERACEAE
***1. GLAUCIUM** Adans.*
G. corniculatum (L.) Rudolph subsp. refractum (Náb.) Cullen (Çömlekçatlatan)
KBAUİ, 02.06.2016, C. Doğar 1154.
KBAUİ, 03.09.2016, C. Doğar 1231.
G. leiocarpum Boiss. (Gavurhaşhaşı)
ABBAUİ, 18.05.2018, C. Doğar 1328.
***2. PAPAVER** L.*
P. rhoeas L. (Gelincik)
ABBAUİ, 29.04.2016, C. Doğar 1069.
ABBAUİ, 12.05.2016, C. Doğar 1112.
ABBAUİ, 18.05.2018, C. Doğar 1396, 1400.
P. dubium L. (Köpekyağı)
KBAUİ, 28.04.2016, C. Doğar 1051.
ABBAUİ, 18.05.2018, C. Doğar 1372, 1373.
P.argemone L. subsp. argemone (Kumhaşhaşı)
ABBAUİ, 18.05.2018, C. Doğar 1395.
P. hybridum L. (Melezgelincik)
ABBAUİ, 18.05.2018, C. Doğar 1383.
***3. HYPECOUM** L.*
1. H. procumbens L. (Yavruağzı)
ABBAUİ, 29.04.2016, C. Doğar 1077.
ABBAUİ, 29.04.2017, C. Doğar 1270.
ABBAUİ, 18.05.2018, C. Doğar 1380.
***4. FUMARIA** L.*
F. officinalis L. (Şahtere)
ABBAUİ, 29.04.2016, C. Doğar 1090.
ABBAUİ, 12.05.2016, C. Doğar 1099.
ABBAUİ, 29.04.2017, C. Doğar 1251.
ABBAUİ, 11.03.2018, C. Doğar 1309.
ABBAUİ, 18.05.2018, C. Doğar 1381, 1382.
F. asepala Boiss.(Akşahtere)
ABBAUİ, 29.04.2017, C. Doğar 1280.
ABBAUİ, 18.05.2018, C. Doğar 1394. Irano-Turanian
3. CRUCIFERAE (BRASSICACEAE)
***1. SINAPIS** L.*
S. arvensis L. (Yabanihardal)
HAUÇ, 27.04.2016, C. Doğar 1001, 1022.
KBAUİ, 28.04.2016, C. Doğar 1063.
ABBAUİ, 29.04.2016, C. Doğar 1074.
ABBAUİ, 12.05.2016, C. Doğar 1117, 1118 and 1120.
ABBAUİ, 16.08.2016, C. Doğar 1204.
ABBAUİ, 01.10.2016, C. Doğar 1245.

ABBAUİ, 29.04.2017, C. Doğar 1276.
***2. DIPLOTAXIS** DC.*
D. tenuifolia (L.) DC. (Türpenk)
HAUÇ, 28.08.2016, C. Doğar 1212, C. Doğar 1217.
ABBAUİ, 11.03.2018, C. Doğar 1320.
***3. LEPIDIUM** L.*
L. draba L. (Diğnik)
HAUÇ, 27.04.2016, C. Doğar 1002.
KBAUİ, 02.06.2016, C. Doğar 1149.
ABBAUİ, 29.04.2017, C. Doğar 1259.
ABBAUİ, 18.05.2018, C. Doğar 1341.
***4. ISATIS** L.*
I. glauca Aucher ex Boiss. subsp. glauca (Soğutot)
HAUÇ, 25.06.2016, C. Doğar 1164. Irano-Turanian
I. tinctoria L. (Çiviotu)
ABBAUİ, 29.04.2017, C. Doğar 1255.
***5. THLASPI** L.*
T. perfoliatum L. (Giyle)
KBAUİ, 28.04.2016, C. Doğar 1062.
ABBAUİ, 29.04.2016, C. Doğar 1089.
ABBAUİ, 29.04.2017, C. Doğar 1273.
HAUÇ, 24.02.2018, C. Doğar 1285.
ABBAUİ, 11.03.2018, C. Doğar 1308.
***6. CAPSELLA** Medik.*
C. bursa-pastoris (L.) Medik. (Çobançantası)
HAUÇ, 27.04.2016, C. Doğar 1030.
ABBAUİ, 12.05.2016, C. Doğar 1092.
ABBAUİ, 29.04.2017, C. Doğar 1257, 1274 and 1281.
ABBAUİ, 11.03.2018, C. Doğar 1325, 1350.
***7. ALYSSUM** L.*
A. desertorum Stapf. var. desertorum (Dumonotu)
ABBAUİ, 11.03.2018, C. Doğar 1317, 1321.
A. strigosum Banks & Sol subsp. strigosum (Dökükkuduzotu)
ABBAUİ, 18.05.2018, C. Doğar 1384.
A. murale Waldst. & Kit var. murale (Sekikkuduzotu)
ABBAUİ, 18.05.2018, C. Doğar 1376.
***8. BARBAREA** R. BR.*
B. brachycarpa subsp. minor var. minor (K.Koch) Parolly & Eren (Nicarcık)
ABBAUİ, 29.04.2016, C. Doğar 1076.
***9. SISYMBRIUM** L.*
S. officinale (L.) Scop. (Ergelenhardalı)
KBAUİ, 28.04.2016, C. Doğar 1053.
ABBAUİ, 29.04.2016, C. Doğar 1068.
ABBAUİ, 29.04.2017, C. Doğar 1263, 1253.
ABBAUİ, 18.05.2018, C. Doğar 1337.
S. altissimum L. (Ergelenotu)
KBAUİ, 02.06.2016, C. Doğar 1138.
ABBAUİ, 29.04.2017, C. Doğar 1252.
S. loeselii L. (Bülbülotu)
ABBAUİ, 12.05.2016, C. Doğar 1100, 1101 and 1102.
KBAUİ, 03.09.2016, C. Doğar 1226.
ABBAUİ, 11.03.2018, C. Doğar 1324.
ABBAUİ, 18.05.2018, C. Doğar 1391.
***10. DESCURAINIA** Webb & Berth.*
D. sophia (L.) Webb ex Prantl (Sadırotu)
HAUÇ, 27.04.2016, C. Doğar 1035.

KBAUİ, 28.04.2016, C. Doğar 1038.
ABBAUİ, 29.04.2016, C. Doğar 1075.
ABBAUİ, 12.05.2016, C. Doğar 1116, 1119.
ABBAUİ, 29.04.2017, C. Doğar 1258, 1278.
KBAUİ, 10.03.2018, C. Doğar 1301.
ABBAUİ, 11.03.2018, C. Doğar 1312.

4. RESEDACEAE

1. RESEDA *L.*
R. lutea L. var. lutea (Muhabbetçiçeği)
HAUÇ, 27.04.2016, C. Doğar 1023.
HAUÇ, 25.06.2016, C. Doğar 1175.
ABBAUİ, 18.05.2018, C. Doğar 1412.

5. VIOLACEAE

1. VIOLA *L.*
V. occulta Lehm. (Saklımenekşe)
KBAUİ, 10.03.2018, C. Doğar 1304.
ABBAUİ, 11.03.2018, C. Doğar 1307.

6. CARYOPHYLLACEAE

1. ARENARIA *L.*
A. serpyllifolia L. (Tarlakumotu)
ABBAUİ, 11.03.2018, C. Doğar 1315.

2. STELLARIA *L.*
S. media (L.) Vill. (Kuşotu)
ABBAUİ, 29.04.2017, C. Doğar 1284.
ABBAUİ, 11.03.2018, C. Doğar 1326.

3. CERASTIUM *L.*
C. perfoliatum L. (Ekinboynuzotu)
ABBAUİ, 29.04.2016, C. Doğar 1078.
ABBAUİ, 29.04.2017, C. Doğar 1282.
HAUÇ, 24.02.2018, C. Doğar 1295.
KBAUİ, 10.03.2018, C. Doğar 1306.

4. HOLOSTEUM *L.*
H. umbellatum L. (Şeytanküpesi)
KBAUİ, 28.04.2016, C. Doğar 1054.
ABBAUİ, 12.05.2016, C. Doğar 1093.

5. GYPSOPHILA *L.*
G. perfoliata L. var. perfoliata (Helvacıçöveni)
ABBAUİ, 16.08.2016, C. Doğar 1207.
G. pilosa Huds.(Tarlaçöveni)
KBAUİ, 02.06.2016, C. Doğar 1125, 1128 and 1158. Irano-Turanian.

6. VACCARIA *N. M. Wolf*
V. hispanica (Mill.) Rauschert (Ekinebesi)
KBAUİ, 28.04.2016, C. Doğar 1056.
KBAUİ, 02.06.2016, C. Doğar 1155.

7. POLYGONACEAE

1. POLYGONUM *L.*
P. persicaria L. (Söğütotu)
ABBAUİ, 18.05.2018, C. Doğar 1392.
P. cognatum Meissn. (Madımak)
ABBAUİ, 18.05.2018, C. Doğar 1374.
P. bellardii All. (Atmercimeleği)
KBAUİ, 02.06.2016, C. Doğar 1124.
KBAUİ, 03.09.2016, C. Doğar 1233.

2. RUMEX *L.*
R. crispus L. (Labada)
ABBAUİ, 18.05.2018, C. Doğar 1338.

R. pulcher L.(Ekşilik)
ABBAUİ, 18.05.2018, C. Doğar 1364.
8. CHENOPODIACEAE
***1. CHENOPODIUM** L.*
C. album L. (Aksirken)
ABBAUİ, 01.10.2016, C. Doğar 1242.
ABBAUİ, 18.05.2018, C. Doğar 1403.
***2. ATRIPLEX** L.*
A. nitens Schkuhr (Dağıspanağı)
HAUÇ, 28.08.2016, C. Doğar 1219, 1220.
KBAUİ, 03.09.2016, C. Doğar 1229.
9. AMARANTHACEAE
***1. AMARANTHUS** L.*
A. retroflexus L. (Tilkikuyruğu)
ABBAUİ, 16.08.2016, C. Doğar 1199.
HAUÇ, 28.08.2016, C. Doğar 1216.
ABBAUİ, 01.10.2016, C. Doğar 1237.
ABBAUİ, 18.05.2018, C. Doğar 1348.
10. MALVACEAE
***1. HIBISCUS** L.*
H. trionum L. (Kerkede)
ABBAUİ, 16.08.2016, C. Doğar 1197.
KBAUİ, 03.09.2016, C. Doğar 1225.
ABBAUİ, 01.10.2016, C. Doğar 1244.
***2. MALVA** L.*
M. alcea L. (Ebecik)
HAUÇ, 25.06.2016, C. Doğar 1168.
M. neglecta Wallr. (Çobançöreği)
HAUÇ, 25.06.2016, C. Doğar 1186.
ABBAUİ, 29.04.2017, C. Doğar 1250.
ABBAUİ, 18.05.2018, C. Doğar 1405.
***3. ALCEA** L.*
A. pallida (Willd.) Waldst. & Kit. (Devegülü)
HAUÇ, 28.08.2016, C. Doğar 1221.
11. LINACEAE
***1. LINUM** L.*
L. nodiflorum L. (Yabanketen)
KBAUİ, 02.06.2016, C. Doğar 1146. Mediterranean.
12. GERANIACEAE
***1. GERANIUM** L.*
G. tuberosum L. (Çakmuz)
ABBAUİ, 29.04.2016, C. Doğar 1081. Irano-Turanian.
G. pyrenaicum Burm. Fil. (Gelinçarşafı)
ABBAUİ, 11.03.2018, C. Doğar 1316.
ABBAUİ, 18.05.2018, C. Doğar 1363.
***2. ERODIUM** L' Herit*
E. ciconium (L.) L'Herit.(Kocakarınığnesi)
ABBAUİ, 18.05.2018, C. Doğar 1343, 1344.
E. cicutarium (L.) L' Herit subsp. Cicutarium (İğnelik)
KBAUİ, 02.06.2016, C. Doğar 1133.
ABBAUİ, 18.05.2018, C. Doğar 1362.
E. acaule (L.) Becherer et Thell. (Leylekgagası)
HAUÇ, 27.04.2016, C. Doğar 1008. Mediterranean.
13.OXALIDACEAE
***1. OXALIS** L.*
O. pes-caprae L. (Kocaekşiyonca)

ABBAUİ, 18.05.2018, C. Doğar 1408.
14. ZYGOPHYLLACEAE
1. TRIBULUS *L.*
T. terrestris L. (Çobançökerten)
ABBAUİ, 18.05.2018, C. Doğar 1386.
15. LEGUMINOSAE (FABACEAE)
1. VICIA *L.*
V. peregrina L. (Kavli)
KBAUİ, 28.04.2016, C. Doğar 1049.
V. sativa L. subsp. sativa (Fiğ)
KBAUİ, 28.04.2016, C. Doğar 1043.
2. TRIFOLIUM *L.*
T. pratense L. var. pratense Boiss. (Çayırgülü)
KBAUİ, 28.04.2016, C. Doğar 1065.
3. MELILOTUS *L.*
M. officinalis (L.) Desr. (Kokuluyonca)
ABBAUİ, 18.05.2018, C. Doğar 1388.
KBAUİ, 02.06.2016, C. Doğar 1157.
4. MEDICAGO *L.*
M. sativa L. (Karayonca)
ABBAUİ, 12.05.2016, C. Doğar 1115.
HAUÇ, 25.06.2016, C. Doğar 1171, 1173 and 1178.
ABBAUİ, 16.08.2016, C. Doğar 1194, 1202.
HAUÇ, 28.08.2016, C. Doğar 1218.
ABBAUİ, 18.05.2018, C. Doğar 1329.
5. LOTUS *L.*
L. corniculatus L. (Gazalboynuzu)
ABBAUİ, 16.08.2016, C. Doğar 1206
6. ONOBRYCHIS Adans.
O. viciifolia Scop. (Korunga)
HAUÇ, 27.04.2016, C. Doğar 1034.
KBAUİ, 02.06.2016, C. Doğar 1121.
7. ALHAGI *Adans.*
A. maurorum Medik. (Aguldikeni)
ABBAUİ, 18.05.2018, C. Doğar 1416. Irano-Turanian.
16. ROSACEAE
1. POTENTILLA *L.*
P. recta L. (Suparmakotu)
ABBAUİ, 18.05.2018, C. Doğar 1369.
P. reptans L. (Reşatınotu)
HAUÇ, 25.06.2016, C. Doğar 1193.
ABBAUİ, 18.05.2018, C. Doğar 1331.
2. ROSA *L.*
R. canina L. (Kuşburnu)
ABBAUİ, 18.05.2018, C. Doğar 1365.
17. UMBELLIFERAE (APIACEAE)
1. ECHINOPHORA *L.*
E. tournefortii Jaub. & Spach (Dikenliçördük)
KBAUİ, 03.09.2016, C. Doğar 1222. Irano-Turanian.
2. BIFORA *Hoffm.*
B. radians Bieb. (Gısbana)
KBAUİ, 02.06.2016, C. Doğar 1156.
3. HERACLEUM *L.*
H. sphondylium L. (Devesil)
ABBAUİ, 18.05.2018, C. Doğar 1409. Euro-Siberian.
4. TURGENIA *Hoffm.*

T. latifolia (L.) Hoffm. (Karaheci)
KBAUİ, 02.06.2016, C. Doğar 1126.
***5. DAUCUS** L.*
D. guttatus Sm. (Beneklihavuç)
HAUÇ, 25.06.2016, C. Doğar 1166.
ABBAUİ, 18.05.2018, C. Doğar 1333.
18. ARALIACEAE
***1. HEDERA** L.*
H. helix L. (Duvarsarmaşığı)
ABBAUİ, 18.05.2018, C. Doğar 1415.
19. CAPRIFOLIACEAE
***1. LONICERA** L.*
L. caucasica Pallas (Çakkana)
KBAUİ, 28.04.2016, C. Doğar 1059.
20. DIPSACACEAE
***1. SCABIOSA** L.*
S. argentea L. (Yazısüpürgesi)
HAUÇ, 25.06.2016, C. Doğar 1188.
S. rotata Bieb. (Topuyuzotu)
KBAUİ, 02.06.2016, C. Doğar 1141, 1145.
HAUÇ, 25.06.2016, C. Doğar 1179. Irano-Turanian.
21. COMPOSITAE (ASTERACEAE)
***1. XANTHIUM** L.*
X. spinosum L. (Pıtrak)
ABBAUİ, 18.05.2018, C. Doğar 1375.
X. strumarium L. subsp. strumarium (Kocapıtrak)
ABBAUİ, 18.05.2018, C. Doğar 1398.
***2. SENECIO** L.*
S. vulgaris L. (Taşakcılotu)
ABBAUİ, 11.03.2018, C. Doğar 1319.
S. vernalis Waldst. & Kit. (Kanaryaotu)
HAUÇ, 27.04.2016, C. Doğar 1005.
ABBAUİ, 29.04.2016, C. Doğar 1087.
ABBAUİ, 29.04.2017, C. Doğar 1260.
S. viscosus L. (Yağlıkanaryaotu)
KBAUİ, 02.06.2016, C. Doğar 1137, 1144 and 1159.
***3. COTA** Gay ex Guss.*
C. tinctoria var. tinctoria (L.) J.Gay (Boyacıpapatyası)
HAUÇ, 25.06.2016, C. Doğar 1191.
C. tinctoria var. pallida (DC.) Özbek & Vural.
KBAUİ, 02.06.2016, C. Doğar 1152.
C. austriaca (Jacq.) Sch.Bip (Babuççа)
KBAUİ, 28.04.2016, C. Doğar 1040.
***4. ACHILLEA** L.*
A. santolinoides subsp. wilhelmsii (K.Koch) Greuter (Kardaşkınası)
KBAUİ, 03.09.2016, C. Doğar 1234. Irano-Turanian.
***5. CIRSIUM** Miller*
C. arvense (L.) Scop. (Köygöçüren)
HAUÇ, 25.06.2016, C. Doğar 1182.
ABBAUİ, 01.10.2016, C. Doğar 1235.
***6. CARDUUS** L.*
C. pycnocephalus L. (Soymaç)
KBAUİ, 28.04.2016, C. Doğar 1044.
KBAUİ, 02.06.2016, C. Doğar 1130.
ABBAUİ, 18.05.2018, C. Doğar 1393.
***7. RHAPONTICUM** Ludwig*

R. repens (L.) Hidalgo (Kekredikeni)
KBAUİ, 02.06.2016, C. Doğar 1142, 1147.
ABBAUİ, 16.08.2016, C. Doğar 1195.
ABBAUİ, 01.10.2016, C. Doğar 1238. Irano-Turanian.
***8. CYANUS** Mill.*
C. depressus (M.Bieb.) Soják (Gökbaş)
KBAUİ, 28.04.2016, C. Doğar 1047.
HAUÇ, 25.06.2016, C. Doğar 1176.
***9. SCOLYMUS** L.*
S. hispanicus L. (Şevketibostan)
HAUÇ, 25.06.2016, C. Doğar 1169. Mediterranean.
***10. CICHORIUM** L.*
C. intybus L. (Hindiba)
HAUÇ, 25.06.2016, C. Doğar 1174, 1183.
HAUÇ, 28.08.2016, C. Doğar 1210.
***11. SCORZONERA** L.*
S. cana (C.A. Meyer) Hoffm. var. cana (Tekesakalı)
HAUÇ, 27.04.2016, C. Doğar 1024.
***12. TRAGOPOGON** L.*
T. dubius Scop. (Atyemliği)
HAUÇ, 27.04.2016, C. Doğar 1020.
T. pratensis L. (Salsifin)
KBAUİ, 02.06.2016, C. Doğar 1136.
***13. TARAXACUM** Wiggers*
T. serotinum (Waldst. & Kit.) Fisch. (Karahindiba)
HAUÇ, 28.08.2016, C. Doğar 1213.
T. androssovii Schischkin (Zeze)
HAUÇ, 27.04.2016, C. Doğar 1025.
ABBAUİ, 29.04.2016, C. Doğar 1084.
***14. CHONDRILLA** L.*
C. juncea L. var. juncea (Karakavuk)
ABBAUİ, 18.08.2016, C. Doğar 1196.
KBAUİ, 03.09.2016, C. Doğar 1227.
C. juncea L. var. acantholepis Boiss.
HAUÇ, 28.08.2016, C. Doğar 1208.
***15. CREPIS** L.*
C. sprengeriana (L.) All.
HAUÇ, 25.06.2016, C. Doğar 1167.
C. alpina L. (Yürekotu)
KBAUİ, 02.06.2016, C. Doğar 1132.
ABBAUİ, 18.05.2018, C. Doğar 1334.
C. foetida L. (Kohum)
HAUÇ, 28.08.2016, C. Doğar 1215.
***16. PICRIS** L.*
P. pauciflora Willd. (Kumşirotu)
HAUÇ, 28.08.2016, C. Doğar 1211. Mediterranean.
***17. SONCHUS** L.*
S. asper L. (Eşekgevreği)
ABBAUİ, 18.05.2018, C. Doğar 1411.
***18. LACTUCA** L.*
L. serriola L. (Eşekhelvası)
ABBAUİ, 18.05.2018, C. Doğar 1413.
22. PRIMULACEAE
***1. ANAGALLIS** L.*
A. arvensis var. caerulea (L.) Gouan (Farekulağı)
KBAUİ, 02.06.2016, C. Doğar 1123.

23. OLEACEAE
1. LIGUSTRUM *L.*
L. vulgare L. (Kurtbağrı)
ABBAUİ, 18.05.2018, C. Doğar 1420. Euro-Siberian.
24. APOCYNACEAE
1. VINCA *L.*
V. herbacea Waldst. & Kit. (Bikirçiçeği)
ABBAUİ, 29.04.2017, C. Doğar 1256.
25. CONVOLVULACEAE
1. CONVOLVULUS *L.*
C. arvensis L. (Tarlasarmaşığı)
KBAUİ, 28.04.2016, C. Doğar 1039, 1042.
ABBAUİ, 12.05.2016, C. Doğar 1113.
KBAUİ, 02.06.2016, C. Doğar 1122, 1143 and 1161.
HAUÇ, 25.06.2016, C. Doğar 1185, 1190.
ABBAUİ, 16.08.2016, C. Doğar 1201.
HAUÇ, 28.08.2016, C. Doğar 1214.
ABBAUİ, 01.10.2016, C. Doğar 1236.
C. galaticus Rotsan ex Choisy (Bozsarmaşık)
ABBAUİ, 12.05.2016, C. Doğar 1110.
ABBAUİ, 16.08.2016, C. Doğar 1203.
ABBAUİ, 18.05.2018, C. Doğar 1399. Irano-Turanian.
26. BORAGINACEAE
1. HELIOTROPIUM *L.*
H. europaeum L. (Akrepotu)
KBAUİ, 02.06.2016, C. Doğar 1160.
ABBAUİ, 18.05.2018, C. Doğar 1340. Irano-Turanian.
H. suaveolens M.Bieb. (Itırlıbambul)
KBAUİ, 03.09.2016, C. Doğar 1223.
ABBAUİ, 16.08.2016, C. Doğar 1205. East Mediterranean.
2. ASPERUGO *L.*
A. procumbens L. (Nevazilotu)
ABBAUİ, 12.05.2016, C. Doğar 1097.
ABBAUİ, 29.04.2017, C. Doğar 1261, 1262. Euro-Siberian.
3. BUGLOSSOIDES *Moench*
B. glandulosa (Velen.) R.Fern. (Sadırlıtaşkeseni)
ABBAUİ, 29.04.2016, C. Doğar 1088. Euxin.
B. arvensis (L.) I. M. Johnston (Tarlataşkeseni)
ABBAUİ, 29.04.2016, C. Doğar 1071.
ABBAUİ, 12.05.2016, C. Doğar 1091.
ABBAUİ, 16.08.2016, C. Doğar 1205.
ABBAUİ, 29.04.2017, C. Doğar 1254.
ABBAUİ, 11.03.2018, C. Doğar 1314.
4. ECHIUM *L.*
E. italicum L. (Kurtkuyruğu)
HAUÇ, 25.06.2016, C. Doğar 1163. Mediterranean.
5. MOLTKIA *Lehm.*
M. coerulea (Willd.) Lehm. (Mavikesen)
KBAUİ, 28.04.2016, C. Doğar 1045. Irano-Turanian.
6. ANCHUSA *L.*
A. leptophylla Roemer & Schultes subsp. Leptophylla (Ballık)
HAUÇ, 27.04.2016, C. Doğar 1029.
HAUÇ, 25.06.2016, C. Doğar 1170.
ABBAUİ, 18.05.2018, C. Doğar 1397.
A. pusilla Guşul. (Kırkgövrek)
KBAUİ, 28.04.2016, C. Doğar 1050.

ABBAUİ, 29.04.2016, C. Doğar 1080.
ABBAUİ, 12.05.2016, C. Doğar 1096.
KBAUİ, 02.06.2016, C. Doğar 1123.
ABBAUİ, 29.04.2017, C. Doğar 1275.
ABBAUİ, 18.05.2018, C. Doğar 1349.

27. SOLANACEAE

1. SOLANUM *L.*
S. americanum Mill. (İtüzümü)
ABBAUİ, 01.10.2016, C. Doğar 1246, 1247.

2. DATURA *L.*
D. stramonium L. (Boruçiçeği)
ABBAUİ, 01.10.2016, C. Doğar 1240, 1243.

3. HYOSCYAMUS *L.*
H. niger L. (Banotu)
KBAUİ, 28.04.2016, C. Doğar 1061.
ABBAUİ, 29.04.2016, C. Doğar 1070.

28. SCROPHULARIACEAE

1. VERBASCUM *L.*
V. lasianthum Boiss. ex Benth. (Yünlüsığırkuyruğu)
HAUÇ, 27.04.2016, C. Doğar 1014.
HAUÇ, 25.06.2016, C. Doğar 1184.
V. ancyritanum Bornm. (Ankarasığırkuyruğu)
ABBAUİ, 18.05.2018, C. Doğar 1351. Irano-Turanian /Endemic.

2. VERONICA *L.*
V. polita Fries (Mavişot)
HAUÇ, 27.04.2016, C. Doğar 1031.
ABBAUİ, 29.04.2017, C. Doğar 1267, 1279.
ABBAUİ, 11.03.2018, C. Doğar 1311.
V. persica Poiret (Cırcamuk)
ABBAUİ, 29.04.2016, C. Doğar 1083.
HAUÇ, 24.02.2018, C. Doğar 1292.
ABBAUİ, 18.05.2018, C. Doğar 1406, 1407.
V. triloba (Opiz) Kerner (Üçmaviş)
ABBAUİ, 29.04.2017, C. Doğar 1263.
HAUÇ, 24.02.2018, C. Doğar 1294.
ABBAUİ, 11.03.2018, C. Doğar 1313.
V. hederifolia L. (Baharmavisi)
ABBAUİ, 29.04.2016, C. Doğar 1079.
ABBAUİ, 12.05.2016, C. Doğar 1209.
HAUÇ, 24.02.2018, C. Doğar 1293.
V. anagallis-aquatica L. (Sugedemesi)
ABBAUİ, 18.05.2018, C. Doğar 1342, 1406 and 1407.

29. OROBANCHACEAE

1. OROBANCHE *L.*
O. ramosa L. (Narincanavarotu)
ABBAUİ, 01.10.2016, C. Doğar 1241.

30. LABIATAE (LAMIACEAE)

1. AJUGA *L.*
A. chamaepitys (L.) Schreber subsp. chia (Schreber) Arcangeli var. Chia (Acıgıcı)
HAUÇ, 27.04.2016, C. Doğar 1011.
KBAUİ, 28.04.2016, C. Doğar 1046.
KBAUİ, 02.06.2016, C. Doğar 1148.
KBAUİ, 03.09.2016, C. Doğar 1228.

2. LAMIUM *L.*
L. amplexicaule L. (Baltutan)
HAUÇ, 27.04.2016, C. Doğar 1036.

ABBAUİ, 29.04.2016, C. Doğar 1067.
ABBAUİ, 12.05.2016, C. Doğar 1095.
ABBAUİ, 29.04.2017, C. Doğar 1271. Euro-Siberian.
L. purpureum L. (Ballıbaba)
ABBAUİ, 12.05.2016, C. Doğar 1094.
ABBAUİ, 29.04.2017, C. Doğar 1272.
ABBAUİ, 11.03.2018, C. Doğar 1322.
ABBAUİ, 18.05.2018, C. Doğar 1404.
L. orientale (Fisch. & C.A.Mey.) E.H.L.Krause (Güzelce)
HAUÇ, 27.04.2016, C. Doğar 1033.
KBAUİ, 28.04.2016, C. Doğar 1055.
ABBAUİ, 12.05.2016, C. Doğar 1106.
KBAUİ, 02.06.2016, C. Doğar 1153. Irano-Turanian
***3. BALLOTA** L.*
B. nigra L. subsp. anatolica P. H. Davis (Gıripotu)
ABBAUİ, 18.05.2018, C. Doğar 1378. Irano-Turanian.
***4. STACHYS** L.*
S. cretica L. subsp. anatolica Rech.fil. (Yağlıkara)
HAUÇ, 25.06.2016, C. Doğar 1162. Endemic.
***5. CLINOPODIUM** L.*
C. graveolens subsp. rotundifolium (Pers.) Govaerts (Filiskin)
KBAUİ, 28.04.2016, C. Doğar 1052.
***6. MENTHA** L.*
M. longifolia (L.) Hudson subsp. typhoides (Briq.) Harley (Derenanesi)
ABBAUİ, 18.05.2018, C. Doğar 1359.
***7. SALVIA** L.*
S. syriaca L. (Çevlikotu)
KBAUİ, 28.04.2016, C. Doğar 1064. Irano-Turanian.
31. PLANTAGINACEAE
***1. PLANTAGO** L.*
P. major L. (Sinirotu)
ABBAUİ, 18.05.2018, C. Doğar 1335.
P. lanceolata L. (Damarlıca)
KBAUİ, 28.04.2016, C. Doğar 1066.
32. ELAEAGNACEAE
***1. ELAEAGNUS** L.*
E. angustifolia L.(İğde)
ABBAUİ, 18.05.2018, C. Doğar 1421.
33. EUPHORBIACEAE
***1. EUPHORBIA** L.*
E helioscopia L. (Feribanotu)
ABBAUİ, 29.04.2016, C. Doğar 1086.
ABBAUİ, 12.05.2016, C. Doğar 1107, 1108.
ABBAUİ, 29.04.2017, C. Doğar 1277.
ABBAUİ, 11.03.2018, C. Doğar 1323.
ABBAUİ, 18.05.2018, C. Doğar 1379.
E. macroclada Boiss. (Neblul)
KBAUİ, 02.06.2016, C. Doğar 1127, 1150.
HAUÇ, 25.06.2016, C. Doğar 1181.
KBAUİ, 03.09.2016, C. Doğar 1230. Irano-Turanian
E. seguieriana Necker (Tasmaotu)
KBAUİ, 28.04.2016, C. Doğar 1060.
34. RUBIACEAE
***1. GALIUM** L.*
G. verum L. subsp. Verum (Boyalık)
HAUÇ, 25.06.2016, C. Doğar 1192. Euro-Siberian.

G. spurium L. subsp. spurium (Arsıziplikçik)
ABBAUİ, 11.03.2018, C. Doğar 1327.
ABBAUİ, 18.05.2018, C. Doğar 1402. Euro-Siberian.
G. aparine L. (Çobansüzgeci)
ABBAUİ, 18.05.2018, C. Doğar 1358, 1402.
***2. RUBIA** L.*
R. tinctorum L. (Kökboyası)
ABBAUİ, 18.05.2018, C. Doğar 1410. Irano-Turanian
Subdivisio: ANGIOSPERMAE
Classis: MONOCOTYLEDONES
1. LILIACEAE
***1. ALLIUM** L.*
A. atroviolaceum Boiss. (Liflikörmen)
HAUÇ, 25.06.2016, C. Doğar 1180.
KBAUİ, 03.09.2016, C. Doğar 1224.
KBAUİ, 10.03.2018, C. Doğar 1296.
***2. ORNITHOGALUM** L.*
O. narbonense L. (Akbaldır)
ABBAUİ, 29.04.2017, C. Doğar 1264. Mediterranean.
O. umbellatum L. (Sunbala)
KBAUİ, 28.04.2016, C. Doğar 1041.
***3. MUSCARI** Miller*
M. neglectum Guss. (Arapüzümü)
KBAUİ, 10.03.2018, C. Doğar 1299, 1300.
***4. GAGEA** Salisb.*
G. villosa (Bieb.) Duby var. villosa (Tüylüyıldız)
KBAUİ, 10.03.2018, C. Doğar 1303.
ABBAUİ, 11.03.2018, C. Doğar 1310. Mediterranean.
***5. COLCHICUM** L.*
C. triphyllum G. Kunze (Öksüzali)
HAUÇ, 24.02.2018, C. Doğar 1287.
KBAUİ, 10.03.2018, C. Doğar 1297, 1298. Mediterranean.
2. IRIDACEAE
***1. CROCUS** L.*
C. danfordiae subsp. danfordiae Maw (İnceçiğdem)
HAUÇ, 24.02.2018, C. Doğar 1286. Endemic.
***2. GLADIOLUS** L.*
G. atroviolaceus Boiss. (Kıraçsüseni)
KBAUİ, 28.04.2016, C. Doğar 1048. Irano-Turanian
3. GRAMINEAE (POACEAE)
***1. ELYMUS** L.*
E. hispidus (Opiz) Melderis subsp. Hispidus (Elimotu)
HAUÇ, 24.02.2018, C. Doğar 1293.
***2. TRITICUM** L.*
T. aestivum L. (Ekmeklikbuğday)
ABBAUİ, 18.05.2018, C. Doğar 1387.
KBAUİ, 02.06.2016, C. Doğar 1134, 1135, 1151.
***3. HORDEUM** L.*
H. murinum L. subsp. glaucum (Steudel) Tzvelev (Duvararpası)
ABBAUİ, 29.04.2016, C. Doğar 1072.
KBAUİ, 02.06.2016, C. Doğar 1131.
HAUÇ, 24.02.2018, C. Doğar 1293.
ABBAUİ, 18.05.2018, C. Doğar 1345.
***4. BROMUS** L.*
B. tectorum L. subsp. tectorum (Kırbromu)
ABBAUİ, 18.05.2018, C. Doğar 1417.

B. sterilis L. (Sağırilcan)
ABBAUİ, 18.05.2018, C. Doğar 1401.
***5. ALOPECURUS** L.*
A. myosuroides Hudson var. myosuroides (Tarlatilkikuyruğu)
HAUÇ, 24.02.2018, C. Doğar 1090.
ABBAUİ, 18.05.2018, C. Doğar 1346. Euro-Siberian.
***6. PHLEUM** L.*
P. bertolonii DC. (Kumulitkuyruğu)
HAUÇ, 27.04.2016, C. Doğar 1028.
ABBAUİ, 29.04.2016, C. Doğar 1073.
***7. POA** L.*
P. angustifolia L. (Darsalkımotu)
HAUÇ, 27.04.2016, C. Doğar 1037.
ABBAUİ, 18.05.2018, C. Doğar 1355.
***8. SCLEROCHLOA P**. Beauv.*
S. dura (L.) P. Beauv. (Mıcırotu)
ABBAUİ, 18.05.2018, C. Doğar 1385. Euro-Siberian.
***9. PHRAGMITES** L.*
P. australis (Cav.) Trin. Ex Steudel (Kamış)
HAUÇ, 27.04.2016, C. Doğar 1027.
HAUÇ, 24.02.2018, C. Doğar 1288.
ABBAUİ, 18.05.2018, C. Doğar 1360. Euro-Siberian.
***10. SETARIA** P.Beauv.*
S. viridis (L.) P.Beauv. (Yeşilsıçansaçı)
HAUÇ, 27.04.2016, C. Doğar 1026.
ABBAUİ, 18.05.2018, C. Doğar 1418.

http://communications.science.ankara.edu.tr

Commun.Fac.Sci.Univ.Ank.Ser. C Biology
Volume 32, Number 2, Pages 174-191 (2023)
ISSN 1303-6025 E-ISSN 2651-3749
DOI: 10.53447/communc.1206230

Research Article; Received: November 17, 2022; Accepted: September 11, 2023

PROFILING THE GENES ASSOCIATED WITH OSMOADAPTATION AND THEIR VARIATION BY SEASONALLY IN TUZ LAKE

SUZAN ŞAHİN DOĞAN[1], AYTAÇ KOCABAŞ[1]

[1]Biology Department, KO Science Faculty of Karamanoglu Mehmetbey University, Karaman, TÜRKİYE

ABSTRACT. Hypersaline environments are one of the extreme habitats in the world. Microorganisms living in a hypersaline environment have developed various molecular adaptation strategies to overcome these extreme conditions. The study aims to investigate the genes associated with osmoadaptation seasonal variation in Tuz Lake by PICRUSt2. Dada2 pipelines were applied for filtering, dereplication, chimera identification, and merging paired-end reads to construct table.qza and rep_seqs.qza files. Therefore, the PICRUSt2 was applied to analyze the metabolic function of archaeal and bacterial diversity in Tuz Lake by using table.qza and rep_seqs.qza files. As a result of metabolic functions based on 16S rDNA amplicon data, the genes related to potassium accumulation played an important role in osmoregulation in Tuz Lake, where the archaea population was dominant. Furthermore, bacteriorhodopsin, halorhodopsin, and sensory rhodopsin functions were determined. The abundance of bacteriorhodopsin and halorhodopsin were increased in summer and spring, respectively.

1. INTRODUCTION

Halophilic microorganisms have developed various molecular mechanisms for adaptation to salt-rich habitats. In general, halophiles use two basic strategies to maintain the osmotic balance between their cytoplasm and environment. First, it is called the salt-in strategy, which is energetically advantageous. The “Salt-in” strategy is a method in which the intracellular salt concentration is kept higher than the environmental osmotic pressure by transporting ions into the cell [1]. It has been observed that halophiles using this method (e.g. *Salinibacter ruber* and *Halobacterium sp.)* have fewer hydrophobic residues and an increase in the synthesis of halophilic protein structures with a predominance of highly acidic amino acids such as aspartic acid. It has been reported that the highly acidic amino acids on the surfaces of halophilic proteins prevent aggregation at a high salt concentration [2, 3]. The second strategy is the accumulation of compatible solutes used by most microorganisms. Most halophilic or halotolerant microorganisms produce or accumulate intracellular small organic compounds (ectoine, trehalose, and sucrose) to maintain osmotic balance in hypersaline environments. Ectoine was first discovered in the haloalkaliphilic photosynthetic sulfur bacterium *Ectothiorhodospira halochloris* but was later found to produce this compound, usually with its 5-hydroxy derivative, by a wide variety of

Keywords. Tuz Lake, PICRUSt2, hypersaline, metabolic functions, osmoregulation

sdogan@kmu.edu.tr- Corresponding author; 0000-0002-1554-0080
aytackocabas@kmu.edu.tr- 0000-0001-7622-1932

halophilic and halotolerant bacteria. It has been reported that ectoine can protect many unstable enzymes and nucleic acids against high salinity, thermal denaturation, and the harmful effects of freezing, thus being important in increasing the shelf life and activity of enzyme preparations [4].

Because of the restricted composition of culture media, it could not reveal all the microbial composition and the dynamic of nutrient cycles. In recent years, the application of next-generation sequencing (NGS) technology to microbial communities has revolutionized environmental microbiological research, allowing cost-effectively both in-depth knowledge and large-scale sequencing of DNA samples without the need for culturing and cloning [5]. As well as sequencing technology, bioinformatics improvements have been advanced by developing powerful new computational tools for practical interpretation and visualization of the taxonomic and functional composition of microbial communities [6]. Nowadays, the prediction of metagenome functions from 16S rRNA gene sequences data by bioinformatics tools like PICRUSt2 allows investigating the metabolomes of complex microbial communities with high precision and confidence at a high taxonomic resolution besides a much lower cost compared to metagenomic sequencing [7]. Tuz Lake, a thalassohaline lake with a salt rate of 32% (w/v), is one of the best biological systems for studying survival strategies of microbial diversity and their response to environmental factors. There are several studies describing the prokaryotic and eukaryotic microbial diversity in Tuz Lake by NGS [8–11]. However, the characterization of metabolic diversity and seasonal variation of related genes are poorly understood in Tuz Lake. The purpose of the present study is to give insights into how osmoadaptation genes fluctuate in response to environmental parameters by seasonally in Tuz Lake, Türkiye. As per our knowledge, there is no reports showing the seasonal variation of genes associated with osmoadaptation in Tuz Lake.

2. MATERIALS AND METHODS

Water samples were collected from Cihanbeyli and Şereflikoçhisar regions of Tuz Lake at three different points of both sites (38°46`33``N-33°14`59``E, 38°45`20``N-33°13`50``E, 38°45`25``N-33°15`6``E, 38°47`1``N-33°26`42``E, 38°46`34``N-33°28`25``E, 38°45`50``N-33°27`6``E) from November 2018 to January 2020. The water samples were collected from the lake's surface at a depth of 10 cm aseptically in sterile bottles on the same day of every month. Water samples could not be taken in August and September because of drought. The water samples collected from each station have been mixed to create a pool for each month. As a result, water samples covering 13 months, which were November 2018, December 2018, January 2019, February 2019, March 2019, April 2019, May 2019, June 2019, July 2019, October 2019, November 2019, December 2019, and January 2020, were obtained. The water samples were clustered to Fall (October and November), Winter (December, January, February), Spring (March, April, May), and Summer (June, July) to evaluate seasonal variation.

2.1. Nucleic acid extraction and 16S rDNA amplicon sequencing

The DNA extraction protocol is same with the previous study [12] which is based on phenol-chloroform method [13]. As summary, 200 ml of water samples for each each month were filtered with 0.22 μm membrane filters and homogenized with liquid nitrogen. Prepared extraction buffer (KCI,Tris-HCI, EDTA) was added to the homogenized filter and centrifuged at 15.000g for 20 min. Then, the supernatant was taken, and RNAse (Thermo Scientific) was added, RNAse was inactivated by keeping it at 37 °C for two hours. Phenol: chloroform: isoamyl alcohol (25: 24: 1), pH,8 was added and centrifuged at 15.000g for 15 min. 3M sodium acetate solution was mixed with the supernatant and kept overnight at -20 °C to precipitate nucleic acids. The pellet was washed with 70% ethanol and dissolved in 10 mM Tris (pH,8) after final centrifugation at 13.000 g. DNA samples were assessed by Qubit DNA Assay (Thermo Scientific Qubit 4.0) and 1% agarose gel electrophoresis. V4 variable region of 16S rDNA was amplified with 515F (5'-GTGYCAGCMGCCGCGGTAA-3') and 806R (5'-GGACTACNVGGGTWTCTAAT-3') primers [14] and sequenced using Illumina MiSeq sequencing platform with 2 × 300 bp paired-end protocol by company (BC, Canada).

2.2. Bioinformatics analysis

The quality of reads was evaluated by FastQC [15] tool and the reads were trimmed to the length of 260 nt (Phred score >20) by trim length function. Dada2 [16] pipelines were used to filter, dereplicate, identify chimera, and merge paired-end reads "table.qza" and "rep_seqs.qza" files were created for functional analysis of reads by the PICRUSt2 pipeline [7]. SILVA database "v.132" [17] was used to assign taxonomy with 97% identity thresholds by classify-consensus-blast algorithm in QIIME2. Initially, the table.qza and rep_seqs.qza files were created by the QIIME2 software [18] and converted to BIOM format for subsequence analysis. place_seqs.py command was applied for ASV placement into a reference phylogenetic tree by EPA-NG and gappa based on the Integrated Microbial Genomes database [19]. The castor R package was used for hidden state prediction. hsp.py script was run in PICRUSt2 to predict the copy number of gene families and output the nearest-sequenced taxon index (NSTI) values for each ASV. NSTI scores that were lower than 2.0 were selected for subsequent analyses. metagenome_pipeline.py script was run for inferring the metagenomes of the communities. the --strat_out command was added to the metagenome_pipeline.py script to figure out how each ASV contributes Enzyme Classification (EC) and Kyoto Encyclopedia of Genes and Genomes (KEGG) orthologs (KO) numbers. After that, KO numbers were used to infer KEGG pathway levels against the KEGG database by pathway_pipeline.py command. Finally, the description of each functional category was added to the output abundance tables with add_descriptions.py command. STAMP [20] tool was used to analyze the functional profile.

3. RESULTS AND DISCUSSION

In the previous study, we investigated and published the composition of prokaryotic diversity in Tuz Lake by 16S amplicon sequencing [12]. Therefore, in the present study, we used the same water samples for generating predictive functional profiles in Tuz Lake. Total number of reads and ASV were detected as 501,654 and 652, respectively [21]. Also, the number of reads per sample were ranged between 4600-86200 after quality filter. High quality paired end reads were obtained. The mean quality scores of the sequences were found in the range of 32-36 [21].

In our previous study it has been shown that microbial diversity consists of 95% of archaea and %5 of bacteria in Tuz Lake [12]. It was determined that *Haloquadratum, Haloparvum, Halonotius, Halorubrum, Halobellus, Halapricum,* and *Haloarcula* were determined as the most abundant archaeal genera. Moreover, *Salinibacter, Pseudomonas, Arhodomonas, Halorhodospira*, and *Chromobacterium* were the most common bacterial genera [12]. Also, it was reported that the archaeal population in Tuz Lake was composed of the *Euryarchaeota* (96%) and *Nanoarchaeaeota* (4%) phyla [12]. Furthermore, the most abundant bacterial phyla were detected as *Bacteroidetes* (74%) and *Proteobacteria* (25%) (Figure S1).

As a result of predictive functional analysis with the PICRUSt2, the genes related to osmoadaptation, and rhodopsin were revealed and their seasonal variation with environmental parameters was assessed. The precision of the metagenome constructed using PICRUSt2 was confirmed by the nearest-sequenced taxon index (NSTI), suggesting the reference genomes closely correlated to the samples in the analysis. The means of NSTI values were 0.19±0.04 (Table S1). Similar findings were obtained with previously reported microbiome studies including rabbit fecal sample (NSTI = 0.19), soil microbiome from Ohio (NSTI = 0.17), hypersaline microbiome (mean NSTI = 0.23), the cold and the hot deserts soil microbiome (mean NSTI = 0.17), and the rhizosphere microbiome (mean NSTI = 0.23) [22–26].

In addition to the seasonal variation, water samples of November and December, taken in both 2019 and 2018, were compared to make year-based comparisons of metabolic functions, and no statistically significant difference was observed.

3.1. Osmoadaptation

Microorganisms overcome the osmotic stress by two mechanisms: KCl accumulation, which requires heavy modification of the enzyme content of the cell, or organic compatible solute deposition, which requires less proteomic modification and allows adaptation to different salt concentrations [27].

As a result of functional genes analysis with PICRUSt2, trkA/B/G/H genes related to potassium accumulation [28] were found predominant (Figure 1). The genes related to the potassium accumulation were predominated in *Haloarchaea,*

which uses a bio energetically efficient "salt in" strategy to move K+ and Cl- ions into the cell and Na+ ions out. High intracellular K+ concentration is maintained by active K+ transport [29]. Trk genes were primarily associated with *Halapricum*, *Haloparvum*, and *Salinibacter* (Table 1). Furthermore, the genes encoding the low-affinity K transporter TrkA/H, driven by the membrane potential [28], were detected. ATPase-K-KdpA/B/C genes were also found (Figure 1). It was seen that TrkA/H genes were higher in spring than in winter. Furthermore, the sequences related to TrkA, which was the most abundant functional gene associated with osmoadaptation, were determined the lowest proportion in December and January (Figure 1 and 2).

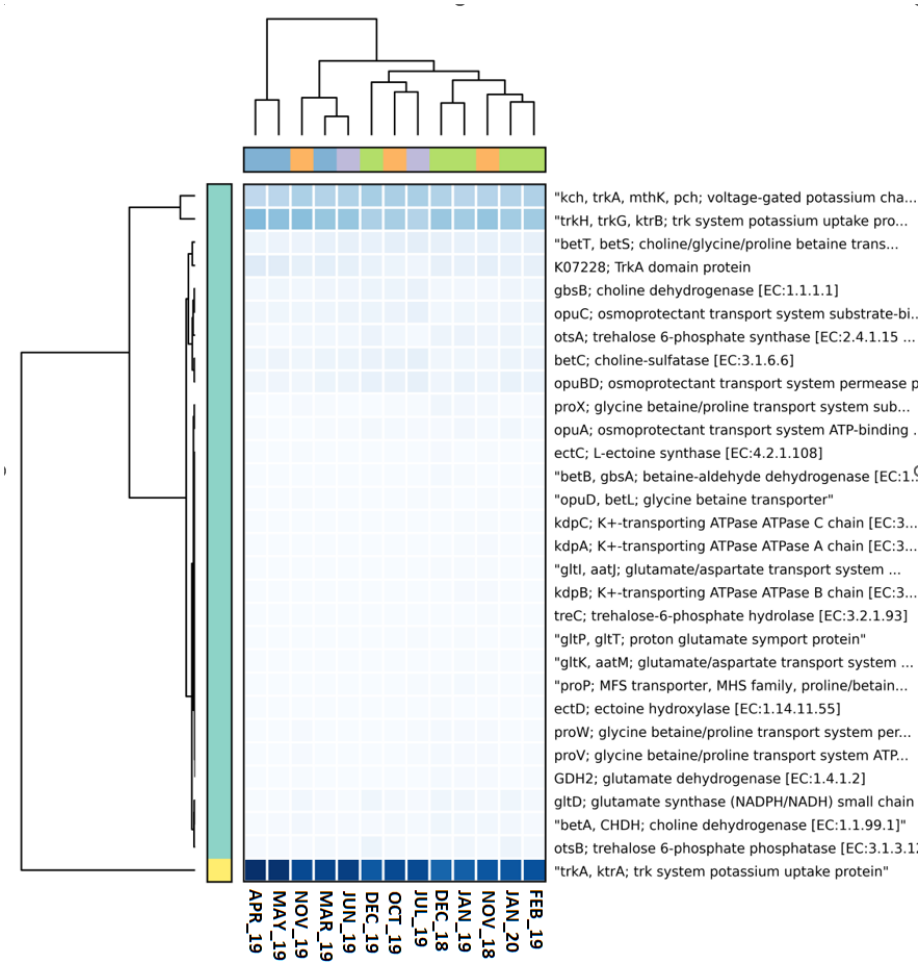

FIGURE 1. The changes of functional genes involved in environmental stress adaptation with heatmap graph by months (Spring:Blue, Fall:Orange, Summer:Purple, Winter:Green).

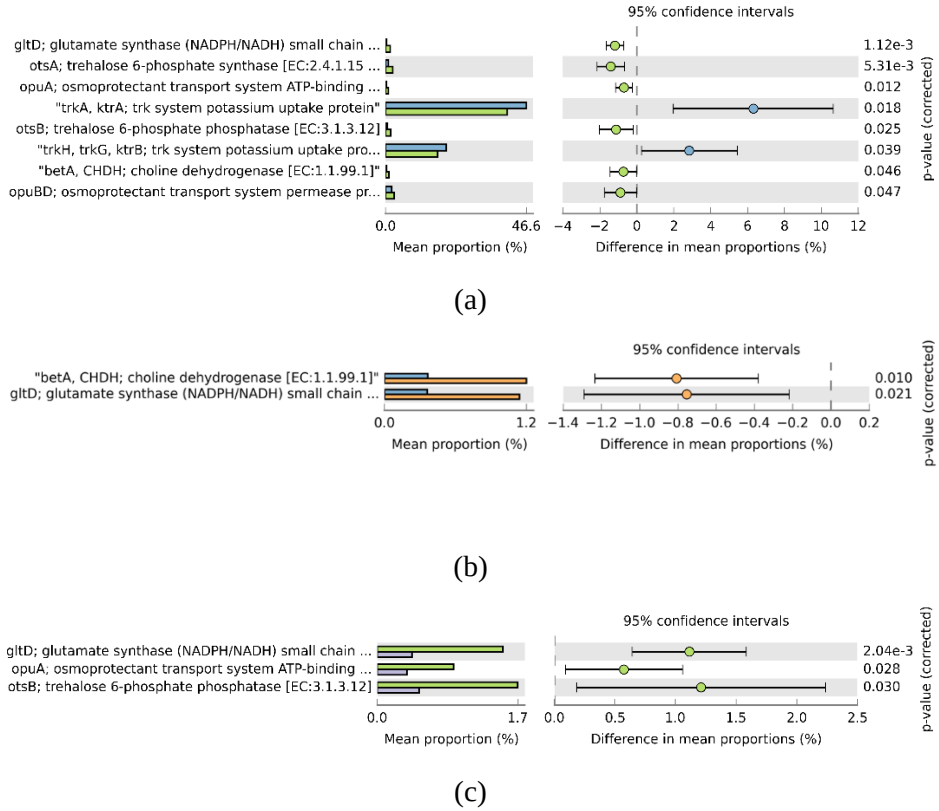

FIGURE 2. Analysis of seasonal variation of the relative abundances of functional genes involved in environmental stress adaptation using the Stamp program and Welch t-test (95% confidence interval, $p < 0.05$) (a) Spring and Winter (b) Spring and Fall (c) Winter and Summer (Spring:Blue, Fall:Orange, Summer:Purple, Winter:Green).

It is more favorable to take osmolytes from the environment instead of their biosynthesis in the cell. Therefore, bacteria and archaea encode multiple osmoregulation-related carrier proteins to take up osmolytes with high affinity [30]. In Tuz Lake, various genes encoding osmolytes transport proteins were revealed, too. BetT (choline transport)/betS (glycine betaine/proline betaine) and opuC were detected as the most abundant functional genes related to compatible solutes accumulation strategy. However, there was no statistical difference between betT/betS and opuC genes between the seasons. In addition, pro X/P/V/W (glycine betaine/proline/betaine transport) and glt (glutamate/aspartate transport) transport genes were also observed (Figure 1). OpuA, OpuBD, and OpuC are high-affinity ABC transporters, OpuD belongs to the betaine-choline-carnitine-transporter (BCCT) family, while the proline transporter OpuE is a member of the sodium-soluble-symport (SSS) family [28]. OpuC is responsible

for the intracellular transport of many compatible solutes, including choline and glycine betaine [31]. It has been reported that ABC transport proteins responsible for betaine transport were transcriptionally increased during the high salt adaptation of *Desulfovibrio vulgaris* [32]. However, present study opuA and opu BD were elevated in winter (Figure 2a and 2c).

The genes responsible for choline synthesis in the samples are pcs (phosphatidylcholine synthase [EC:2.7.8.24]), betT/betS (choline/glycine/proline betaine transport protein), betC (choline sulfatase [EC:3.1.6.6]), betaA (choline dehydrogenase [EC:1.1.99.1]) was observed in all months. The main function of choline in most species is to form a precursor metabolite for glycine betaine biosynthesis [33]. Most bacteria produce glycine betaine through the oxidation of choline with products of two genes encoding betB and betA, respectively [30]. While functional genes related to proline, glycine betaine such as proX, betaS/T/C were found at high proportion, genes for ectoine metabolism such as ectC (L-ectoine synthase [EC:4.2.1.108]) were observed at a very low proportion (Figure 1). A bioinformatics study showed that ectoine biosynthesis was predominantly found in bacteria and only in a few archaea [30]. In Tuz lake samples, genes encoding the ectoine synthase were predominantly observed in *Halorhodospira* (Table 1). In Tuz Lake, the sequences related to glycine betaine were found to be more abundant than the sequences associated with ectoine. In the metagenomic research conducted in the hypersaline Santa Pola saltern, it has been reported that genes required for betaine synthesis and especially betaine and choline transport were found in various halotolerant bacteria and cyanobacteria species [34]. In addition, it was stated that very few sequences related to ectoine transport and trehalose biosynthesis were obtained [34]. Trehalose, a glucose disaccharide, is found in a wide variety of microorganisms and helps to protect many biological structures against the stresses generated by typical extreme conditions such as drought, high temperature, and hyperosmotic conditions in saline environments [35]. In the current study, otsA (trehalose 6-phosphate synthase) and otsB (trehalose 6-phosphate phosphatase) genes were observed at a high level (Figure 1). OtsAB uses UDP-glucose and glucose-6-phosphate precursors for trehalose metabolism. Also, trehalose is synthesized as a nitrogen-free alternative to nitrogen-containing glycine betaine and ectoine, especially at low nitrogen concentrations [34]. It has been reported that the nitrate concentration of Tuz Lake was lower in winter than in spring [36]. The present study showed that genes related to trehalose metabolism were generally higher in winter. In addition, the genes related to trehalose synthesis were predominantly linked to *Halonotius* and *Salinibacter* (Table 1). Furthermore, it was reported that trehalose concentration decreased with increasing NaCl concentrations [37]. The sequences related to trehalose metabolism might be increased in the winter because of the low temperature and salinity [12,36].

The gltD (glutamate synthase) gene, involved in glutamate synthesis, was also detected at a high ratio (Figue 1 and 2). It has been reported that the synthesis of

this osmolyte is mostly found in bacteria, especially in the *Salinibacter* sequences [38]. In present study, the gltD gene was associated with the most abundant bacterial genus *Salinibacter*, as well *as Chitinophagales*; uncultured bacterium. Moreover, the gene encoding glumate dehydrogenase was primarily observed in the bacterial genera *Marinobacter* and *Halorhodospira* (Table 1).

TABLE 1. Taxonomic units associated with functional profiles of osmoregulation.

Month	Function	Taxon	Taxon abundance	Taxon relative abundance	Predicted copy number of function per taxon	Taxon function abundance	Taxon relative function abundance
November -2018	K15371	*Halorhodospira*	481	2.0	1	481	2
December -2018	K15371	*Marinobacter*	238	1.2	2	476	2.5
November -2018	K06720	*Halorhodospira*	481	2.0	1	481	2
February -2019	K06720	*Nitrococcaceae; g__uncultured*	416	0.5	1	416	0.5
April -2019	K04642	*Haloparvum*	5761	9.0	1	5761	9
February -2019	K04641	*Haloquadratum*	3717	4.8	2	7434	9.6
December -2018	K03499	*Halapricum*	505	13.0	5	2525	65.0
April -2019	K03499	*Haloparvum*	5761	9.0	6	34566	53.9
April -2019	K03498	*Haloparvum*	5761	9.0	3	17283	27.0
December -2018	K03498	*Salinibacter*	454	11.7	2	908	23.3
May-2019	K03499	*Haloparvum*	5074	8.7	6	30444	51.7
March -2019	K00697	*Halonotius*	313	0.5	1	313	0.5
April -2019	K00697	*Salinibacter*	269	0.4	1	269	0.4
May-2019	K03499	*Haloparvum*	5074	8.6	6	30444	51.7

Finally, when the seasonal variations of the glt (glutamate), bet (glycine betaine), ots (trehalose) and ect (ectoine) genes were assessed, it was seen that they were generally high proportion in winter (Figure 1 and 2). Therefore, the sequences related to the osmolyte accumulation might be increased in the winter because of the low temperature and salinity [12,36]. Furthermore, it was also stated that *Haloarchaea* typically prefers the salt-in strategy at high salt concentrations to maintain osmotic balance. Thus, organic solutes such as simple sugars, glycerol, and amino acids are taken into the cell are probably consumed as substrates [39].

In Tuz Lake, trkA were found the most abundant genes related to K+ uptake. The functional genes related to the intracellular osmolyte accumulation strategy predominantly increased in winter and fall, while trkA genes were found in high abundance in spring and summer (Figure 1 and 2). Moreover, the genes encoding potassium uptake proteins showed similar fluctuations with the archaeal population that increased in the summer and spring [12].

Finally, when the gene profile associated with osmoadaptation was assessed in principal component analysis (PCA) graph, it might be said that although there is no complete seasonal separation, a roughly grouping was observed in the spring and winter seasons (Figure S2).

3.2. Rhodopsin

Bacteriorhodopsin (K04641), halorhodopsin (K04642), and sensor rhodopsin (K04643) functions were observed in Tuz Lake (Figure 3a). Light is widely used as an energy source by rhodopsins in hypersaline environments [40]. Bacteriodopsin is an integral membrane protein that acts as a light-driven proton pump. The ion gradient produced across the membrane is then converted into chemical energy (ATP). Halorhodopsin is a bacteriorhodopsin-like retinal protein but an inwardly directed electrogenic chloride ion pump rather than an outwardly directed proton pump [41]. It was reported that along the salinity gradient, an increase in the number of sequences related to bacteriorhodopsins as well as sensory rhodopsins and halorhodopsins was observed, and it was stated that this was due to the more abundant species at higher salinities, *H. walsbyi* and *S. ruber* [42]. In Tuz Lake, the abundance of bacteriorhodopsin and halorhodopsin was increased in summer and spring, respectively. Also, bacteriorhodopsin was observed as the predominant rhodopsin gene (Figure 3a, 3b and 3c). In addition, the genes related to halorhodopsin and bacteriorhodopsin was primarily assigned to *Haloparvum* and *Haloquadratum*, respectively (Table 1). Archaea also use these structures for protection against high salinity and harmful light [43].

Halorhodopsin regulates intracellular osmotic pressure by carrying chloride ions into the cell. It also plays a role in transporting betaine into the cell for osmoregulation [35]. Moreover, the increase in ion concentration may also be a factor, as the conductivity is high during these months. The sequences related to the sensor rhodopsin genes were observed at the lowest proportion in summer while at the highest ratio in fall (Figure 3d). The experiment was conducted under microoxic conditions with *Halobacterium sp.* NRC-1 showed that three of the four rhodopsin types were expressed to harness solar energy and support periods of phototrophic growth. It has also been observed that sensory rhodopsin I (SRI) directs the phototaxis of the cell to wavelengths of light, where both bacteriorhodopsin and halorodopsin can be efficiently absorbed from solar energy and used most efficiently [44]. In the experiment with extremely

halophilic *Salinibacter*, SRI is synthesized only under low oxygen stress (like the proton pump BR and chloride pump HR) and mediates the absorption of the orange light that drives the proton pumps; it has been also determined that SRII is produced in high oxygen conditions and as a photophobic response to blue light when the cell bioenergetics are activated by the respiratory chain [43]. No statistical difference was observed between the seasons in the sequences related to sensory rhodopsin (Figure 3d). However, the sequences associated with sensory rhodopsin (SOP) function were observed as the lowest proportion in the summer (Figure 3d). SOP could be increased to direct bacteriorhodopsin and halorhodopsin to absorb solar energy efficiently.

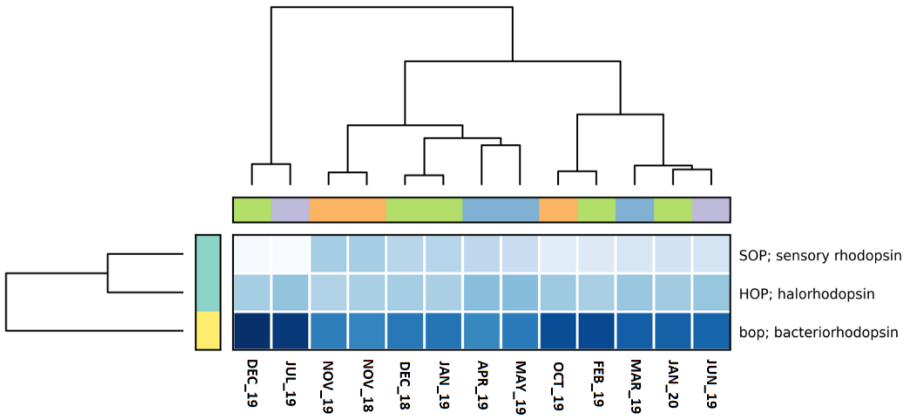

(a)

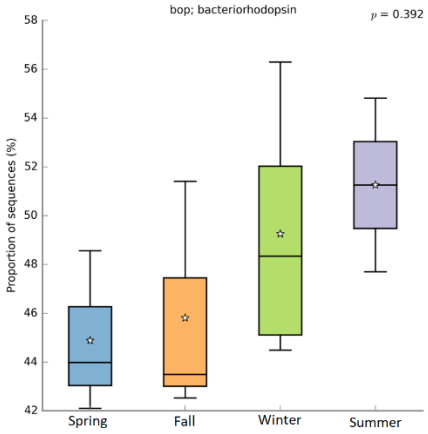
bop; bacteriorhodopsin
p = 0.392
Proportion of sequences (%)
58
56
54
52
50
48
46
44
42
Spring
Fall
Winter
Summer

(b)

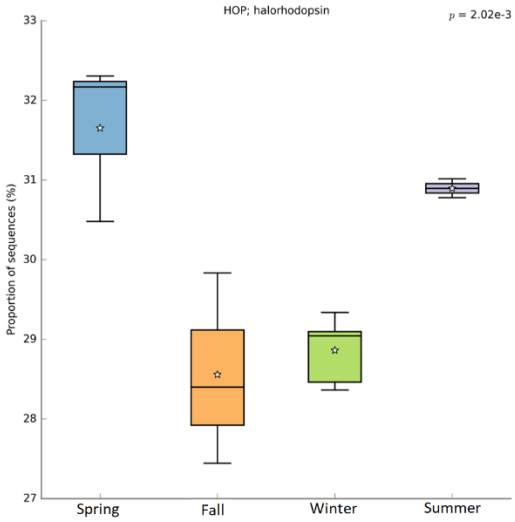
HOP; halorhodopsin
p = 2.02e-3
Proportion of sequences (%)
33
32
31
30
29
28
27
Spring
Fall
Winter
Summer

(c)

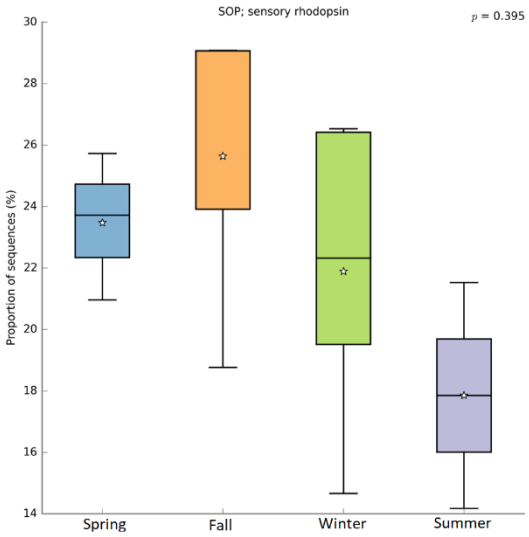

(d)

FIGURE 3. (a) Change of functional genes related to rhodopsin by months with heatmap graph (b) Seasonal variation of bacteriodopsin (c) Seasonal variation of halorodopsin (d) Seasonal variation of sensor rhodopsin (Spring:Blue, Fall:Orange, Summer:Purple, Winter:Green). ANOVA statistical test and Tukey-Kramer post-hoc test was applied by Stamp software (95% confidence interval, $p < 0.05$).

4. CONCLUSIONS

The genes related to osmoadaptation, and rhodopsins in Tuz Lake were analyzed, and its seasonal variation was investigated. The sequence associated with K+ uptake genes seems to play an essential role in osmoregulation in Tuz Lake, where the archaeal population was dominant with 95% abundance. Bacteriorhodopsin, halorhodopsin, and sensory rhodopsin functions were observed as rhodopsin functions. The abundance of bacteriorhodopsin and halorhodopsin was increased in summer and spring, respectively. Also, bacteriorhodopsin was observed as the predominant rhodopsin gene. These functional profiles in Tuz Lake might be valuable sources for future ecological and biotechnological research. Moreover, predictive functional profile could be beneficial to indentify candidate microorganisms for commercially significant genes. Further studies are required to reveal the regulation mechanisms of osmoadaptation in halophiles response to environmental parameters.

Acknowledgement This work was supported by the TUBITAK (Turkish Scientific and Technical Research Council) – [Project no: 117Z966].

Author Contribution Statements SŞD: designed the study, performed the wet-lab work and analyzed the data, wrote and reviewed the manuscript; AK: designed the study and applied for funding.

Declaration of Competing Interests The authors declare no conflict of interest.

REFERENCES

[1] Simachew, A., Lanzén, A., Gessesse, A., Øvreås, L., Prokaryotic community diversity along an increasing salt gradient in a soda ash concentration pond, *Microbial Ecology*, 71 (2) (2016), 326–338. https://doi.org/10.1007/s00248-015-0675-7.

[2] Paul, S., Bag, S.K., Das, S., Harvill, E.T., Dutta, C., Molecular signature of hypersaline adaptation: insights from genome and proteome composition of halophilic prokaryotes, *Genome Biology*, 9 (4) (2008), R70. https://doi.org/10.1186/gb-2008-9-4-r70.

[3] Rhodes, M.E., Fitz-Gibbon, S.T., Oren, A., House, C.H., Amino acid signatures of salinity on an environmental scale with a focus on the Dead Sea, *Environmental Microbiology*, 12 (9) (2010), 2613–2623. https://doi.org/10.1111/j.1462-2920.2010.02232.x.

[4] Lentzen, G., Schwarz, T., Extremolytes: natural compounds from extremophiles for versatile applications, *Applied Microbiology and Biotechnology*, 72 (4) (2006), 623–634. https://doi.org/10.1007/s00253-006-0553-9.

[5] Check Hayden, E., Technology: The $1,000 genome, *Nature*, 507 (7492) (2014), 294–295. https://doi.org/10.1038/507294a.

[6] Hauser, M., Steinegger, M., Söding, J., MMseqs software suite for fast and deep clustering and searching of large protein sequence sets, *Bioinformatics*, 32 (9) (2016), 1323–1330. https://doi.org/10.1093/bioinformatics/btw006.

[7] Douglas, G.M., Maffei, V.J., Zaneveld, J.R., Yurgel, S.N., Brown, J.R., Taylor, C.M., Huttenhower, C., Langille, M.G.I., PICRUSt2 for prediction of metagenome functions, *Nature Biotechnology*, 38 (6) (2020), 685–688. https://doi.org/10.1038/s41587-020-0548-6.

[8] Akpolat, C., Fernández, A.B., Caglayan, P., Calli, B., Birbir, M., Ventosa, A., Prokaryotic communities in the Thalassohaline Tuz Lake, Deep Zone, and Kayacik, Kaldirim and Yavsan salterns (Turkey) assessed by 16S rRNA amplicon sequencing, *Microorganisms*, 9 (7) (2021), 1525. https://doi.org/10.3390/microorganisms9071525.

[9] Çınar, S., Mutlu, M.B., Prokaryotic community compositions of the hypersaline sediments of Tuz Lake demonstrated by cloning and high-throughput sequencing, *Microbiology*, 89 (6) (2020), 756–768. https://doi.org/10.1134/S0026261720060028.

[10] Şahin Doğan, S., Kocabaş, A., Seasonal dynamics of eukaryotic microbial diversity in hypersaline Tuz Lake characterized by 18S rDNA sequencing, *Journal of Eukaryotic Microbiology*, (2023),. https://doi.org/10.1111/jeu.12993.

[11] Sahin Dogan, S., Kocabaş, A., Seasonal gene profiling in Tuz Lake with regard to biogeochemical cycling, *Kahramanmaraş Sütçü İmam Üniversitesi Tarım ve Doğa Dergisi*, (2023). https://doi.org/10.18016/ksutarimdoga.vi.1212062.

[12] Doğan, S.Ş., Kocabaş, A., Metagenomic assessment of prokaryotic diversity within hypersaline Tuz Lake, Turkey, *Microbiology*, 90 (5) (2021), 647–655. https://doi.org/10.1134/S0026261721050118.

[13] Ausubel, F., Brent, R., Kingston, R.E.,Moore, D.D.,Seidman, J.G., Smith, J.A., Struhl K., Short protocols in molecular biology, third edition, John Wiley & Sons, New York, 1996. https://doi.org/10.1002/bmb.1996.5690240143.

[14] Caporaso, J.G., Lauber, C.L., Walters, W.A., Berg-Lyons, D., Lozupone, C.A., Turnbaugh, P.J., Fierer, N., Knight, R., Global patterns of 16S rRNA diversity at a depth of millions of sequences per sample, *Proceedings of the National Academy of Sciences*, 108 (supplement_1) (2011), 4516–4522. https://doi.org/10.1073/pnas.1000080107.

[15] Andrews, S., FastQC: A quality control tool for high throughput sequence data, (2010).

[16] Callahan, B.J., McMurdie, P.J., Rosen, M.J., Han, A.W., Johnson, A.J.A., Holmes, S.P., DADA2: High-resolution sample inference from Illumina amplicon data, *Nature Methods*, 13 (7) (2016), 581–583. https://doi.org/10.1038/nmeth.3869.

[17] Quast, C., Pruesse, E., Yilmaz, P., Gerken, J., Schweer, T., Yarza, P., Peplies, J., Glöckner, F.O., The SILVA ribosomal RNA gene database project: improved data processing and web-based tools, *Nucleic Acids Research*, 41 (D1) (2012), D590–D596. https://doi.org/10.1093/nar/gks1219.

[18] Bolyen, E., Rideout, J.R., Dillon, M.R., Bokulich, N.A., Abnet, C.C., Al-Ghalith, G.A., Alexander, H., Alm, E.J., Arumugam, M., Asnicar, F., Bai, Y., Bisanz, J.E., Bittinger, K., Brejnrod, A., Brislawn, C.J., Brown, C.T., Callahan, B.J., Caraballo-Rodríguez, A.M., Chase, J., Cope, E.K., Da Silva, R., Diener, C., Dorrestein, P.C., Douglas, G.M., Durall, D.M., Duvallet, C., Edwardson, C.F., Ernst, M., Estaki, M., Fouquier, J., Gauglitz, J.M., Gibbons, S.M., Gibson, D.L., Gonzalez, A., Gorlick, K., Guo, J., Hillmann, B., Holmes, S., Holste, H., Huttenhower, C., Huttley, G.A., Janssen, S., Jarmusch, A.K., Jiang, L., Kaehler, B.D., Kang, K. Bin, Keefe, C.R., Keim, P., Kelley, S.T., Knights, D., Koester, I., Kosciolek, T., Kreps, J., Langille, M.G.I., Lee, J., Ley, R., Liu, Y.-X., Loftfield, E., Lozupone, C., Maher, M., Marotz, C., Martin, B.D., McDonald, D., McIver, L.J., Melnik, A. V., Metcalf, J.L., Morgan, S.C., Morton, J.T., Naimey, A.T., Navas-Molina, J.A., Nothias, L.F., Orchanian, S.B., Pearson, T., Peoples, S.L., Petras, D., Preuss, M.L., Pruesse, E., Rasmussen, L.B., Rivers, A., Robeson, M.S., Rosenthal, P., Segata, N., Shaffer, M., Shiffer, A., Sinha, R., Song, S.J., Spear, J.R., Swafford, A.D., Thompson, L.R., Torres, P.J., Trinh, P., Tripathi, A., Turnbaugh, P.J., Ul-Hasan, S., van der Hooft, J.J.J., Vargas, F., Vázquez-Baeza, Y., Vogtmann, E., von Hippel, M., Walters, W., Wan, Y., Wang, M., Warren, J., Weber, K.C., Williamson, C.H.D., Willis, A.D., Xu, Z.Z., Zaneveld, J.R., Zhang, Y., Zhu, Q., Knight, R., Caporaso, J.G., Reproducible, interactive, scalable and extensible microbiome data science using QIIME 2, *Nature Biotechnology*, 37 (8) (2019), 852–857. https://doi.org/10.1038/s41587-019-0209-9.

[19] Markowitz, V.M., Chen, I.-M.A., Palaniappan, K., Chu, K., Szeto, E., Grechkin, Y., Ratner, A., Jacob, B., Huang, J., Williams, P., Huntemann, M., Anderson, I., Mavromatis, K., Ivanova, N.N., Kyrpides, N.C., IMG: the integrated microbial genomes database and comparative analysis system, *Nucleic Acids Research*, 40 (D1) (2012), D115–D122. https://doi.org/10.1093/nar/gkr1044.

[20] Parks, D.H., Tyson, G.W., Hugenholtz, P., Beiko, R.G., STAMP: statistical analysis of taxonomic and functional profiles, *Bioinformatics*, 30 (21) (2014), 3123–3124. https://doi.org/10.1093/bioinformatics/btu494.

[21] Doğan, S.Ş., Metagenomik yaklaşım ile Tuz gölündeki alg, bakteri ve arke çeşitliliğinin araştırılması, Karamanoğlu Mehmetbey University, 2022.

[22] Langille, M.G.I., Zaneveld, J., Caporaso, J.G., McDonald, D., Knights, D., Reyes, J.A., Clemente, J.C., Burkepile, D.E., Vega Thurber, R.L., Knight, R., Beiko, R.G., Huttenhower, C., Predictive functional profiling of microbial communities using 16S rRNA marker gene sequences, *Nature Biotechnology*, 31 (9) (2013), 814–821. https://doi.org/10.1038/nbt.2676.

[23] Zeng, B., Han, S., Wang, P., Wen, B., Jian, W., Guo, W., Yu, Z., Du, D., Fu, X., Kong, F., Yang, M., Si, X., Zhao, J., Li, Y., The bacterial communities associated with fecal types and body weight of rex rabbits, *Scientific Reports*, 5 (1) (2015), 9342. https://doi.org/10.1038/srep09342.

[24] Lopes, L.D., Pereira e Silva, M. de C., Andreote, F.D., Bacterial abilities and adaptation toward the rhizosphere colonization, *Frontiers in Microbiology*, 7 (2016). https://doi.org/10.3389/fmicb.2016.01341.

[25] Yuan, Z., Druzhinina, I.S., Labbé, J., Redman, R., Qin, Y., Rodriguez, R., Zhang, C., Tuskan, G.A., Lin, F., Specialized microbiome of a halophyte and its role in helping non-host plants to withstand salinity, *Scientific Reports*, 6 (1) (2016), 32467. https://doi.org/10.1038/srep32467.

[26] Hariharan, J., Sengupta, A., Grewal, P., Dick, W.A., Functional predictions of microbial communities in soil as affected by long-term tillage practices, *Agricultural & Environmental Letters*, 2 (1) (2017). https://doi.org/10.2134/ael2017.09.0031.

[27] Oren, A., Microbial life at high salt concentrations: phylogenetic and metabolic diversity, *Saline Systems*, 4 (1) (2008) 2. https://doi.org/10.1186/1746-1448-4-2.

[28] Hoffmann, T., Bremer, E., Guardians in a stressful world: the Opu family of compatible solute transporters from *Bacillus subtilis*, *Biological Chemistry*, 398 (2) (2017), 193–214. https://doi.org/10.1515/hsz-2016-0265.

[29] Oren, A., Diversity of halophilic microorganisms: environments, phylogeny, physiology, and applications, *Journal of Industrial Microbiology & Biotechnology*, 28 (1) (2002), 56–63. https://doi.org/10.1038/sj/jim/7000176.

[30] Gregory, G.J., Boyd, E.F., Stressed out: Bacterial response to high salinity using compatible solute biosynthesis and uptake systems, lessons from Vibrionaceae, *Computational and Structural Biotechnology Journal*, 19 (2021), 1014–1027. https://doi.org/10.1016/j.csbj.2021.01.030.

[31] Rath, H., Reder, A., Hoffmann, T., Hammer, E., Seubert, A., Bremer, E., Völker, U., Mäder, U., Management of osmoprotectant uptake hierarchy in *Bacillus subtilis* via a SigB-dependent antisense RNA, *Frontiers in Microbiology*, 11 (2020), 1-17. https://doi.org/10.3389/fmicb.2020.00622.

[32] He, Q., He, Z., Joyner, D.C., Joachimiak, M., Price, M.N., Yang, Z.K., Yen, H.-C.B., Hemme, C.L., Chen, W., Fields, M.M., Stahl, D.A., Keasling, J.D., Keller, M., Arkin, A.P., Hazen, T.C., Wall, J.D., Zhou, J., Impact of elevated nitrate on sulfate-reducing bacteria: a comparative study of *Desulfovibrio vulgaris*, *The ISME Journal*, 4 (11) (2010), 1386–1397. https://doi.org/10.1038/ismej.2010.59.

[33] Wargo, M.J., Homeostasis and catabolism of choline and glycine betaine: Lessons from *Pseudomonas aeruginosa*, *Applied and Environmental Microbiology*, 79 (7) (2013), 2112–2120. https://doi.org/10.1128/AEM.03565-12.

[34] Fernández, A.B., Ghai, R., Martin-Cuadrado, A.-B., Sánchez-Porro, C., Rodriguez-Valera, F., Ventosa, A., Prokaryotic taxonomic and metabolic diversity of an intermediate salinity hypersaline habitat assessed by metagenomics, *FEMS Microbiology Ecology*, 88 (3) (2014), 623–635. https://doi.org/10.1111/1574-6941.12329.

[35] Oyewusi, H.A., Muhammad, M., Abdul Wahab, R., Huyop, F., A review on enzymatic response to salt stress and genomic/metagenomic analysis of adaptation protein in hypersaline environment, *The Journal of Tropical Life Science*, 11 (3) (2021), 339–360.

[36] Kırkağaç, M., Gümüş, E., Yokuş, G., Tuz Gölü'nde çevresel faktörlerin Artemia Populasyonu'na etkisi, *Iğdır Üniversitesi Fen Bilimleri Enstitüsü Dergisi*, 7 (2) (2017), 303–312.

[37] Ding, R., Yang, N., Liu, J., The osmoprotectant switch of potassium to compatible solutes in an extremely halophilic archaea Halorubrum kocurii 2020YC7, *Genes*, 13 (6) (2022), 939. https://doi.org/10.3390/genes13060939.

[38] Saum, S.H., Müller, V., Salinity-Dependent switching of osmolyte strategies in a moderately halophilic bacterium: glutamate induces proline biosynthesis in *Halobacillus halophilus*, *Journal of Bacteriology*, 189 (19) (2007), 6968–6975. https://doi.org/10.1128/JB.00775-07.

[39] Williams, T.J., Allen, M.A., DeMaere, M.Z., Kyrpides, N.C., Tringe, S.G., Woyke, T., Cavicchioli, R., Microbial ecology of an Antarctic hypersaline lake: genomic assessment of ecophysiology among dominant haloarchaea, *The ISME Journal*, 8 (8) (2014), 1645–1658. https://doi.org/10.1038/ismej.2014.18.

[40] Inoue, K., del Carmen Marín, M., Tomida, S., Nakamura, R., Nakajima, Y., Olivucci, M., Kandori, H., Red-shifting mutation of light-driven sodium-pump rhodopsin, *Nature Communications*, 10 (1) (2019), 1993. https://doi.org/10.1038/s41467-019-10000-x.

[41] Nakajima, Y., Tsukamoto, T., Kumagai, Y., Ogura, Y., Hayashi, T., Song, J., Kikukawa, T., Demura, M., Kogure, K., Sudo, Y., Yoshizawa, S., Presence of a haloarchaeal halorhodopsin-like Cl^- pump in marine bacteria, *Microbes and Environments*, 33 (1) (2018), 89–97. https://doi.org/10.1264/jsme2.ME17197.

[42] Ghai, R., Pašić, L., Fernández, A.B., Martin-Cuadrado, A.-B., Mizuno, C.M., McMahon, K.D., Papke, R.T., Stepanauskas, R., Rodriguez-Brito, B., Rohwer, F., Sánchez-Porro, C., Ventosa, A., Rodríguez-Valera, F., New abundant microbial groups in aquatic hypersaline environments, *Scientific Reports*, 1 (1) (2011), 135. https://doi.org/10.1038/srep00135.

[43] Mongodin, E.F., Nelson, K.E., Daugherty, S., DeBoy, R.T., Wister, J., Khouri, H., Weidman, J., Walsh, D.A., Papke, R.T., Sanchez Perez, G., Sharma, A.K., Nesbo, C.L., MacLeod, D., Bapteste, E., Doolittle, W.F., Charlebois, R.L., Legault, B., Rodriguez-Valera, F., The genome of Salinibacter ruber: convergence and gene exchange among hyperhalophilic bacteria and archaea, *Proceedings of the National Academy of Sciences*, 102 (50) (2005), 18147–18152. https://doi.org/10.1073/pnas.0509073102.

[44] Sharma, A.K., Walsh, D.A., Bapteste, E., Rodriguez-Valera, F., Ford Doolittle, W., Papke, R.T., Evolution of rhodopsin ion pumps in haloarchaea, *BMC Evolutionary Biology*, 7 (1) (2007), 79. https://doi.org/10.1186/1471-2148-7-79.

SUPPLEMENTARY MATERIALS

TABLE S1. Weighted_NSTI values of the samples.

Samples/Month	Weighted_NSTI values
NOV_18	0.18
DEC_18	0.17
JAN_19	0.16
FEB_19	0.15
MAR_19	0.17
APR_19	0.23
MAY_19	0.22
JUN_19	0.18
JUL_19	0.16
OCT_19	0.18
NOV_19	0.27
DEC_19	0.17
JAN_20	0.16

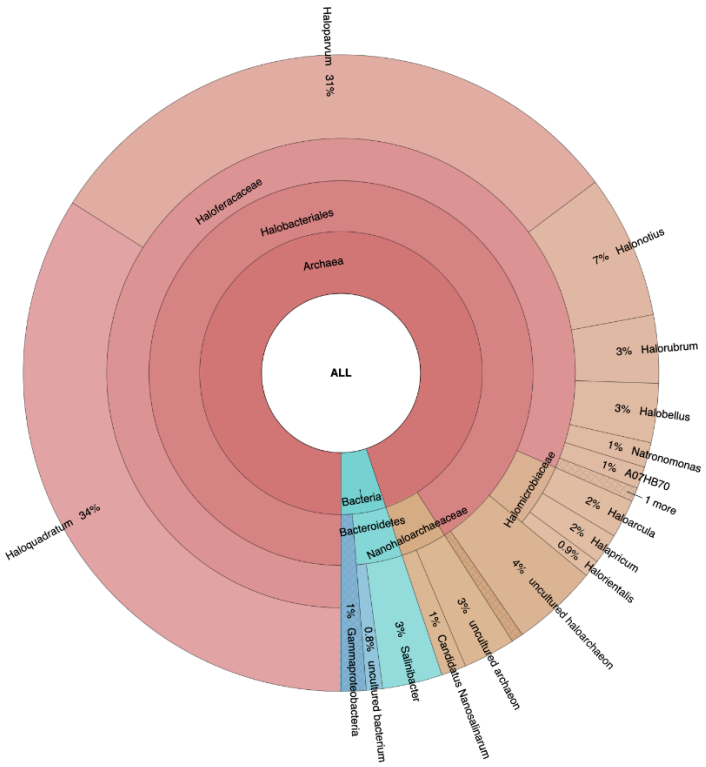

FIGURE S1. The composition of archaea and bacteria in Tuz Lake [12].

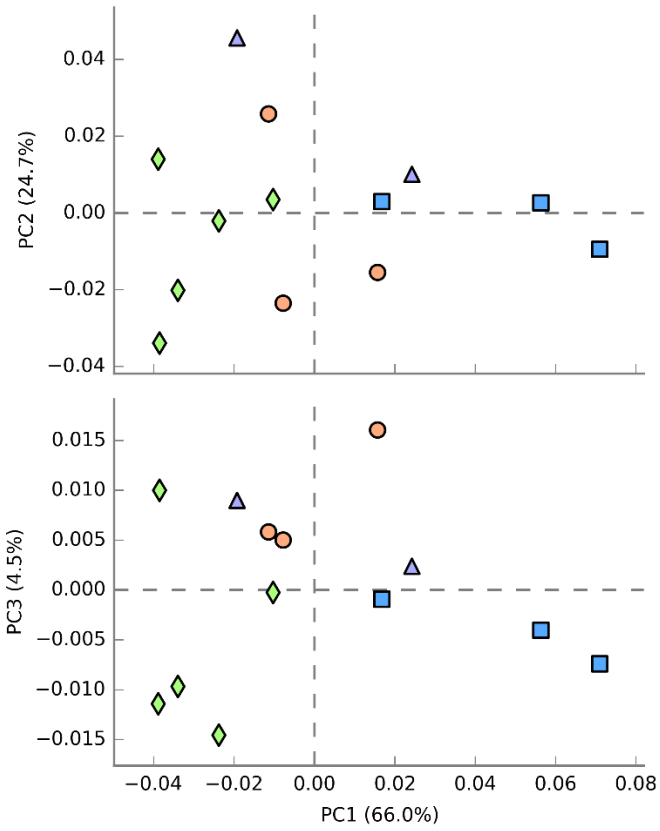

FIGURE S2. PCA plot representing metabolic functions related to osmoadaptation (Spring:Blue, Fall:Orange, Summer:Purple, Winter:Green)

http://communications.science.ankara.edu.tr

Commun.Fac.Sci.Univ.Ank.Ser. C Biology
Volume 32, Number 2, Pages 192-207 (2023)
ISSN 1303-6025 E-ISSN 2651-3749
DOI: 10.53447/communc.1350057

Research Article; Received: August 25, 2023; Accepted: October 03, 2023

EMBRYONIC DEVELOPMENT OF THE LEMON-YELLOW TREE FROG, *Hyla savignyi* AUDOUIN, 1827

ŞEFİK KARANLIK[1], ELNAZ NAJAFI-MAJD[1], ELİF YILDIRIM[2,3], UĞUR KAYA[1]

[1]Ege University, Faculty of Science, Biology Department, Zoology Section, Bornova, İzmir, TÜRKİYE
[2]Dokuz Eylül University, Biology Department, Zoology Section, Buca, İzmir, TÜRKİYE
[3]Dokuz Eylül University, Fauna and Flora Applied and Research Centre, Buca, İzmir, TÜRKİYE

ABSTRACT. Amphibians are widely used in temperature adaptation studies due to their compatibility in laboratory experiments. We investigated the embryonic development stages (from fertilization to 25th) of *Hyla savignyi* following Gosner's generalized table. Three pairs of *H. savignyi* were collected during the breeding season (February 2015) from Northern Cyprus, Kalkanlı Region and maintained at 21±1 °C in the laboratory. The samples were set in 3 groups and examinations of embryos and photographs taken every 10 minutes were carried out during the 9-days embryonic period. Embryos hatched at stage 20 or 21 come up to 3rd – 4th days after fertilization. Embryonic development of *H. savignyi* is about 157 hours (7 days). Cleavage is unequal holoblastic. The embryonic developmental stages of *H. savignyi* were compared with the result of a similar study of two other *Hyla* species (*H. orientalis* and *H. annectans*) at various temperatures, and the possible temporal effect of the temperature and ovum size on the growth rate of these species was discussed.

1. INTRODUCTION

Amphibians have been considered model organisms for developmental studies for a long time. Although the South African clawed frog, *Xenopus laevis* (Daudin, 1802) is currently the most popular amphibian model, others had already been spotlighted for the issue [1, 2, 3]. *X. laevis* was raised through its use in pregnancy testing, and it was established by Nieuwkoop and Fischberg as a model for development [2]. Among the frogs, several *Rana* species have been used in developmental studies [4, 5, 6, 7].

Different salamander species were used in classic embryological studies [8, 9, 10, 11, 12, 13, 14, 15, 16]. While the Spanish ribbed newt, *Pleurodeles waltl* Michahelles, 1830 was popular in French labs, the lowland newt, *Cynops pyrrhogaster* (Boie, 1826) was in Japanese laboratories. The Mexican axolotl, *Ambystoma mexicanum* (Shaw and Nodder, 1798)

Keywords. Fertilization, cleavage, gastrula, tadpole, growth rate, ovum size, gosner stages, hylidae

sefikkaranlik@gmail.com- 0009-0008-1995-963X
elnaz.najafi.majd@gmail.com- Corresponding author; 0000-0001-7710-1625
yildirim.elif@deu.edu.tr- 0000-0001-9614-5754
kuagyuar@gmail.com- 0000-0002-6718-5842

became the most popular one because it could be easily bred and kept in captive conditions and laboratory colonies [17, 18].

There are fundamental differences in development within different groups of amphibians. Fertilization is monospermic in most anurans, frogs, as in mammals, but fertilization is polyspermous in most urodeles; newts and salamanders [19, 20]. Primordial germ cells form a cytoplasmic localization in anurans via germ plasm, but by induction in urodeles [21, 22]. The shape of the body changes completely and abruptly at anurans metamorphosis, but the body form undergoes minimal and gradual changes in urodeles. Also, urodeles possess remarkable regeneration abilities, not found in anurans [23].

In 1960 Gosner proposed a table that is now used as a standard for development in anurans. The table contains 46 stages but just the first 25 stages are embryonic or prefeeding and the other 21 are larval stages and investigates metamorphosis in the frog as stages [24]. However, the sequence of changes in the early embryo from fertilization to cleavage, the blastula and the gastrula is essentially similar in most species.

Published data of the development of hylid species referred only to *Hyla regilla* Cocroft, 1994, *Hyla avivoca* Viosca, 1928 and *Hyla japonica* Günther, 1859 [25, 26, 27, 28]. Recently, the developmental stages of *Hyla orientalis* Bedriaga, 1890 and *Hyla annectans* Jerdon, 1870 have been described in detail [29, 30]. However not much is known about the embryonic development of *H. savignyi* Audouin, 1827.

This is the first study on the embryonic development of *H. savignyi* that provides a staging temporal table and a complement to previous studies in the literature. This laboratory work also reveals the timing and characterization of similar species' external development to understand the embryonic process's importance and define the hylid life history.

2. MATERIALS AND METHODS

The fertilized eggs of *H. savignyi* were obtained from two mating pairs that were collected during the breeding season (09 Feb. 2015) from Northern Cyprus (Kalkanlı Region, 35° 15′ 59.48″ N, 33° 02′ 34.22″ E). These pairs were separately transferred to the laboratory and placed in a glass container (26 × 38 × 16 cm) with de-chlorinated tap water. Spawns were observed three to five hours later. The fertilized eggs obtained by this procedure were reared at 21 ± 1°C, with natural ambient lighting, in de-chlorinated and gently aerated tap water. In order to obtain a sequence of developmental stages, groups of 10 embryos were removed at any one

time, and the rest were left in the clutch for further development. During the development of the embryos, a thermoregulation device was used to stabilize the ambient temperature. The experiment was set in 3 groups based on the observation of 30 embryos from two mating pairs in different sets of spawning eggs. Live embryos were reared in petri dishes in their jelly coatings were observed and photographed using a stereomicroscope (Olympus SZ61) attached to a digital camera (Camedia C-5060) every 10 minutes to describe the stages of species' embryonic development according to Gosner (1960). Sampled pairs were released back to nature.

3. RESULTS

The embryonic development monitoring study started on 10 February 2015 and lasted about 18 days. In 30 zygotes embryonic stages were studied and the mean time (age in an hour) for each stage was obtained. Embryos hatched at stages 20 - 21 about 3^{rd} – 4^{th} days after fertilization. The embryonic development process of *H. savignyi* from fertilization to the 25^{th} stage lasted about 157 hours (7 days) at 21±1 °C (Table 1).

This study presents temporal data and the morphologic characteristics of embryonic development prefeeding stages (from fertilization to 25^{th}) of *H. savignyi*. Like other frogs their egg is telolecithal with a large amount of yolk. Fertilization is monospermic and they undergo unequal holoblastic cleavage. Embryonic developmental stages have been divided into four major categories: (1) Fertilization, two stages (2) Cleavage, seven stages (3) Gastrula, three stages (4) Tadpole, seven stages. Developmental features include the tail bud, indicated initially by a strong upward arching of the back. Embryo hatching occurs at stage 19, when the cornea is just beginning to become transparent. However, it is not until the end of stage 20 and the beginning of stage 21 that the cornea becomes fully clear. At stage 20, circulation begins in the caudal fin, but the caudal fin is not transparent as in the Gosner stages and remains dark.

Embryonic Developmental Stages Categories

Fertilization stages

Stage 1. The spherical egg has differentiation including an animal and a vegetal pole (Figure 1A).

Stage 2. The gray crescent, seen as a pigmented area, is visible between the animal and vegetal poles (Figure 1B).

Cleavage stages

Stage 3. Meridional furrow, advancing from animal pole to vegetal pole, divides the egg in equal halves (Figure 1C).

Stage 4. The second meridian furrow divides the egg into four cells from the animal pole to the vegetal pole at a right angle to the first (Figure 1D).

Stage 5. The third division, consisting of eight unequal cells, is at latitude slightly above the equator (Figure 1E).

Stage 6. Eight cells divide vertically to form sixteen cells (Figure 1F).

Stage 7. Sixteen cells divide latitudinally to form thirty-two cells (Figure 1G).

Stage 8. The number of cells exceeded 64 (Figure 1H).

Stage 9. The animal polar surface has a granular appearance (Figure 2A).

Gastrulation stages

Stage 10. The dorsal lip of the crescent-shaped blastopore is formed on the animal polar surface (Figure 2B).

Stage 11. It reduces the exposed area of non-pigmented macromeres surrounded by the lateral lips of the circular blastopore with epibolism of micromeres at the vegetal pole (Figure 2C and D).

Stage 12. The embryo is slightly elongated and the dorsal surface of the embryo flattens to form th*e neural plate* (Figure 2E).

Stage 13. The posterior part of the embryo enlarges. The neural plate forms a wider neural groove in the cerebral region (Figure 2F).

Rotation. Sperm entry affects the rotation of the cell's cortex relative to the inner cell mass. This rotation moves the determinants on the vegetal side of the egg towards the animal-vegetal boundary and the gray crescent appears (Figure 2G).

Stage 14. The neural folds are completely fused to form the neural tube (Figure 2H).

Stage 15. The tail is wider than the length of the bud and extends dorsoposteriorly (Figure 3A).

Stage 16. The muscular response is produced by unilateral flexion of the head, which is well defined by optic bulges and prominent protrusions of

the gill plates. As the embryo elongates, the tail begins to curl to the right or left (Figure 3B).

Stage 17. The heartbeat is seen below and behind the gill bud. A pair of external gill buds emerged from each gill plate. Dorsal and ventral fins are translucent. The stomodeal pit is triangular in shape (Figure 3C).

Stage 18. In branched gills, circulation is seen as the movement of bodies through the external gill filaments (Figure 3D).

Tadpole stages

Stage 19. The olfactory pit becomes prominent. The cornea of the optic lobes begins to become transparent. The stomodeum, which has no feeding activity yet, becomes triangular to form a simple mouth. The anterior end of the head bulges the vitelline membrane. At this point the membrane ruptures, the larva comes out and settles at the bottom (Figure 3E).

Stage 20. The caudal fin circulation begins at the base of the anterior part of the fin and moves slowly through the vessel (Figure 4A).

Stage 21. The operculum has a small fold of skin and covers the base of the external gills (Figure 4B).

Stage 22. The opercular fold covering the external gills on the right is fused with the skin of the abdomen on the right. The upper and lower lips around the mouth become prominent and keratinized (Figure 4C).

Stage 23. The operculum closes and the gills disappear. Spiracle occurs. The feeding of the tadpole begins (Figure 4D).

Stage 24. Hind limbs formed and straightened mediolaterally to form a foot paddle.

Stage 25. Formation of all toes in the posterior parts.

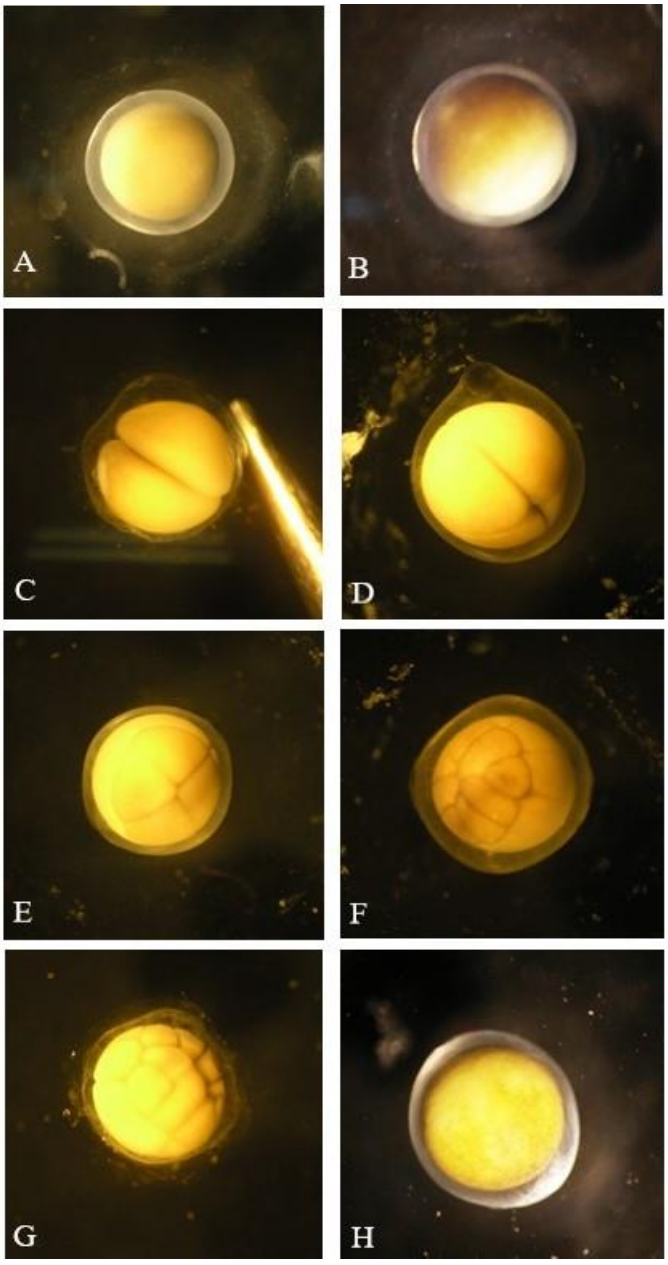

FIGURE 1. **A.** Fertilization, **B.** Gray crescent, **C.** Two cell stage, **D.** Four cell stage, **E.** Eight cell stage, **F.** Sixteen cell stage, **G.** Thirty-two cell stage, **H.** Mid-cleavage.

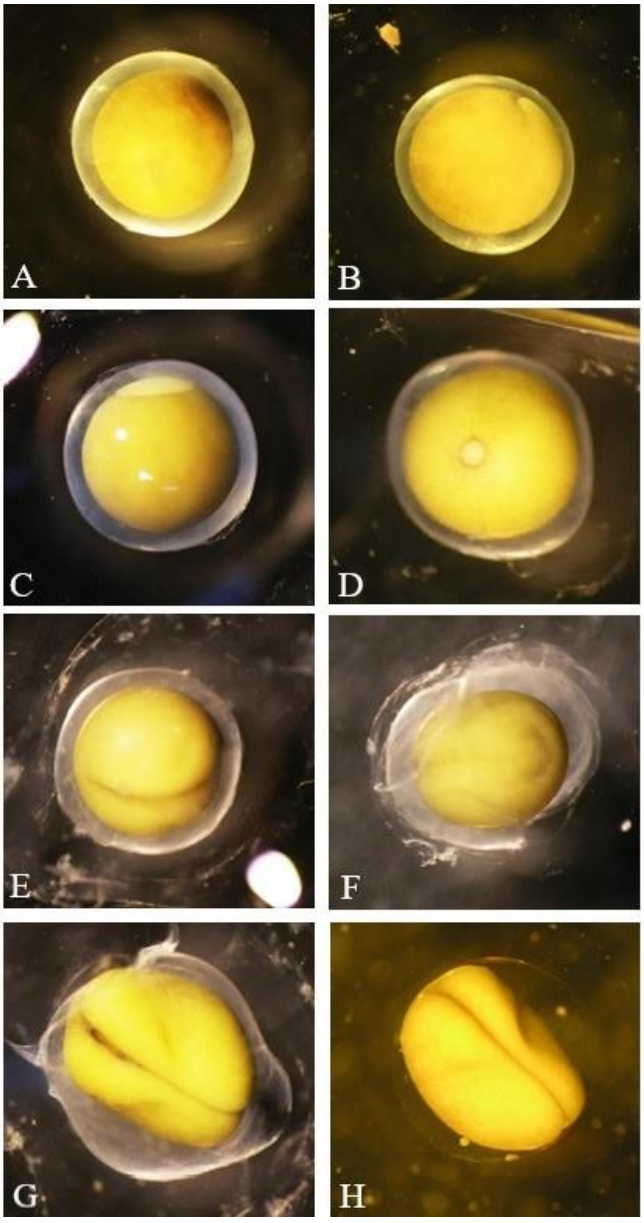

FIGURE 2. **A.** Late cleavage, **B.** Dorsal lip, **C.** Mid-gastrula, **D.** Late gastrula, **E.** Neural plate, **F.** Neural fold, **G.** Rotation, **H.** Neural tube.

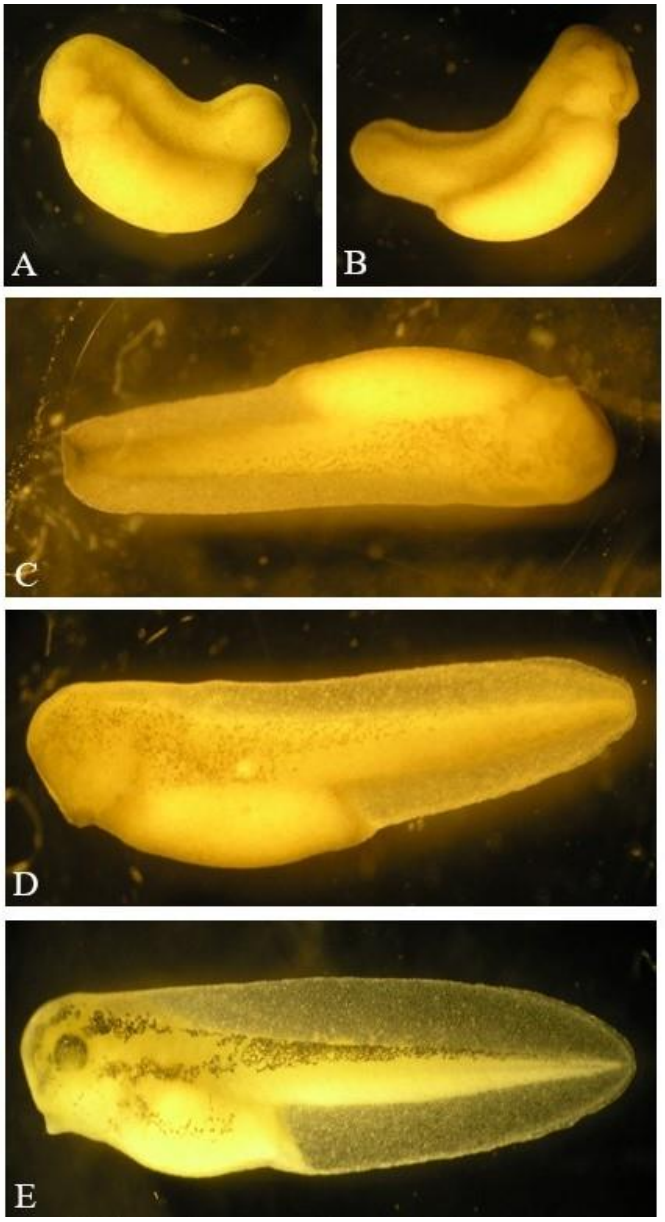

FIGURE 3. **A.** Tail bud, **B.** Muscular response, **C.** Heartbeat, **D.** Gill circulation, **E.** Cornea transparent

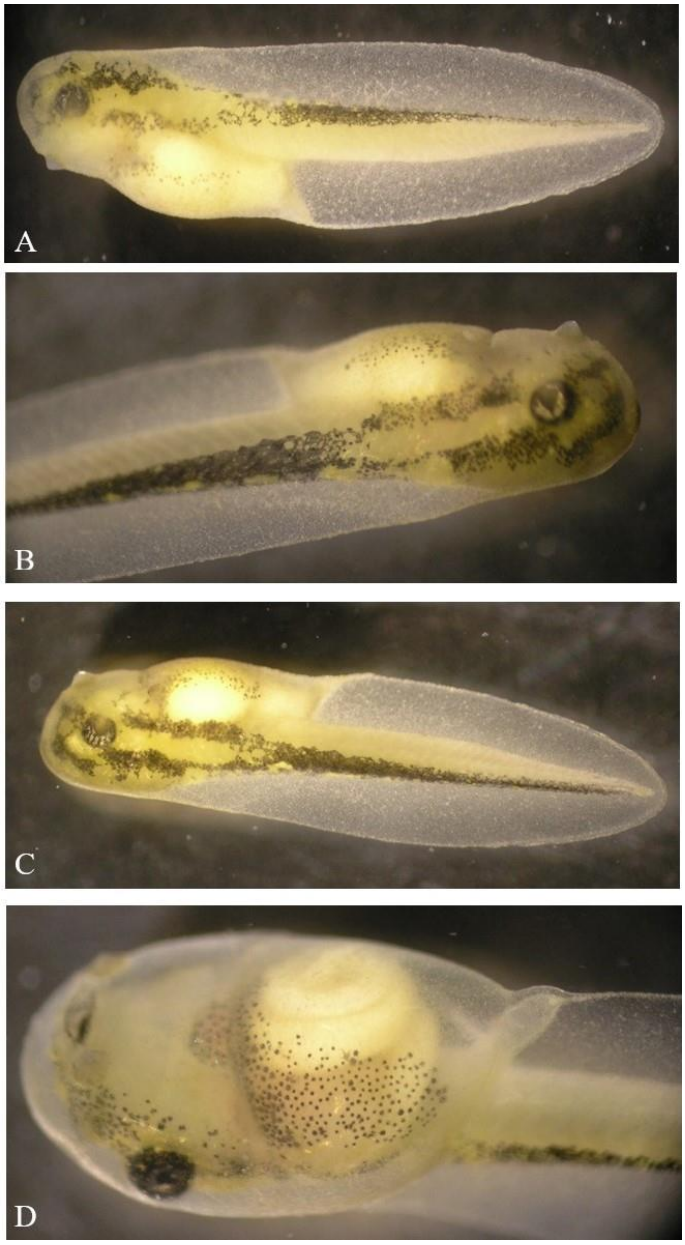

FIGURE 4. **A.** Tail fin circulation, **B.** Operculum fold, **C.** Operculum closed on right, **D.** Operculum closed on the left and a spiracle formed.

TABLE 1. The embryonic stages of *H. orientalis*, *H. annectans* and *H. savignyi* follow Gosner stages (1960).

Stage	Characteristics of embryos Gosner stages (1960)		Age in hours		
			H. orientalis	*H. annectans*	*H. savignyi*
1	Fertilization		0	0	0
2	Second polar body released		0.30	0.55	0.45
3	First cleavage (meridional); 2 blastomeres	Cleavage	2.00	1.50	3.00
4	Second cleavage (meridional); 4 blastomeres		2.20	2.20	4.00
5	Third cleavage (latitudinal); 8 blastomeres		3.00	2.45	4.30
6	Fourth cleavage (meridional); 16 blastomeres		3.30	3.20	5.30
7	Fifth cleavage (latitudinal); 32 blastomeres		4.10	3.52	7.00
8	Mid-cleavage; early blastula		7.30	7.54	7.30
9	Late cleavage; late blastula		9.30	12.10	11.30
10	Involution at dorsal lip of blastopore; beginning of gastrulation	Gastrula	16.00	15.05	20.30
11	Mid-gastrula; large yolk plug		21.00	16.50	23.00
12	Late gastrula; small yolk plug		25.30	34.40	26.00
13	Dorsal flattening; formation of neural plate	Neurula	28.30	38.20	33.30
14	Early neurula stage; neural folds approach each other		33.30	40.50	35.30
15	Mid neurula stage; neural folds coalesce; body begins to elongate		34.30	42.50	37.00
16	Formation of the neural tube; body elongated		35.30	60	39.30
17	Tail bud; adhesive organs begin to develop		38.30	70.07	41.00
18	Muscular response; differentiation of gill arches; olfactory pits form		52.30	72.29	54.00
19	Heart beat		73.30	102.29	65.30
20	Gill circulation begins		88.00	117.29	76.30
21	Cornea transparent		112.00	143.59	92.33
22	Tail fins become transparent; circulation begins in fins		117.00	172.29	101.00
23	Opercular fold covers base of gills		139.30	185.29	119.00
24	Opercular fold closes on the right side		163.30	748.00	132.30
25	Opercular fold closes on the left side; spiracle forms		211.30	1136.00	157.00
Duration of the embryonic development from fertilization to 25th stage			8.8 days	94.6 days	7 days
Temperature			20 ± 1°C	16 – 22 °C	21±1 °C
Ovum size (mm)			1.4	1.52	1.4

4. CONCLUSIONS

The pattern of development of hylid species is generally the same as Ranidae. Although comparing our results by embryonic development of *H. orientalis* and *H. annectans* show morphologic similarity, the duration of each stage and inter stages time is different in the three species.

The embryonic development process of *H. savignyi* from fertilization to the 25th stage lasted about 157 hours (7 days) at 21±1 °C but this period for H. *orientalis* was about 211.30 hours (9 days) at 20 ±1 °C. This rate in *H. annectans* is slower and the process lasts 1136 hours (94.6 days) at 16 – 22 °C (Table 1).

The rate of development to different stages may depends primarily on temperature and secondly on ovum size [30]. While these three species are from the same genus, the ovum size is the same in *H. orientalis* and *H. savignyi* (1.4 mm) and a bit larger in *H. annectans* (1.52 mm). The rate of embryonic development in *H. savignyi* is slower than *H. orientalis* up to 18th stage but from 19th stage the rate increases in *H. savignyi* and completes the process earlier than *H. orientalis*.

It is known that the development rate in anurans with larger eggs is slower than smaller ones [31, 32, 33, 34], which may occur due to oxygen limitations in the larger eggs which slows the rate of embryonic tissue synthesis [35]. Generally, there is a correlation in animals [36], smaller eggs may result in faster hatching, and it's also possible for smaller offspring to be produced after hatching [32, 37]. However, more research studies are needed on the relationship between egg size and post-hatch development between species. After hatching, the offspring can use environmental resources, which affects the rate of development [38]. The comparison of temporal data on embryonic development of *H. savignyi*, *H. orientalis* and *H. annectans* shows a slower embryonic development rate in *H. annectans* (1136 hours = 94.6 days) that could be related to its larger ovum size in this species.

Of course, in addition to the size of the eggs, other external factors such as the environmental temperature also play a crucial role in the rate of development during the incubation [30, 39, 40] that must be taken into account. Even after hatching, the egg size can still have a direct impact on the development time of the amphibian offspring.

Considering that the world is experiencing unprecedented anthropogenic changes [41], including global climate change [42], and since amphibians are sensitive to changes in their environment [43], studying the impact of

these temperatures' changes on the development and growth of amphibians in and throughout their early life history is critical to conservation activities [44].

Most laboratory studies that investigate the effects of the environment on development have taken place under stable environmental conditions. Naturally occurring thermal environments can vary widely, so it is not clear that working models in stable environments provide an adequate representation for the variations. Temperature is the most important factor affecting embryonic development [45, 30]. For this reason, there have been studies on the embryogenesis of many amphibian species since the 1900s [46, 47, 48, 49, 50, 28]. Several studies in the literature have investigated the effects of diel temperature fluctuation on amphibian development, which particularly is sensitive to variable environmental conditions [51, 52]. Extensive studies about the effects of temperature fluctuations on the developmental rate of ectotherms show that these variations may increase, decrease, or have no effect on development rates [52, 53, 54]. The result of research on models and experiential data reveals that temperature fluctuations are ecologically significant when individuals are temporarily exposed to temperatures within their physiologically relevant temperature range [55, 56, 58, 59] and that fluctuations between cooler and warmer temperatures can have different or opposing impacts on developmental traits [53, 56].

Low temperatures can slow metabolic rate and development, and reduce growth, swimming and feeding activity [59]. The temperature effect may be the reason why the development period of *H. annectans*, whose embryonic development was examined in the laboratory between 16 – 22 °C, was completed in a longer time. The completion times of cleavage and gastrula stages seem to be almost parallel to each other in all three hylid species (Table 1). The difference is towards the end of the neurulation. After the neural tube is formed, the rate of embryonic development slows down in the *H. annectans* species (Table 1). In *H. savignyi*, embryonic development progresses more slowly to muscle response than *H. orientalis* whereas it accelerates after the 18th stage (Table 1). As a result, the *H. savignyi* species completed its embryonic development faster than the other two hylid species (Table 1). Completing the embryonic development process earlier may be advantageous for adapting *H. savignyi* to warmer zones where it lives and increasing the survival chance of the species.

Author Contribution Statements ŞK- conceptualization, analysis, writing, EN- validation, editing, review, writing, EY- validation, editing, review, writing, UK- review.

Declaration of Competing Interests The authors declare no conflict of interest.

REFERENCES

[1] Callery, E. M., There's more than one frog in the pond: A survey of the Amphibia and their contributions to developmental biology, *Seminars in cell & developmental biology*, Academic Press, 17 (2006), 80–92. https://doi.org/10.1016/j.semcdb.2005.11.001

[2] Gurdon, J.B., Hopwood, N., The introduction of *Xenopus laevis* into developmental biology: of empire, pregnancy testing and ribosomal genes, *International Journal of Developmental Biology*, 44 (1) (2000), 43–50.

[3] Holtfreter, J., Amphibians. In: Willier, BH.; Weiss, PA.; Hamburger, V. Editors. Analysis of development. W. B. Saunders Company; Philadelphia: (1955), 230–296.

[4] Ancel, P., Vintemberger, P., Recherches sur le déterminisme de la symétrie bilatérale dans l'oeuf des Amphibiens, *Bulletin biologique de la France et de la Belgique. Suppléments*, 31 (1948), 1–182.

[5] Barth, L.G., Barth, L.J., Differentiation of Cells of the *Rana pipiens* Gastrula in Unconditioned Medium, *Development*, 7 (2) (1959), 210–222. https://doi.org/10.1242/dev.7.2.210

[6] Briggs, R., King, T.J., Transplantation of living nuclei from blastula cells into enucleated frogs' eggs, *Proceedings of the National Academy of Sciences*, 38 (5) (1952), 455–463. https://doi.org/10.1073/pnas.38.5.455

[7] Pasteels, J., Les effets de la centrifugation sur la blastula et la jeune gastrula des Amphibiens: I. Mécanisme de la formation des organes secondaires aux dépens de l'ectoblaste, *Development*, 1 (2) (1953), 125–145. https://doi.org/10.1242/dev.1.1.5

[8] Fankhauser, G., The effects of changes in chromosome number on amphibian development, *The Quarterly Review of Biology*, 20 (1) (1945), 20-78. https://doi.org/10.1086/394703

[9] Harrison, R.G., Experiments in transplanting limbs and their bearing upon the problems of the development of nerves, *Journal of experimental zoology*, 4 (2) (1907), 239–281.

[10] Holtfreter, J., Über die aufzucht isolierter teile des amphibienkeimes: II. Züchtung von keimen und keimteilen in salzlösung. *Wilhelm Roux'Archiv für Entwicklungsmechanik der Organismen*, 124 (1931), 404–466. https://doi.org/10.1007/BF00652482

[11] Spemann, H., Entwickelungsphysiologische Studien am Triton-Ei. *Archiv für Entwicklungsmechanik der Organismen*, 12 (1901), 224-264 + 1 pI. (V).

[12] Spemann, H., Über Transplantationen an Amphibienembryonen im Gastrulastadium. Sitz. Ber. Gesel!, *Naturf. Freunde zu Berlin* (1916), 306–320.

[13] Spemann, H., Experimentelle forschungen zum determinations-und individualitätsproblem, *Naturwissenschaften*, 7 (1919), 581–591. https://doi.org/10.1007/BF01498212

[14] Vogt, W., Morphologische und physiologische Fragen der Primitiventwicklung, Versuche zu ihrer Lösung mittels vitaler Farbmarkierung, *Sitz. Ber. Ges. Morph. Physiol. Munchen.*, 35 (1924), 22–32.
[15] Vogt, W., Gestaltungsanalyse am Amphibienkeim mit örtlicher Vitalfarbung. II. Gastrulation und Mesodermbildung bei Urodelen und Anuren, *Arch. Entw.Mech.*, 120 (1) (1929), 384–706
[16] Beetschen, J.C., How did urodele embryos come into prominence as a model system?, *The International journal of developmental biology*, 40 (4) (1996), 629–636.
[17] Malacinski, G.M., Rufus R. Humphrey (1892–1977), *American Zoologist.* 18 (1978), 191–193.
[18] Smith, J.J., Putta, S., Zhu, W., Pao, G.M., Verma, I.M., Hunter, T., Bryant, S.V., Gardiner, D.M., Harkins, T.T., Voss, S.R., Genic regions of a large salamander genome contain long introns and novel genes, *BMC Genomics*, (2009), 10–19. https://doi.org/10.1186/1471-2164-10-19
[19] Elinson, R.P., Fertilization in amphibians: the ancestry of the block to polyspermy, *International review of cytology*, 101 (1986), 59–100. https://doi.org/10.1016/S0074-7696(08)60246-6
[20] Iwao, Y., Fertilization in amphibians. In: Tarin, JJ.; Cano, A. Editors. Fertilization in protozoa and metazoan animals, cellular and molecular aspects. Springer-Verlag; Berlin: (2000), 147-191. https://doi.org/10.1007/978-3-642-58301-8_4
[21] Johnson, A.D., Richardson, E., Bachvarova, R.F., Crother, B.I., Evolution of the germ line-soma relationship in vertebrate embryos. *Reproduction*, 141 (3) (2011), 291–300. https://doi.org/10.1530/rep-10-0474
[22] Nieuwkoop, P.D., Sutasurya, L.A., Primordial germ cells in the chordates. Cambridge University Press, Cambridge, 1979.
[23] Stocum, D.L., The role of peripheral nerves in urodele limb regeneration. *European Journal of Neuroscience*, 34 (6) (2011), 908–916. https://doi.org/10.1111/j.1460-9568.2011.07827.x
[24] Gosner, K.L., A simplified table for staging anuran embryos and larvae with notes on identification, *Herpetologica*, 16 (3) (1960), 183–190.
[25] Duellman, W.E., Trueb, L. Biology of Amphibians. Baltimore and London, The Johns Hopkins University Press, 1994.
[26] Iwasawa, H., Futagami, J., Normal stages of development of a Tree Frog, *Hyla japonica* Günther. Jpn. *J. Herpetol.*, 14 (1992), 129–142. (in Japanese with English abstract)
[27] Rugh, R., Experimental embryology; techniques and procedures. Burgess Publishing, Minneapolis, 1962.
[28] Volpe, E.P., Embryonic temperature tolerance and rate of development in *Bufo valliceps*, *Physiological Zoology*, 30 (2) (1957), 164–176.
[29] Ao, J.M., Development of *Hyla annectans* Jerdon, 1870 from Nagaland, India, *Rüsıe: A Journal Of Contemporary Scıentıfic, Academıc and Socıal Issues*, 2 (2015), 6–11.
[30] Sayim, F., Kaya, U., Embryonic development of the tree frog, *Hyla arborea*, *Biologia*, 63 (2008), 588–593. https://doi.org/10.2478/s11756-008-0086-z
[31] McLaren, I.A., Cooley, J.M., Temperature adaptation of embryonic development rate among frogs, *Physiological Zoology*, 45 (3) (1972), 223–228.

[32] Salthe, S.N., Duellman, W.E., Quantitative constraints associated with reproductive mode in anurans, In: *Evolutionary Biology of the Anurans. Contemporary Research on Major Problems.* Vial, JL (ed.). University of Missouri Press. Columbia, Missouri. (1973), 229–249.
[33] Kuramoto, M., Embryonic temperature adaptation in development rate of frogs, *Physiological Zoology*, 48 (4) (1975), 360–366.
[34] Kaplan, R.H., Maternal influences on offspring development in the California newt, *Taricha torosa*, *Copeia*, (1985), 1028–1035. https://doi.org/10.2307/1445258
[35] Seymour, R.S., Bradford, D.F., Respiration of amphibian eggs. *Physiological Zoology*, 68 (1) (1995), 1–25.
[36] Guinnee, M.A., Gardner, A., Howard, A.E., West, S.A., Little, T.J., The causes and consequences of variation in offspring size: a case study using Daphnia, *Journal of Evolutionary Biology*, 20 (2) (2007), 577–587. https://doi.org/10.1111/j.1420-9101.2006.01253.x
[37] Kaplan, R.H., The implications of ovum size variability for offspring fitness and clutch size within several populations of salamanders (*Ambystoma*), *Evolution*, 34 (1) (1980), 51-64. https://doi.org/10.2307/2408314
[38] Doughty, P., Roberts, J.D., Plasticity in age and size at metamorphosis of *Crinia georgiana* tadpoles: responses to variation in food levels and deteriorating conditions during development, *Australian Journal of Zoology*, 51 (3) (2003), 271–284. https://doi.org/10.1071/ZO02075
[39] Bradford, D.F., Incubation time and rate of embryonic development in amphibians: the influence of ovum size, temperature, and reproductive mode, *Physiological Zoology*, 63 (6) (1990), 1157–1180.
[40] Beattie, R.C., Tyler-. Tones, R., Baxter, M.J., The effects of pH, aluminium concentration and temperature on the embryonic development of the European common frog, *Rana temporaria*, *Journal of Zoology*, 228 (4) (1992), 557-570. https://doi.org/10.1111/j.1469-7998.1992.tb04455.x
[41] Steffen, W., Crutzen, P.J., McNeill, J.R., The Anthropocene: are humans now overwhelming the great forces of nature, *Ambio-Journal of Human Environment Research and Management*, 36 (8) (2007), 614-621. https://doi.org/10.18574/nyu/9781479844746.003.0006
[42] Intergovernmental Panel on Climate Change. "Ipcc." Climate change, 2014
[43] Hopkins, W.A., Amphibians as models for studying environmental change, *ILAR journal*, 48 (3) (2007), 270-277. https://doi.org/10.1093/ilar.48.3.270
[44] Walther, G.R., Post, E., Convey, P., Menzel, A., Parmesan, C., Beebee, T.J., Fromentin, J.M., Hoegh-Guldberg, O., Bairlein, F., Ecological responses to recent climate change, *Nature*, 416 (6879) (2002), 389–395. https://doi.org/10.1038/416389a
[45] Bachmann, K., Temperature adaptations of amphibian embryos. *The American Naturalist*, 103 (930) (1969), 115–130.
[46] Guyetant, R., Influence du facteur temperature sur le développement embryonnaire de *Rana temporaria* et *Rana dalmatina*, *Vie et Milieu*, 20 (1969), 231–242.
[47] Harkey, G.A., Semlitsch, R.D., Effects of temperature on growth, development, and color polymorphism in the Ornate Chorus Frog *Pseudacris ornate*, *Copeia*, 4 (1988), 1001–1007. https://doi.org/10.2307/1445724
[48] Kuramoto, M., Embryonic temperature adaptation in development rate of frogs, *Physiological Zoology*, 48 (4) (1975), 360–366.

[49] Mitchell, N.J., Seymour, R.S., Effects of temperature on energy cost and timing of embryonic and larval development of the terrestrially breeding Moss Frog, *Bryobatrachus nimbus*, *Physiological and Biochemical Zoology*, 73 (6) (2000), 829–840.

[50] Smith, G.D., Hopkins, G. R., Mohammadi, S., Skinner, H.M., Hansen, T., Brodie, E.D., French, S.S., Effects of temperature on embryonic and early larval growth and development in the rough-skinned newt (*Taricha granulosa*), *Journal of Thermal Biology*, 51 (2015), 89–95. https://doi.org/10.1016/j.jtherbio.2015.03.010

[51] Kaplan, R.H., Phillips, P.C., Ecological and developmental context of natural selection: maternal effects and thermally induced plasticity in the frog *Bombina orientalis*, *Evolution*, 60 (1) (2006), 142–156. https://doi.org/10.1111/j.0014-3820.2006.tb01089.x

[52] Niehaus, A.C., Angilletta Jr, M.J., Sears, M.W., Franklin, C.E., Wilson, R.S., Predicting the physiological performance of ectotherms in fluctuating thermal environments, *Journal of Experimental Biology*, 215 (4) (2012), 694–701. https://doi.org/10.1242/jeb.058032

[53] Hagstrum, D.W., Milliken, G.A., Modeling differences in insect developmental times between constant and fluctuating temperatures, *Annals of the Entomological Society of America*, 84 (4) (1991), 369–379. https://doi.org/10.1093/aesa/84.4.369

[54] Kingsolver, J.G., Feeding, growth, and the thermal environment of cabbage white caterpillars, *Pieris rapae* L, *Physiological and Biochemical Zoology*, 73 (5) (2000), 621–628. https://doi.org/10.1086/317758

[55] Shine, R., Harlow, P.S. Maternal manipulation of offspring phenotypes via nest-site selection in an oviparous lizard, *Ecology*, 77 (6) (1996), 1808–1817. https://doi.org/10.2307/2265785

[56] Du, W.G., Feng, J.H., Phenotypic effects of thermal mean and fluctuations on embryonic development and hatchling traits in a lacertid lizard, *Takydromus septentrionalis*, *Journal of Experimental Zoology Part A: Ecological Genetics and Physiology*, 309 (3) (2008), 138–146. https://doi.org/10.1002/jez.442

[57] Kingsolver, J.G., Ragland, G.J., Diamond, S.E., Evolution in a constant environment: thermal fluctuations and thermal sensitivity of laboratory and field populations of *Manduca sexta*. *Evolution*, 63 (2) (2009), 537–541.

[58] Georges, A., Beggs, K., Young, J.E. and Doody, J.S., Modelling development of reptile embryos under fluctuating temperature regimes, *Physiological and Biochemical Zoology*, 78 (1) (2005), 18–30. https://doi.org/10.1111/j.1558-5646.2008.00568.x

[59] Yee, E. H., Murray, S. N., Effects of temperature on activity, food consumption rates, and gut passage times of seaweed-eating *Tegula* species (Trochidae) from California, *Marine Biology*, 145 (2004), 895– 903. https://doi.org/10.1007/s00227-004-1379-6.

INSTRUCTIONS TO CONTRIBUTORS

Communications Faculty of Sciences University of Ankara Series C Biology (Commun. Fac. Sci. Univ. Ank. Ser. C-Biology.) is a single-blind peer reviewed open access journal which has been published biannually since 1948 by Ankara University, accepts original research articles written in English in the field of Biology. Review articles written by eminent scientists can also be invited by the Editor.

The publication costs for Communications Faculty of Sciences University of Ankara Series C-Biology are covered by the journal, so authors do not need to pay an article-processing and submission charges. The PDF copies of accepted papers are free of charges and can be downloaded from the website. Hard copies of the paper, if required, are due to be charged for the amount of which is determined by the administration each year.

All manuscripts should be submitted via our online submission system https://dergipark.org.tr/en/journal/2987/submission/step/manuscript/new. Manuscripts should be submitted in the PDF form used in the peer-review process together with THE COVER LETTER and the TEX file (Source File). In the cover letter the authors should suggest the most appropriate Field Editor for the manuscript and potential four reviewers with full names, universities and institutional email addresses. Proposed reviewers must be experienced researchers in your area of research and at least two of them should be from different countries. In addition, proposed reviewers must not be co-auhors, advisors, students, etc. of the authors. In the cover letter, the author may enter the name of anyone who he/she would prefer not to review the manuscript, with detailed explanation of the reason. Note that the editorial office may not use these nominations, but this may help to speed up the selection of appropriate reviewers.

Manuscripts should be typeset using a word processor editor. Authors should prepare the article using the COMMUNICATIONS style before submission to the editor via our submission system. A template of manuscript can be downloaded in doc form from the link http://dergipark.org.tr/download/journal-file/13889 (or can be reviewed in pdf form). The title page should contain the title of the paper, full names of the authors, affiliations addresses and e-mail addresses of all authors. Authors are also required to submit their Open Researcher and Contributor ID (ORCID)'s which can be obtained from http://orcid.org as their URL address in the format http://orcid.org/xxxx-xxxx-xxxx-xxxx. Please indicate the corresponding author. The abstract should state briefly the purpose of the research. The length of the Abstract should be between 50 to 5000 characters. At least 3 keywords are required. Formulas should be numbered consecutively in the parentheses ( ). All tables must have numbers (TABLE 1) consecutively in accordance with their appearance in the text and a legend above the table. Please submit tables as editable text not as images. All figures must have numbers (FIGURE 1) consecutively in accordance with their appearance in the text and a caption (not on the figure itself) below the figure. Required final resolution is 300 dpi for coloured images (RGB), 300–600 dpi for black and white images and 600–1200 dpi for line art. Pictures and line drawings should be saved as TIFF files. Authors Contribution Statement, Declaration of Competing Interests and Acknowledgements should be given at the end of the article before the references. The following format for the references should be used. Authors are urged to use the Communication.csl style (https://dergipark.org.tr/en/download/journal-file/18514) in Mendeley Desktop or Zotero automated bibliography. If manual entry is prefered for bibliography, then all citations must be listed in the references part and vice versa. The Editor may seek the advice of two, or three referees, depending on the response of the referees, chosen in consultation with appropriate members of the Editorial Board, from among experts in the field of specialization of the paper. The reviewing process is conducted in strict confidence and the identity of a referee is not disclosed to the authors at any point since we use a single-blind peer review process.

Declarations/Ethics:
With the submission of the manuscript authors declare that:

- All authors of the submitted research paper have directly participated in the planning, execution, or analysis of study;
- All authors of the paper have read and approved the final version submitted;
- The contents of the manuscript have not been submitted, copyrighted or published elsewhere and the visual-graphical materials such as photograph, drawing, picture, and document within the article do not have any copyright issue;
- The contents of the manuscript will not be copyrighted, submitted, or published elsewhere, while acceptance by the Journal is under consideration.
- The article is clean in terms of plagiarism, and the legal and ethical responsibility of the article belongs to the author(s). Author(s) also accept that the manuscript may go through plagiarism check using IThenticate software;
- The objectivity and transparency in research, and the principles of ethical and professional conduct have been followed. Authors have also declared that they have no potential conflict of interest (financial or non-financial), and their research does not involve any human participants and/or animals.

Research papers published in **Communications Faculty of Sciences University of Ankara** are archived in the Library of Ankara University (Volume 1-67) and in Dergipark immediately following publication with no embargo.

Editor in Chief
http://communications.science.ankara.edu.tr
Ankara University, Faculty of Sciences
06100, Besevler - ANKARA TÜRKİYE